



TN2: SIMULATION REPORT ON COMPARISON OF DVB-RCS2 AND 3GPP NR NTN TECHNOLOGIES IN LEO SYSTEMS.





Change history

Date	Author(s)	Comment	
11.02.2025	Tuomas Huikko	Template for other content, simulation assumptions	
18.03.2025	Tuomas Huikko	Simulator overview (section 2), clarified simulation description	
20.03.2025	Tuomas Huikko, Verneri Rönty	Added results, analysis	
21.03.2025	Tuomas Huikko, Verneri Rönty	Finished results, analysis, conclusions, added abbreviations, minor changes	





Abbreviations

3GPP 3rd Generation Partnership Project

5G 5th Generation

ACM Adaptive Coding and Modulation

ARQ Automatic Repeat reQuest

AWGN Additive White Gaussian Noise

BBFrame Baseband Frame

BLER Block Error Rate

C/N0 Carrier-to-noise Density Ratio

CA Carrier Aggregation

CBS Code Block Size

CL Coupling Loss

CRC Cyclic Redundancy Check

DL Downlink

DSS Dynamic Spectrum Sharing

DVB Digital Video Broadcasting

EIRP Equivalent Isotropic Radiated Power

Es/N0 Energy per symbol to Noise Density Ratio

ESA European Space Agency, Electronically Steered Antenna

FER Frame Error Rate

FRF Frequency Reuse Factor

FSPL Free Space Path Loss

GEO Geostationary Orbit

GNSS Global Navigation Satellite System

GSE Generic Stream Encapsulation

HARQ Hybrid ARQ

ICI Inter-carrier Interference

ISI Inter-symbol Interference



TN2-Simulation report



KPI Key Performance Indicator

L2S Link-to-System

LEO Low Earth Orbit

LLC Logical Link Control

LLS Link Level Simulation

LOS Line-of-Sight

MAC Medium Access Control

MC Multi-Connectivity

MCS Modulation and Coding scheme

MF-TDMA Multi Frequency-Time Division Multiple Access

MODCOD Modulation and Coding scheme

NR New Radio

ns-3 Network Simulator 3

NTN Non-terrestrial Network

OFDM Orthogonal Frequency Division Multiplex

PC Power Control

PDCP Packet Data Convergence Protocol

PL/PHY Physical Layer

PRB Physical Resource Block

PTRS Phase Tracking Reference Signal

PUSCH Physical Uplink Shared Channel

RCS2 Return Channel Satellite 2nd Generation

RF Radio Frequency

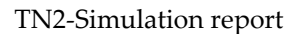
RLC Radio Link Control

RLE Return Link Encapsulation

RNG Random Number Generator

RR Round Robin

RRC Radio Resource Control







S2X Second Generation Satellite Extensions

SCS Subcarrier Spacing

SINR Signal-to-interference-plus-noise Ratio

SLS System Level Simulation

SNR Signal-to-noise Ratio

SNS3 Satellite Network Simulator 3

TB Transport Block

TBTP Terminal Burst Time Plan

TN Terrestrial Network

Tx Transmit

UL Uplink

UT User Terminal

VSAT Very Small Aperture Terminal





Table of Contents

1	Int	trodu	ction	8
2	Sir	nulat	or overview	9
	2.1	SNS	3	9
	2.2	ALI	x	9
	2.3	Phas	se 1.5 features	10
	2.3	3.1	Doppler degradation	10
	2.3	3.2	Expanded LLS results	12
	2.3	3.3	Electronically Steered Antenna model	14
3	Sy	stem	Level Metrics Description	14
	3.1	Gen	eral parameters, assumptions and scenario	14
	3.1	.1	Simulation flow	19
	3.1	.2	Traffic model	20
	3.2	Stati	stics	20
4	Sy	stem	Level Simulation Evaluation	21
	4.1	Info	rmative statistics	21
	4.2	DVE	3-RCS2 vs. NR NTN comparison results: ideal Doppler compensation	27
	4.2	2.1	DVB-RCS2 waveforms vs. NR PUSCH	27
	4.2	2.2	Burst-mode DVB-S2X waveforms vs. NR PUSCH	32
	4.2	2.3	Continuous carrier DVB-S2X waveforms vs. NR PUSCH	37
	4.2	2.4	Summary	42
	4.3 term		3-RCS2 vs. NR NTN comparison results: Doppler compensation of synchronised non-G	NSS 43
	4.3	3.1	DVB-RCS2 waveforms vs. NR PUSCH	44
	4.3	3.2	Burst-mode DVB-S2X waveforms vs. NR PUSCH	50
	4.3	3.3	Continuous carrier DVB-S2X waveforms vs. NR PUSCH	55
	4.3	3.4	Summary	59
	4.4	DVE	3-RCS2 vs. NR NTN comparison results: Doppler compensation of GNSS terminal	61
	4.4	l .1	DVB-RCS2 waveforms vs. NR PUSCH	61
	4.4	1.2	Burst-mode DVB-S2X waveforms vs. NR PUSCH	67
	4.4	1.3	Continuous carrier DVB-S2X waveforms vs. NR PUSCH	72



TN2-Simulation report



	4.4.4 Summary	77
5	Conclusions	78
6	References	80





1 Introduction

This document contains a detailed description of the simulation- and simulator development work done for DVB project to compare the 5th Generation (5G) New Radio (NR) Non-terrestrial Networks (NTN) technology to Digital Video Broadcasting (DVB) Return Channel Satellite 2nd Generation (RCS2) in Low Earth Orbit (LEO) environments. This comparison is a continuation of previous simulation work [1] and introduces new effects such as signal degradation from the Doppler shift and losses in gain when using Electronically Steered Antennas (ESA). The main intent is to compare how the DVB-RCS2 technology performs vs. another major candidate for current and future satellite systems, namely 3rd Generation Partnership Project (3GPP) NR NTN. The comparison methodology is similar to previous comparison work in Geostationary Orbit (GEO) [2] satellite systems.

Section 2 briefly describes the used simulators as well as the newly developed features. Section 3 describes the general simulation assumptions, the evaluated scenario and targeted Key Performance Indicators (KPIs) and statistics. Section 4 presents the simulation results, detailed parameters, and discussion concerning the results and the factors that contribute to the results. Section 5 concludes the document.





2 Simulator overview

2.1 SNS3

The simulator was previously described in [1] and since the core functionality of the simulator has not changed, the content is not repeated here. Any new developments are described in section 2.3.

2.2 ALIX



Magister Solutions has implemented a 5G (TN-)NTN System Level Simulator (SLS) [3] called ALIX, primarily within the European Space Agency (ESA) ALIX project [4] targeting successful standardization of NTN in 3GPP. Like Satellite Network Simulator 3 (SNS3), the simulator is an extension of Network Simulator 3 (ns-3)

[5], with its own link-to-system (L2S) mapper for different modulation and coding schemes (MCS). The simulator calculates Signal-to-Interference plus Noise Ratio (SINR) for each received packet including received power, noise and co-channel interference and uses the L2S to convert that into a Block Error Rate (BLER). To model 5G networks, ns-3 has been extended with 5G LENA [6] which models physical (PHY) and Medium Access Control (MAC) layers of NR and implements terrestrial propagation and channel models of 3GPP TR 38.901 [7]. 5G LENA implements the channel, NR PHY and MAC protocol layers, algorithms, and procedures, but Radio Resource Control (RRC), Packet Data Convergence Protocol (PDCP) and Radio Link Control (RLC) layers are reused from the ns-3 LTE module. 5G LENA focuses only on terrestrial network deployment scenarios. To support NTN-specific features, 5G LENA and ns-3 have been extended by adding support for 3GPP TR 38.811 [8] based channel and antenna/beam modelling, along with the global coordinate system, and the system level calibration scenarios presented in TR 38.821 [9]. The ns-3 platform shall also provide the higher protocol layers, i.e., network, transport, and application layers. An overview protocol architecture of the simulator is presented in Figure 1.

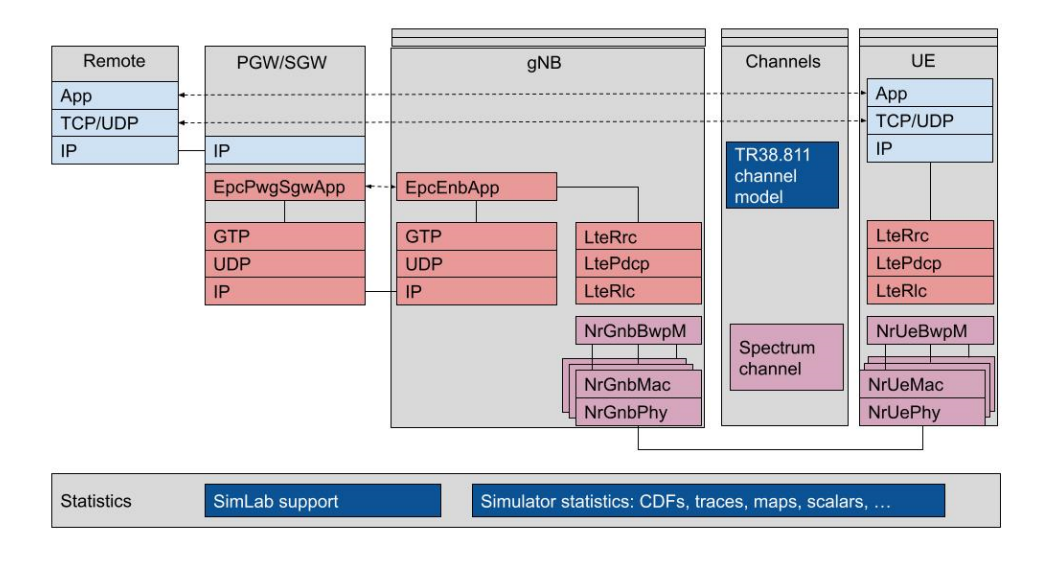


Figure 1. Protocol architecture of ALIX 5G NTN SLS.





The system level calibration scenarios presented in TR 38.821 [9] function as a baseline for satellite scenario deployments and parameterizations. This contains for example different satellite orbits (LEO-600, LEO-1200, GEO), frequency bands (S-, Ka-band), terminal assumptions (VSAT, handheld) and frequency reuse patterns (reuse 1, 3 and 2+2). These function as baseline scenarios, but all parameters can be also configured separately. In addition, hybrid TN and NTN scenarios can be studied, e.g., deployed to overlapping, adjacent, or completely separated frequency bands. Satellites assume so called Bessel equation-based beam patterns defined in TR 38.811 [8] where the beam parameters, beam count and beam spacing can be configured by means of different parameters.

The primary use case has been the 3GPP RAN standardization support related to NTN by means of system/network level simulations focusing on the air interface protocols such as PHY, MAC and RLC. The simulator has been used, e.g., to produce some RAN1, RAN2 and RAN4 contributions, as the following:

- System level calibration simulations and HARQ operation, [10][11].
- TN/NTN Multi-Connectivity (MC) and Dynamic Spectrum Sharing (DSS) between TN and NTN researched in the DYNASAT project, [12][13][14][15][16][17][18]
- Application layer performance of railway control communications for GEO satellite network with 5G air interface, [19].
- TN/NTN adjacent channel coexistence simulations in S-band for handheld terminals [20][21]. RAN4 calibration simulation results for both TN and NTN simulation scenarios can be found in [22]. The resulting coexistence simulation results have been contributed to 3GPP RAN4 working group meetings [23][24].

2.3 Phase 1.5 features

Within this activity, the following features were developed for the simulation tools:

- Regenerative payload for ALIX.
- Signal degradation of the Line-of-sight (LOS) component from Doppler shift, including reduction in received power and resulting Inter-carrier Interference (ICI).
- Expanded Link Level Simulation (LLS) results, based on the link level comparison work in [25].
- ESA modelling, including scanning loss resulting from the steering of the beam pattern.
- Non-persistent continuous-carrier mode for DVB- Second Generation Satellite Extensions (S2X) waveforms implemented to DVB return link [26].
- Generic Stream Encapsulation (GSE) implemented to DVB-RCS2, to enable using DVB-S2X waveforms in the return link.

2.3.1 Doppler degradation

The Doppler modelling in both simulators utilizes a generated trace of satellite positions and other information e.g. satellite velocity and associated timestamp along an orbit, which is then used to calculate the resulting Doppler shift for each individual connection between User Terminal (UT) and satellite. The elevation angle between a satellite and UT is calculated individually for every connection and every time the Doppler is needed. The Doppler shift is calculated followingly [8]:

$$\Delta f = \frac{v_{sat}}{c} * \left(\frac{R}{R+h}\cos\alpha\right) * f_c \tag{1}$$





where v_{sat} is the satellite speed, c is the speed of light, R is the radius of the Earth, h is satellite altitude, α is the elevation angle between satellite and UT and f_c is the carrier center frequency.

The Doppler shift is calculated in the UT at the time of reception, and the full Doppler is compensated to get the residual Doppler shift, that is finally applied to the signal to get the degradation. The Doppler compensation is implemented as a compensation percentage. The main rationale behind this approach is to avoid evaluating specific Doppler compensation techniques but rather evaluate the system under different levels of compensation efficiency. The compensation is applied as follows:

$$\Delta f_{comp} = \Delta f * \frac{100\% - D_{comp,percentage}}{100\%}$$
 (2)

where Δf is the full Doppler shift and $D_{comp,percentage}$ is the Doppler compensation percentage.

The effect of the residual Doppler shift on the frequency spectrum is calculated as follows. First the frequency shift is applied to the received spectrum:

$$f_{rx,low,shifted} = f_{rx,low} + \Delta f_{comp}$$
, $f_{rx,high,shifted} = f_{rx,high} + \Delta f_{comp}$ (3)

where $f_{rx,low}$ and $f_{rx,high}$ are the expected received start and end frequency of the signal spectrum under consideration and Δf_{comp} is the calculated residual Doppler shift. For NR the considered frequency band limited by $f_{rx,low}$ and $f_{rx,high}$ is the subcarrier (bandwidth equal to Subcarrier Spacing (SCS)), whereas for DVB it is the carrier (bandwidth in the order of tens to hundreds of times larger than SCS). Then the overlap between the expected and actually received frequency is calculated to get an overlap factor $F_{overlap}$:

$$F_{overlap} = \frac{minimum\left(f_{rx,high}, f_{rx,high,shifted}\right) - maximum\left(f_{rx,low}, f_{rx,low,shifted}\right)}{f_{rx,high} - f_{rx,low}}$$
(4)

where *minimum* and *maximum* denote generic functions to get the minimum or maximum value from the pair of given values. Finally, the effective received carrier power $C_{shifted}$ and inter-carrier interference power ICI are determined using the $F_{overlap}$:

$$C_{shifted} = C * F_{overlap}, ICI = C * (1 - F_{overlap})$$
 (5)

where *C* is the original received carrier power. Note that the ICI is calculated for NR using the same overlap factor as in the received power, but since DVB employs waveforms with a roll-off and carrier spacing in frequency, the overlap factor for the adjacent carrier is calculated separately and used for the ICI calculation. A visualization of the Doppler modelling for both simulators is given below in Figure 2.







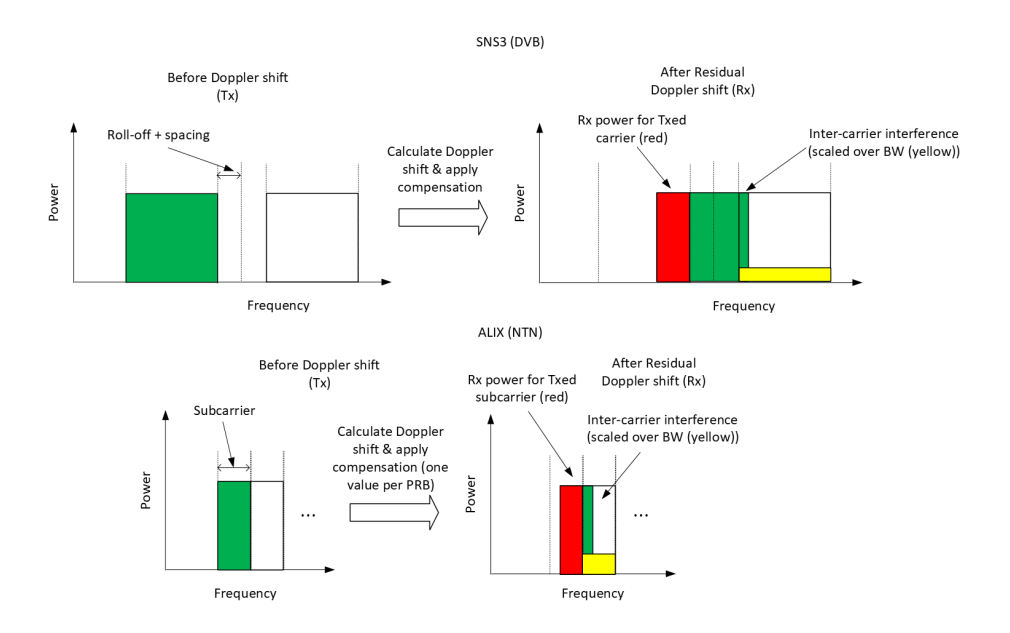


Figure 2. Residual Doppler shift and degradation implementation.

Note that the current approach considers only the frequency domain degradation and compensation, but particularly for DVB-S2X waveforms, the time domain degradation from Inter-symbol Interference (ISI) over the transmission duration, caused by the drifting of the phase of the signal, and the efficiency of symbol rate compensation will have an effect. This degradation model could be improved in the future to take into account the time-domain effects in some capacity. Furthermore, the frequency domain degradation observed for NR could be reduced by ICI compensation and Doppler estimation methods, utilizing e.g. Phase Tracking Reference Signal (PTRS) [27]. Similarly, the pilots embedded within the DVB waveforms can also be used to correct those errors. This, however, requires some further work to realize on system level.

2.3.2 Expanded LLS results

The LLS results for DVB-S2X waveforms (Additive White Gaussian Noise (AWGN)), achieved within the ESA MARINA project [28], have been expanded by calculating the common trend i.e., the average change in Energy per symbol to noise power density ratio (Es/N0) between data points, for all available Modulation and Coding (MODCOD) schemes. This common trend has then been applied to the MODCODs that were missing from the LLS results. This new expanded list of MODCODs has been utilized for the L2S mapping in the DVB simulations. The LLS results from the MARINA activity have been used for NR Physical Uplink Shared Channel (PUSCH) and DVB-RCS2 as well. The Es/N0 to spectral efficiency distribution of the used link results is presented below in Figure 3. The same distribution is further represented within a more relevant Es/N0 range in Figure 4. Note that some of the waveforms have been left out due to decreasing relevance, namely waveforms below -4 dB Es/N0. Additionally, the NR waveforms are presented only with a Code Block Size (CBS) of either 3752 (MCS 8 and 9) or 4224 (MCS 9-27). When all CBS are included, some variation in the position of the NR curve can be observed (smaller CBS have higher Es/N0 requirement, while larger CBS require less).





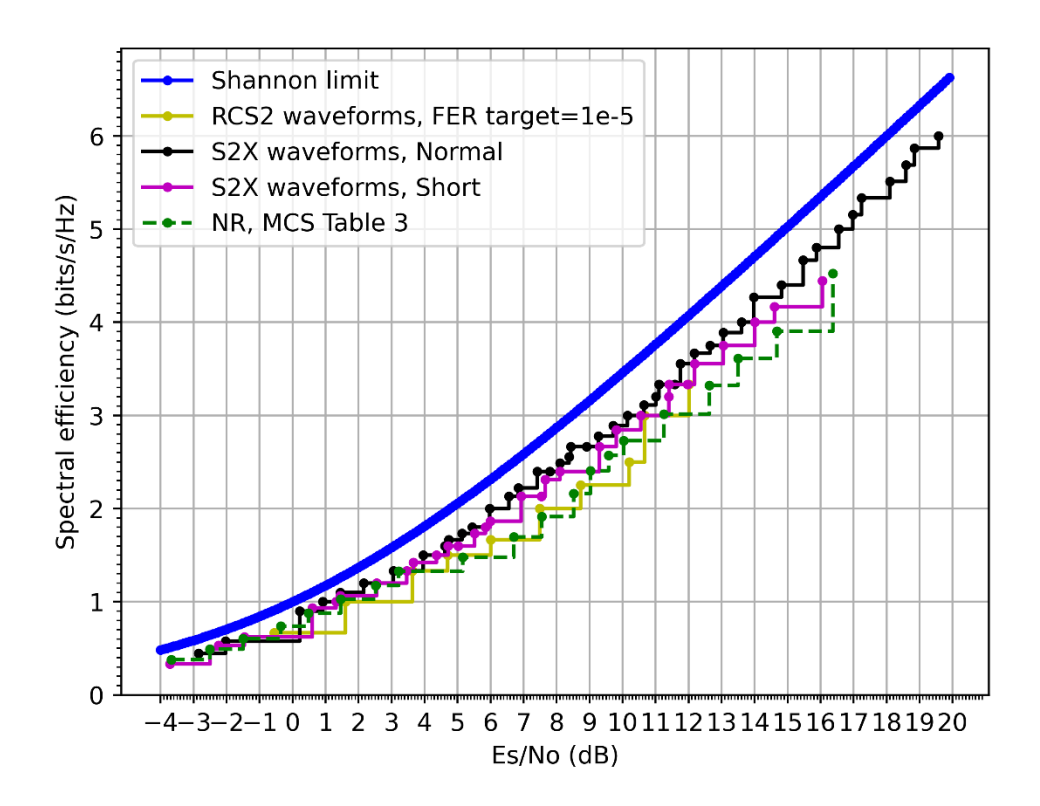


Figure 3. Es/N0 vs. spectral efficiency of LLS results.

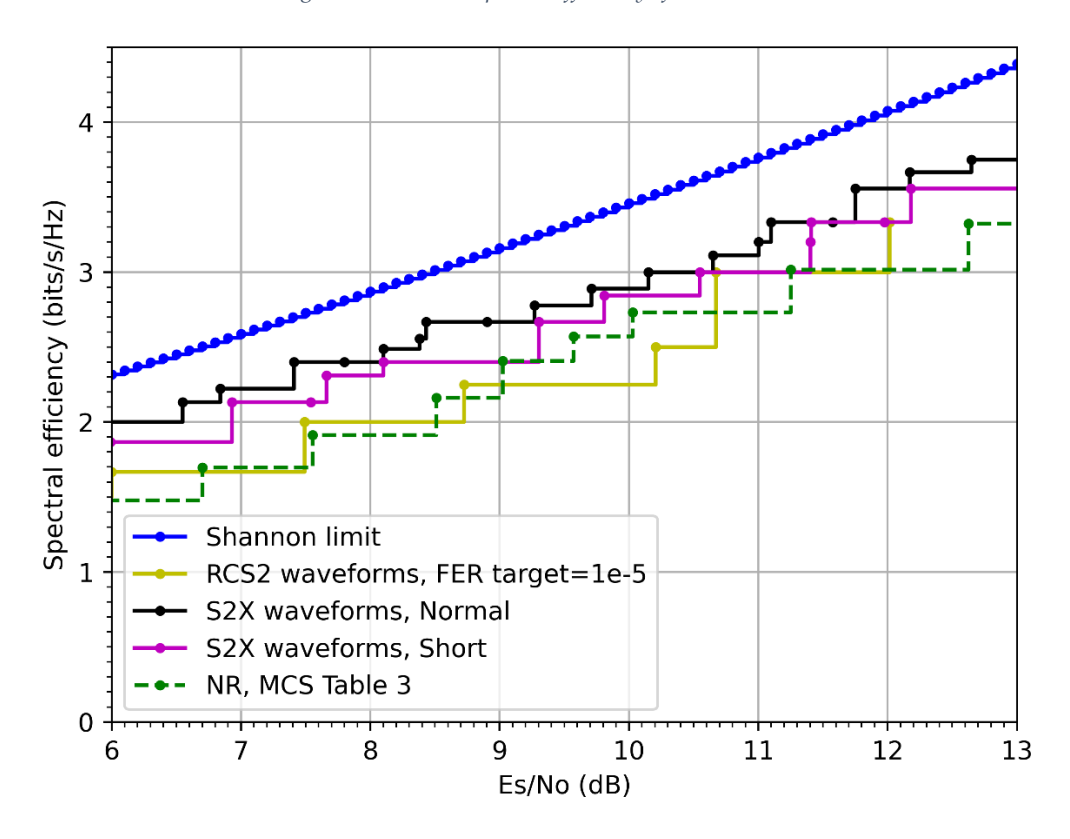


Figure 4. Es/N0 vs. spectral efficiency of LLS results, subset.





2.3.3 Electronically Steered Antenna model

The implemented ESA scanning loss model is applied to the gain of the UT antenna. The scanning loss depends on the configured scanning loss curve, such as in the Figure 5 below. The application of such scanning loss curve is based on the observations in [29], that this kind of curve is a good approximation of antenna performance. Note that the scan angle denotes the angle of deviation from the reference plane (e.g. elevation angle of 70° is equal to scan angle of 30° because the reference plane points to the zenith).

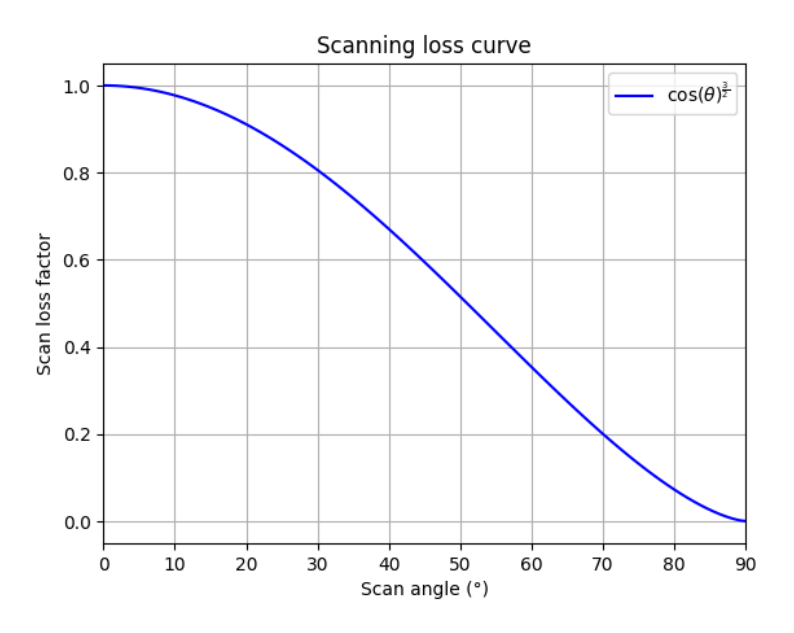


Figure 5. Example scanning loss curve.

To get both the elevation and azimuth angle, the same satellite orbital position trace that was used for Doppler, is used. The resulting scan loss factor *S*, accounting for both elevation and azimuth angles (2D scanning), is calculated followingly:

$$S = \cos \alpha^P * \cos \beta^P, \tag{6}$$

where α is the elevation angle (radians), β is the azimuth angle (radians) and P is the configured power for the cosine that defines the scanning loss curve. The scan loss factor is further applied to the antenna gain G_{SCAP} of the UT:

$$G_{scan} = G_{lin} * S \tag{7}$$

where *G_{lin}* is the linear gain value of the used antenna before scanning loss.

3 System Level Metrics Description

3.1 General parameters, assumptions and scenario

The simulated scenario is a Ka-band LEO-600 scenario with a single satellite, a single beam with 90-degree elevation angle, and 1 surrounding tier of beams for background interference. The satellite assumes constant position within the simulation i.e. no satellite movement. This assumption, coupled





with the short simulation time, gives a snapshot of the whole system performance on a single point on the satellites orbit. This limitation is planned to be addressed in future work. The satellite assumes 3GPP Set-1 parameterization (narrow, high gain beams) from 3GPP TR 38.821 Table 6.1.1.1-1 [9]. The total system bandwidth is assumed to be 1 GHz, but the frequency configuration uses 3GPP frequency re-use (FRF) Option 3 [9] (FRF 2+2), meaning that effectively 500 MHz of bandwidth (within single polarization) is available for the simulated beams. Note that realistically, NTN will have to employ Carrier Aggregation (CA) to reach this bandwidth, and the current approach assumes that works ideally. The frequency configuration assumes that beam hopping is not used. This setup corresponds to single simulated colour, which is illustrated in Figure 6.

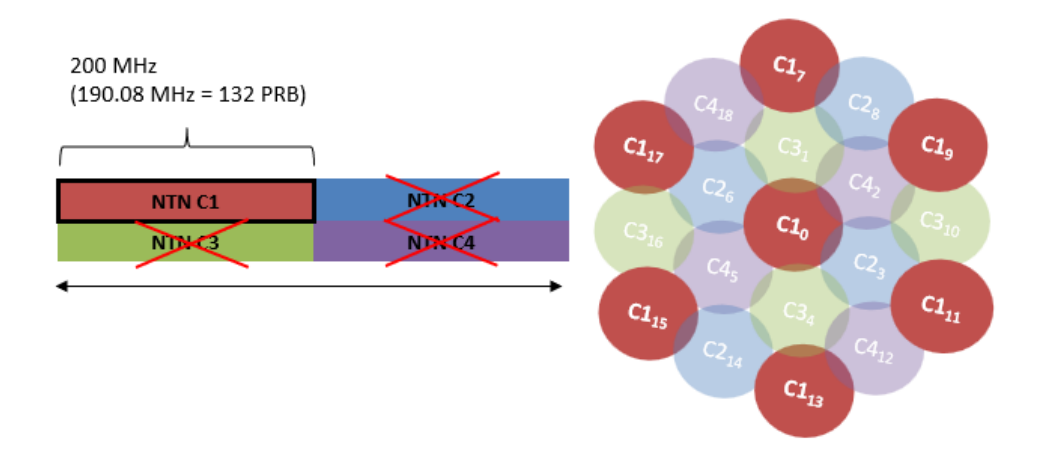


Figure 6. Simulated beam layout.

The general parameters used are presented in Table 1. The satellite payload characteristics are given in Table 2. The characteristics used by the Very Small Aperture Terminals (VSATs) are given in Table 3. The UT antennas are assumed to be perfectly pointed towards satellite (i.e. no pointing loss). The UTs with ESAs assume the same parameters as regular VSAT, only with loss in antenna gain applied according to section 2.3.3. The 30 UTs per cell are randomly placed within the width of each beam, with equivalent positions between the simulators.

Simulation duration

4.2 s (4.8 s for DVB-S2X waveforms), statistics collection duration 3.2 s per drop (total 5 simulation drops i.e., different RNG number realizations)

Satellite & beam layout

LEO satellite (altitude 600 km) with 1 statistics beam + 1 tier of surrounding, interfering beams of same colour (see Figure 6).

Central beam elevation angle 90 deg.

Satellite altitude ~606.5 km within utilized positions, speed

7.5191 km/s, orbit passes directly over central beam centre

Table 1. General parameters.

Satellite parameters for Doppler

and ESA scan loss model





	position, elevation angles between satellite and users roughly
	between 56.9–67.4 ° over the 5 drops.
ESA scan loss configuration	Scanning loss modelled according to section 2.3.3, with <i>P</i> -value
	of 1.5.
Frequency configuration and	Ka-band: 30 GHz on Uplink (UL).
waveforms	500 MHz effective bandwidth.
	DVB-RCS2 Superframe: Assumes a single waveform configuration option for all superframes per simulation scenario (either burst- or continuous carrier-mode DVB-S2X (Normal or Short) or DVB-RCS2 bursts), single frame (referring to DVB-RCS2 resource structure) per superframe, superframe duration of 10.35 ms, 20 carriers of 25 MHz (0.05 roll-off, 0.02 carrier spacing, effective symbol rate of 23.342 Msps) in superframe. Timeslots dynamically allocated to carriers for burst-mode operation, with constant duration in time for DVB-RCS2, and duration for DVB-S2X depending on the used
	waveform. DVB-RCS2 waveforms: waveform ids 13-22 used, 24 symbol guard period
	DVB-S2X waveforms: Available DVB-S2 and DVB-S2X MODCODs used, Normal and Short BBFrames, 24 symbol guard period, pilot blocks enabled, 1 waveform per burst (DVB-S2X superframing not used)
	NR waveforms: MCS table 3, numerology 3 (120 kHz SCS), effective bandwidth 480 MHz/333 Physical Resource Blocks (PRB) (4% guard band).
Continuous carrier configuration	Continuous carrier DVB-S2X configured as "non-persistent", with an allocation duration of 2 contiguous superframes. Continuous carriers assigned and UT MODCOD allocations updated with Terminal Burst Time Plan (TBTP) messages.
Physical layer overheads	DVB-S2X: BBFrame header, Physical Layer (PL) header, pilot blocks. DVB-RCS2: Waveform and burst overheads (guard symbols, pilots, pre-amble, post-amble), Cyclic Redundancy Check (CRC). NR: Demodulation Reference Signal (DMRS), PTRS, Transport Block (TB) overheads i.e., CRC, code rate.
Frequency re-use factor	2+2 (Option 3 of Table 6.1.1.1-5 in [9]) with single simulated colour.



TN2-Simulation report



User terminals per cell (per drop)	30
Channel model	Free-space Path Loss (FSPL), Line-of-sight (LOS) only with scintillation and atmospheric attenuation models from 3GPP TR 38.811 [8]. Optimistic clear sky (no rain loss) for Ka-band is assumed.
Interference sources	Neighbour beams of same colour, ICI caused by Doppler shift.
Uplink Power Control (PC)	Disabled
ACM	Enabled. Details under specific sections.
	BLER/Frame Error Rate (FER) target: 1e-5
Channel estimation	C/N_0 (SINR for NTN) reported as minimum or average value in a moving window. Each used channel estimation configuration is listed under the specific section.
Traffic model	Full buffer (Logical Link Control (LLC)/RLC layer) as described below.
Scheduler	Similar for both technologies, aiming to allocate resources evenly between users. DVB: Resource-fair.
	NR NTN: Round Robin (RR).
Control channel and signalling	Ideal signalling with delay. Control channel resource occupancy is assumed 0%.
Mobility	No satellite or UT mobility (constant positions).
Beam Hopping	Disabled.
HARQ/ARQ	Disabled.

Table 2. Satellite characteristics [1]

Satellite orbit		LEO-600
Satellite altitude		600 km
Payload cha	nsmissions	
Equivalent satellite antenna aperture	Ka-band (i.e. 20 GHz for DL)	0.5 m
Satellite EIRP density		4 dBW/MHz





Satellite Tx max Gain		38.5 dBi
3dB beamwidth		1.7647 deg
Satellite beam diameter		20 km
Payload ch	aracteristics for UL tra	nsmissions
Equivalent satellite antenna aperture	Ka-band (i.e. 30 GHz for UL)	0.33 m
G/T		13 dB K ⁻¹
Satellite RX max Gain		38.5 dBi

Table 3. Terminal characteristics [1]

Characteristics	VSAT
Frequency band	Ka-band (i.e., 30 GHz UL and 20 GHz DL)
Antenna type and configuration	Directional with 60 cm equivalent aperture diameter
Polarization	circular
Rx Antenna gain	39.7 dBi
Antenna temperature	150 K
Noise figure	1.2 dB
Tx transmit power	2 W (33 dBm)
Tx antenna gain	43.2 dBi

The simulated scenario is further visualized in Figure 7.







Figure 7. Scenario visualization.

3.1.1 Simulation flow

The simulation scenario involves a single satellite, seven spot beams, and 210 user terminals. Each spot beam contains a random distribution of 30 UTs, all possessing identical Radio Frequency (RF) characteristics. The UT positions are identical between the two simulators. Among these, one beam is designated as the statistical beam, while the remaining six serve as interference beams. The statistical and interference beams differ solely in that performance metrics from the statistical beam, as well as the user terminals associated with it, are collected for inclusion in the final analysis. The simulation execution uses a warm-up phase, during which statistics are not collected.

During the warm-up phase, all user terminals establish connections with the satellite, ensuring that statistics are not collected when connection establishment has not completed fully. This phase also initiates data transmission, allowing the satellite to dynamically allocate resources in response to user demands. However, samples are not collected during this period to exclude the duration of initial access from the final analysis.

After the warm-up phase, the simulation transitions into the data collection phase. During this period, performance metrics for the central beam, referred to as the statistical beam, and its associated 30 user terminals are recorded. Key metrics such as throughput and SINR are collected. Incorporating a warm-up phase ensures that the collected statistics represent the steady-state operational performance of the system, free from initialization artifacts.

This one simulation run is referred to as a single simulation drop, in which the same random number seed is used in the generation of random variables, such as the spatial distribution of user terminals. The comparative simulation analysis consists of five simulation drops, with samples aggregated across





all the five executed simulations. In the results this approach yields, for instance, 150 unique random user positions within the statistical beam and 900 unique random user positions within the interference beams, serving as sources of interference. However, at any given time, each beam contains 30 user terminals, resulting in a total of 210 user terminals across the single satellite.

3.1.2 Traffic model

The full buffer traffic model generates traffic at the LLC layer i.e. the Return Link Encapsulation (RLE) or GSE layer for DVB and the RLC layer for NR. The model always reports full LLC/RLC buffers, which results in the maximum assignable capacity always being requested and allocated in scheduling, although the scheduler attempts to allocate resources evenly between all users, when all users have requested the maximum capacity. Additionally, the upper layer packets are not fragmented using this model, instead the queued packets are generated based on need, fitting the available capacity in the allocated waveform. Essentially, the full buffer traffic model does not have any meaningful data transmitted within the packets, only aiming to generate full system load. This leads to scenarios where the maximum system capacity is tested.

3.2 Statistics

The following statistics are used as KPIs for the simulations:

- User throughput (kbps)
- Beam throughput (Mbps)
- Spectral efficiency (bit/s/Hz)
- Link performance (BLER/FER performance)

The throughput for DVB is calculated using the information on how much data bits fit each waveform (specified by MODCOD and symbol length), considering the modulation order (number of modulated bits per symbol) and coding rate. NR NTN uses a similar approach, utilizing the knowledge of transmitted TB sizes and used MCS. Additionally, possible overheads (e.g. BBFrame header, CRC for DVB) are reduced from the payload that is available for data traffic. With the full buffer traffic model, higher layer packets equal to the size of the data available in the waveform are then created. The final throughput considers all the packets that were received successfully within the statistics beam, within the statistics collection duration, and measures the throughput in kbits per second. The difference in user and beam throughput is that the statistics are sampled per user and per beam (sum of total user throughput within beam), respectively. The spectral efficiency is calculated considering the relation of realized beam throughput with the system bandwidth. Link (BLER/FER) performance is calculated as the frame or block error ratio over all transmitted packets in the system, sampled from the statistics beam.

The following metrics are used for calibration/informative purposes:

- Coupling loss (dB)
- Signal ratios (SINR and SNR) (dB)
- Superframe symbol load ratio (ratio of allocated vs. available symbols), allocated UTs
- MODCOD/MCS usage





• Doppler/ESA related stats: elevation angle, Doppler shift (Hz), scanning loss (dB)

Coupling loss is a useful metric used for calibration, defined as the total signal power loss between the antenna port of the transmitter and the antenna port of the receiver, used by e.g. 3GPP for calibrating system level simulations. This metric helps identifying the geometric configuration of a scenario and ensuring consistent terminal positions and conditions when comparing the performance of different simulation variations. Contributing factors to the coupling loss is the path loss, transmitter- and receiver gain. The terminal characteristics are listed in Table 3 and the satellite characteristics are listed in Table 2 for LEO-600 Ka-band.

Defined in 6.6-1 [8] the path loss (PL) is composed of components:

$$PL = PL_b + PL_a + PL_s + PL_e, (8)$$

where PL is the total path loss in dB, PL_b is the basic path loss in dB, PL_g is the attenuation due to atmospheric gasses in dB, PL_s is the attenuation due to either ionospheric or tropospheric scintillation in dB and Pl_e is building entry loss in dB.

Basic path loss is defined in Section 6.6.2 of [8], accounting for the signal's free-space propagation, clutter loss, and shadow fading. In the simulation assumptions in Table 1, the propagation channel is defined as FSPL with scintillation and atmospheric attenuation. Scenario with continuous LOS conditions is considered. Therefore, as specified in the basic path loss model, clutter loss and shadow fading are not considered in the simulations.

Additionally, attenuation due to atmospheric gases is considered as per Section 6.6.4 of [8], while scintillation loss is modelled according to the description in Section 6.6.6 of [8]. Building entry loss was not considered due to simulation assumptions, which considered terminals located outdoors. Neither was rain or other precipitation losses.

Coupling loss (CL) is calculated as:

$$CL = PL - Tx_{gain} - Rx_{gain}, (9)$$

where CL is the coupling loss in dB, PL is the path loss in dB, Tx_{gain} is the gain of the transmitter antenna gain in dB and Rx_{gain} is the gain of the receiver antenna in dB.

4 System Level Simulation Evaluation

This section presents the results of the technology comparison in various Doppler compensation capabilities and analyses the impact of the residual Doppler as well as other impacting factors on the performance. Additionally, some informative statistics are presented in section 4.1.

4.1 Informative statistics

This section presents informative statistics related to the simulated Doppler and ESA models as well as some other commonly applicable statistics. The ESA scanning loss statistics, common to all results with ESA terminals, are presented in Figure 8. The elevation angle distribution between satellite and centre cell terminals, used by the Doppler and ESA models, is presented in Figure 9. The uncompensated Doppler shift for the scenario is presented in Figure 10. The compensated/residual Doppler shifts for





97.5% and 99.3% compensation are presented in Figure 11 and Figure 12. The PRB allocation distribution for NR is given in Figure 13. One PRB equals to 12 subcarriers, which have the simulated bandwidth equal to the SCS, resulting in one PRB occupying a frequency band of 12*SCS=1.44 MHz. This means that the effective used bandwidth per user transmission in this scenario is either 15.84 MHz or 17.28 MHz. The superframe data symbol load ratios for DVB-RCS2, DVB-S2X bursts and DVB-S2X continuous carriers are given in Figure 14, Figure 15 and Figure 16, respectively.

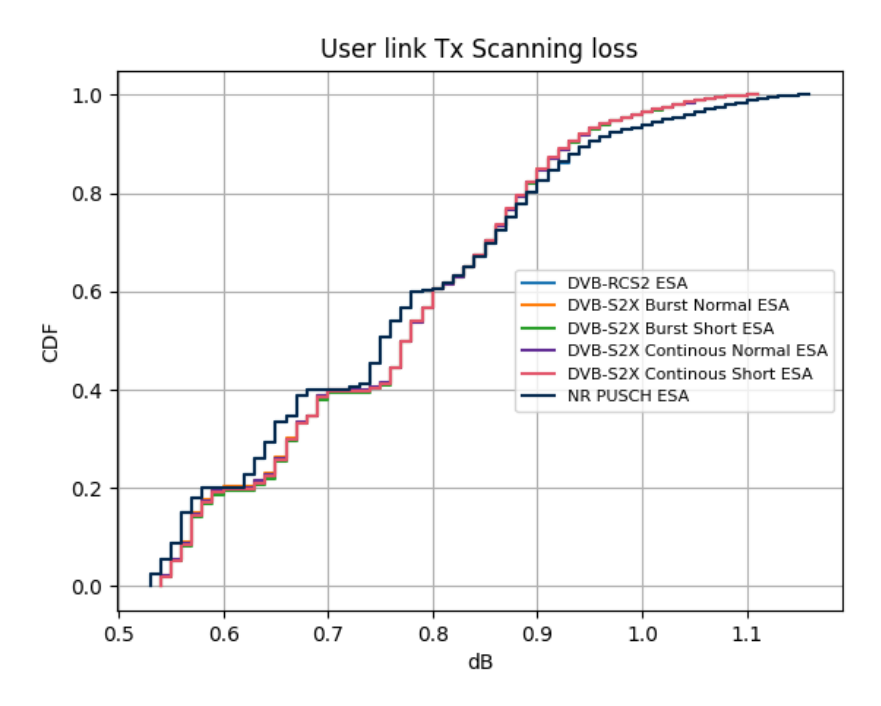


Figure 8. User link ESA scanning loss.





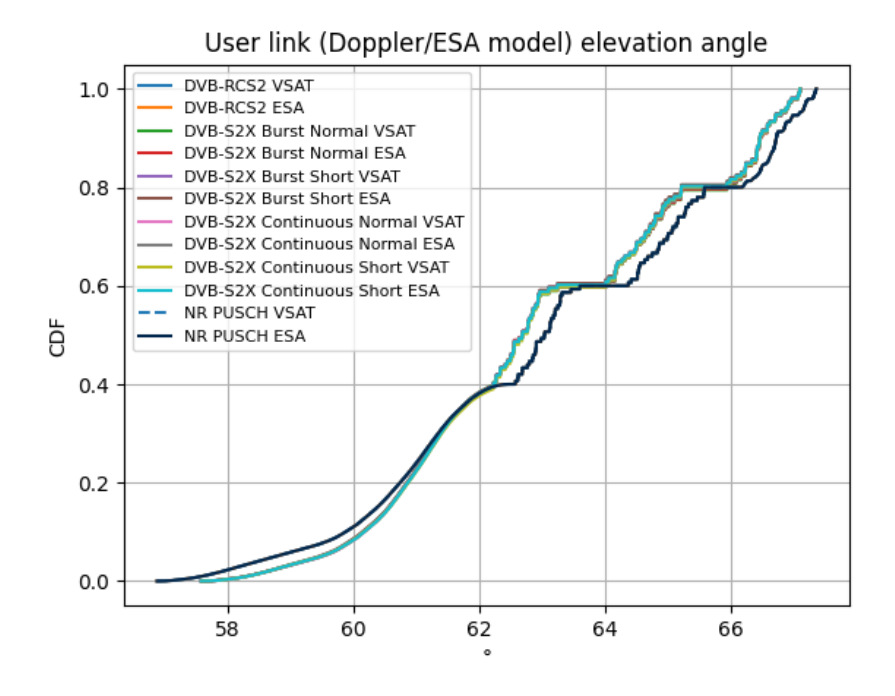


Figure 9. User link elevation angle, Doppler/ESA models.

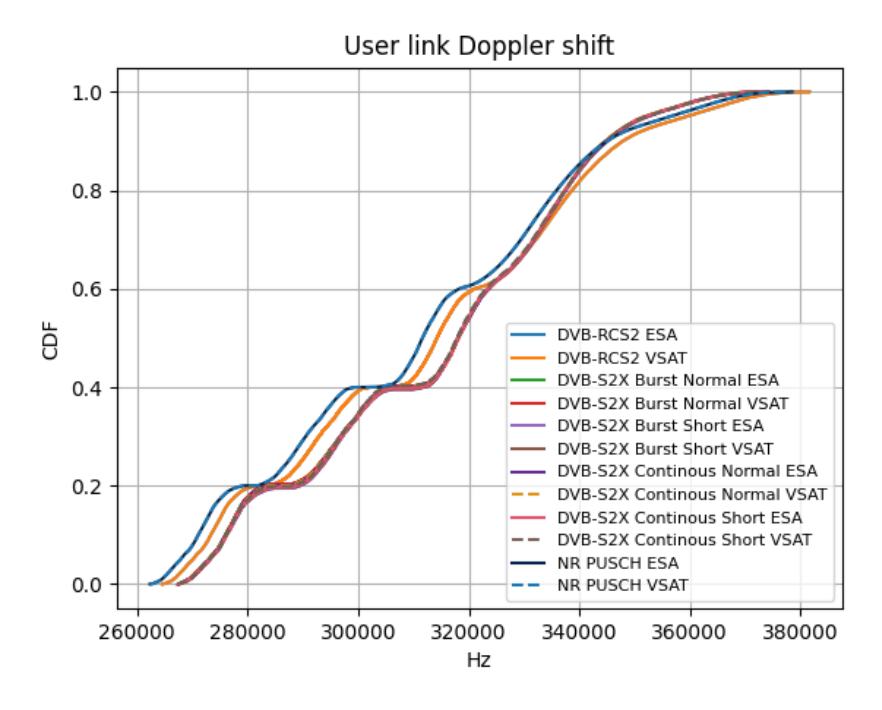


Figure 10. User link Doppler shift.





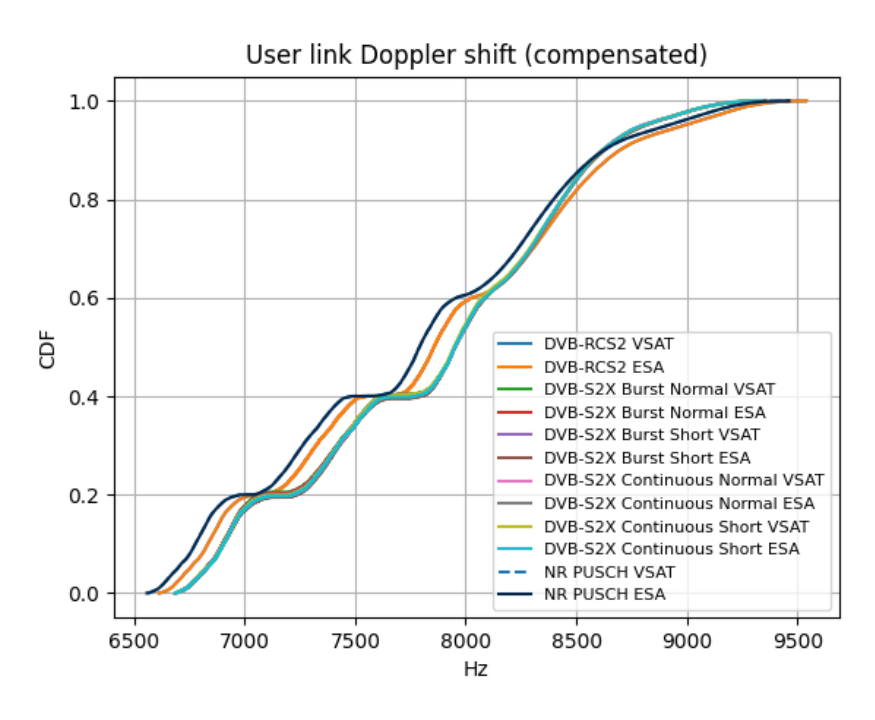


Figure 11. User link compensated Doppler shift, 97.5% compensation.

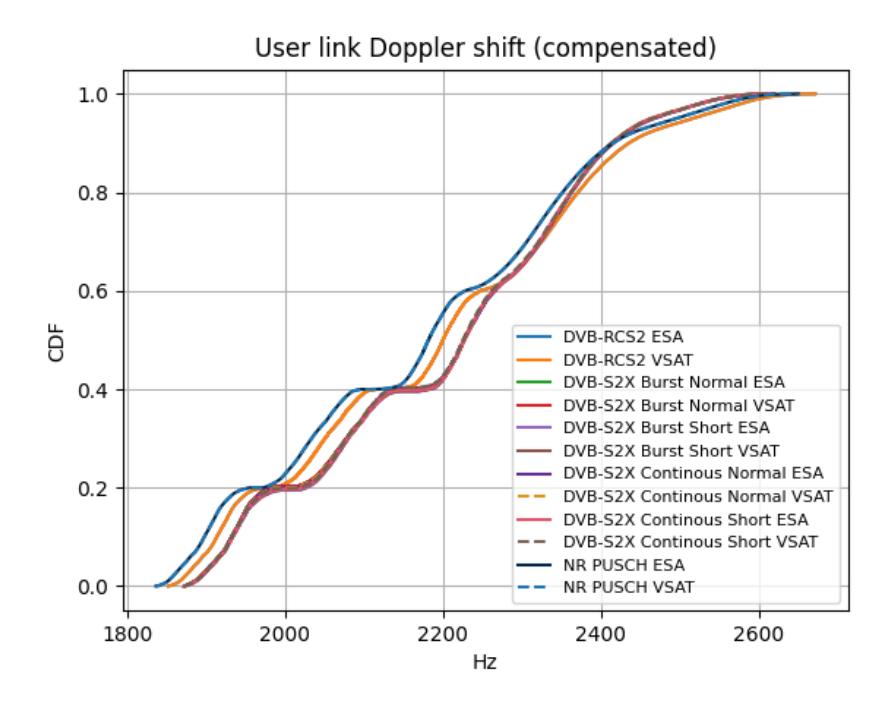


Figure 12. User link compensated Doppler shift, 99.3% compensation.





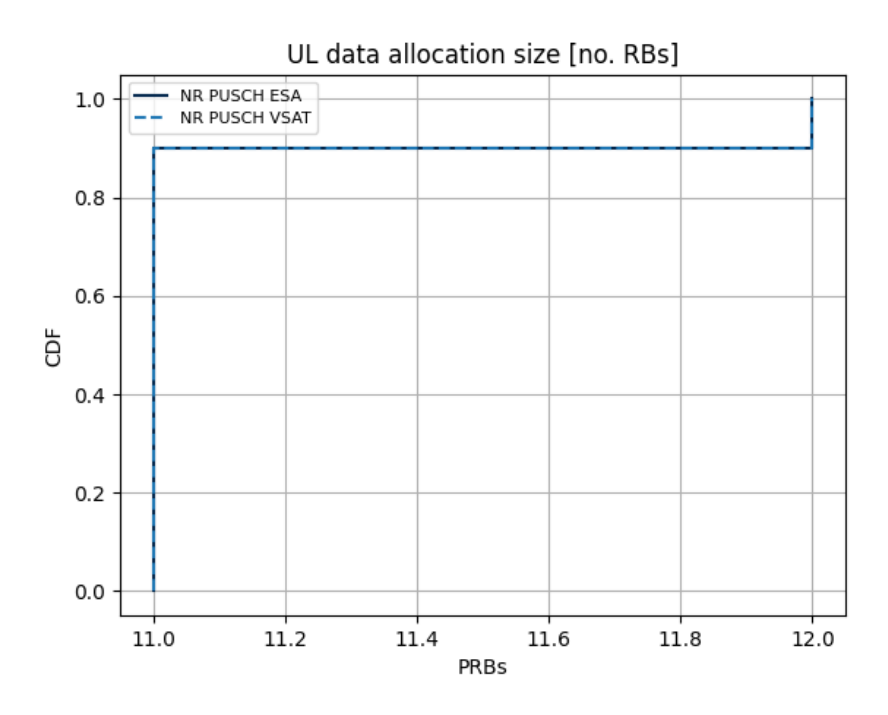


Figure 13. User data transmission PRB allocation size.

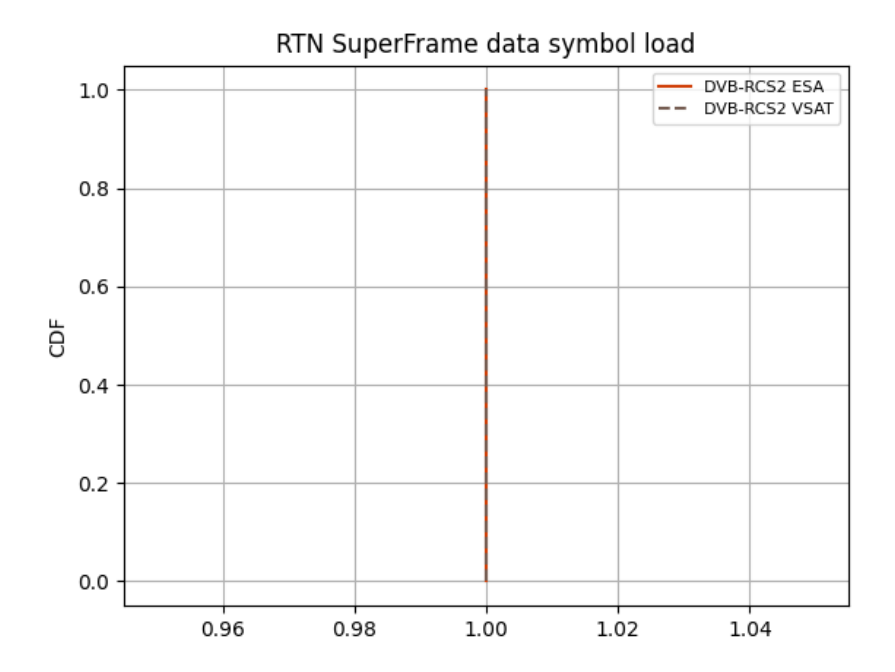


Figure 14. DVB-RCS2 data symbol load.





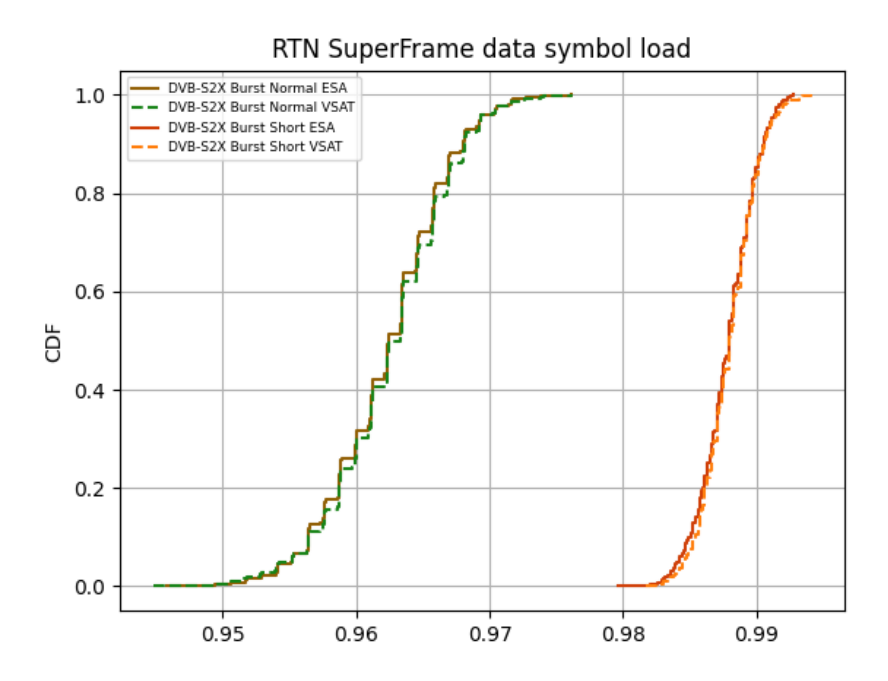
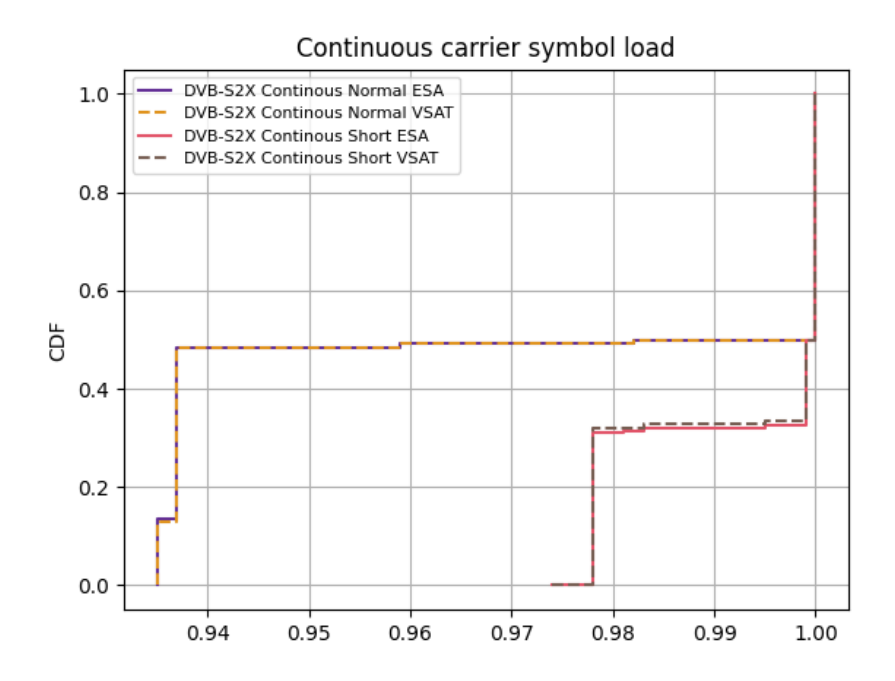


Figure 15. DVB-S2X data symbol load.



Figure~16.~Continuous~DVB-S2X~data~symbol~load.





4.2 DVB-RCS2 vs. NR NTN comparison results: ideal Doppler compensation

First, the technologies are compared under ideal Doppler compensation (100% compensated). The comparison is split into 3 sections: DVB-RCS2 waveforms vs. NR PUSCH, DVB-S2X waveforms vs. NR PUSCH and continuous mode DVB-S2X vs. NR PUSCH. The simulation parameters specific to this comparison are given below in Table 4.

Table 4. Simulation specific parameters, ideal Doppler compensation.

Parameter	Value
Channel estimation and ACM configuration	DVB-RCS2: 300ms minimum window
	DVB-S2X Burst: 300ms minimum window &
	0.6/0.4 dB ACM offset for Normal/Short frames
	DVB-S2X Continuous: 400ms minimum window
	& 1 dB ACM offset
	NR PUSCH: 2ms average window & 0.6 dB ACM
	offset
UT type	VSAT vs. ESA

4.2.1 DVB-RCS2 waveforms vs. NR PUSCH

The coupling loss, Signal-to-noise Ratio (SNR) and SINR results are presented in Figure 17, Figure 18 and Figure 19, respectively. The coupling loss shows aligned values for both technologies, verifying the scenario geometry and similarity of simulated effects. Additionally, the figure shows the effect of scanning loss when using ESAs. The SNR shows lower total noise for NR compared to DVB-RCS2. This is caused by the fact that the DVB waveform after filtering contains additional noise from the roll-off frequency bands, whereas the NR waveform does not. The SINR shows slightly better SINR for NR compared to DVB-RCS2, mostly due to the better SNR. The scanning losses due to using ESAs can be seen to not affect the resulting SINR, as it is dominated by the interference.





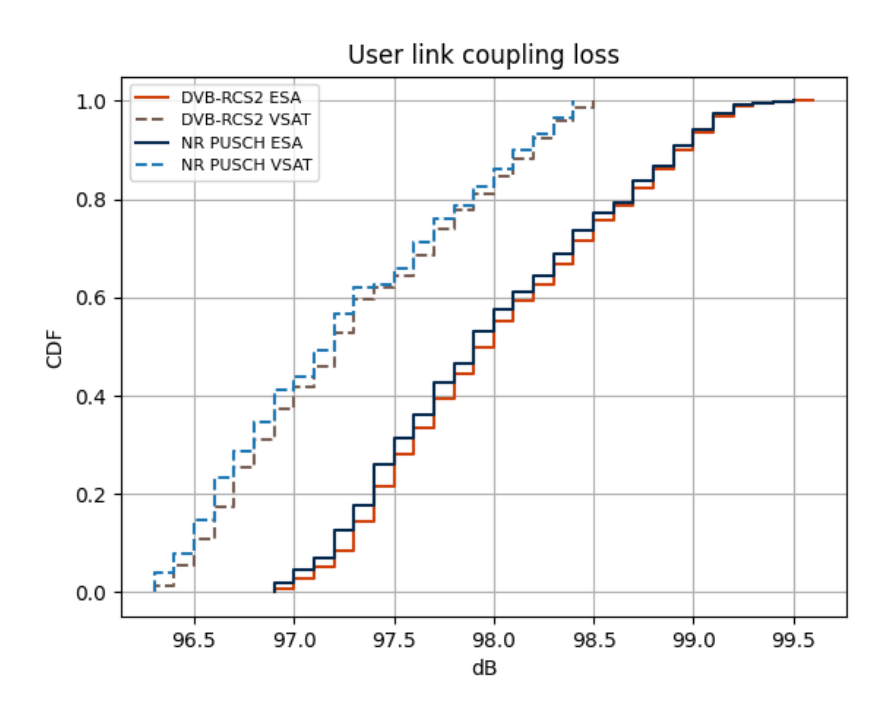
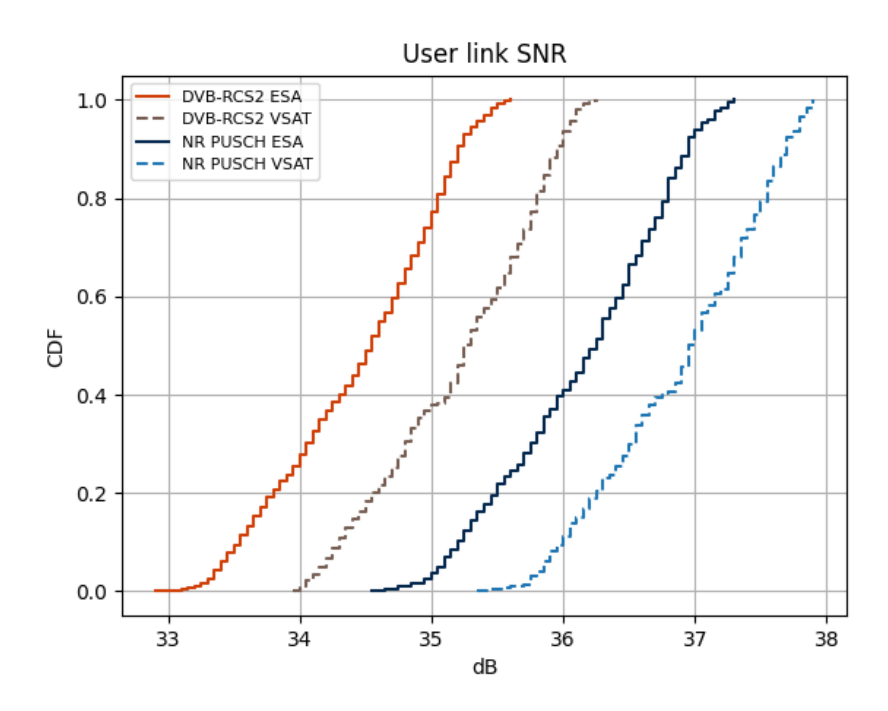


Figure 17. User link coupling loss, DVB-RCS2 vs. NR PUSCH, ideal Doppler compensation.



Figure~18.~User~link~SNR,~DVB-RCS2~vs.~NR~PUSCH,~ideal~Doppler~compensation.





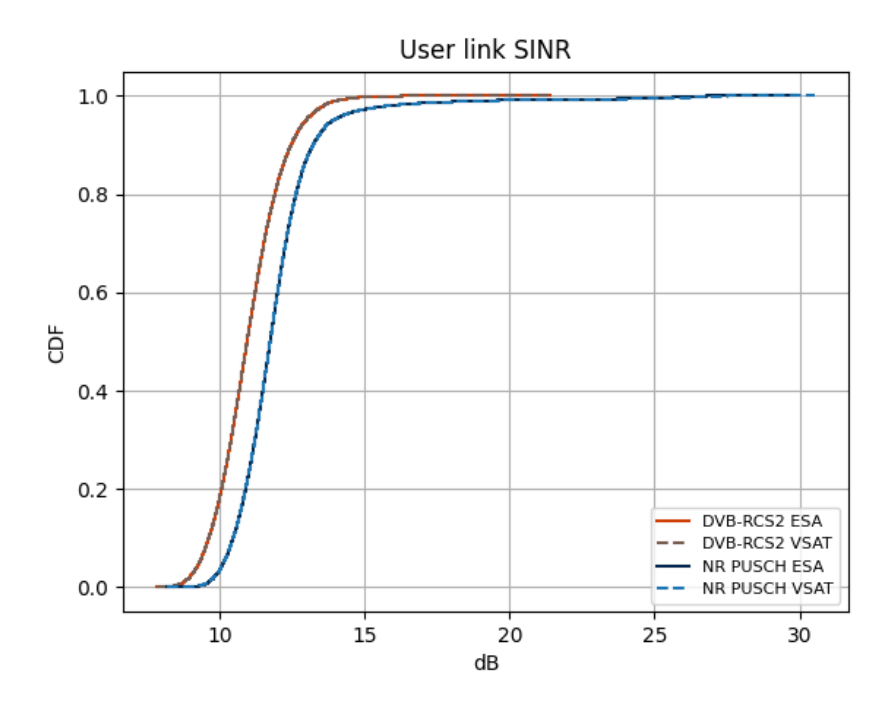


Figure 19. User link SINR, DVB-RCS2 vs. NR PUSCH, ideal Doppler compensation.

The performance of the technologies is presented with user- and system throughput, and system spectral efficiency (over 1 GHz) in Figure 20, Figure 21 and Figure 22, respectively. The user throughput shows a very large gain in favor of NR PUSCH compared to DVB-RCS2. The system level metrics reflect the user level results. The gap in throughput is mainly due to the better spectral efficiency observed for the MCS used by NR PUSCH, presented in Figure 23, combined with less overhead due to generally larger data payloads for NR TBs, compared to typical data payloads of DVB-RCS2 waveforms. The realized FER/BLER of the comparison is presented in Figure 24.





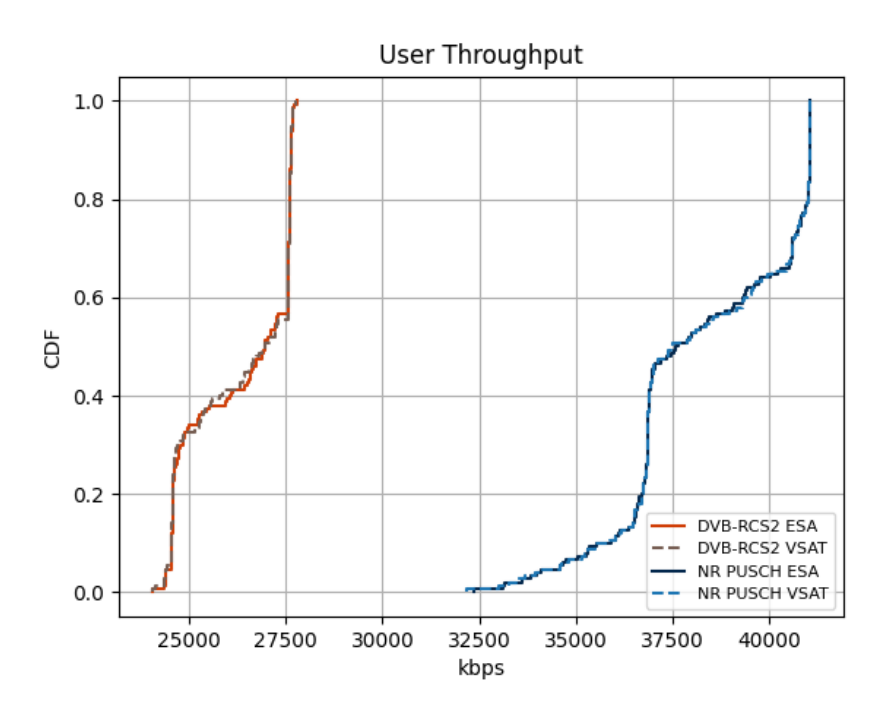
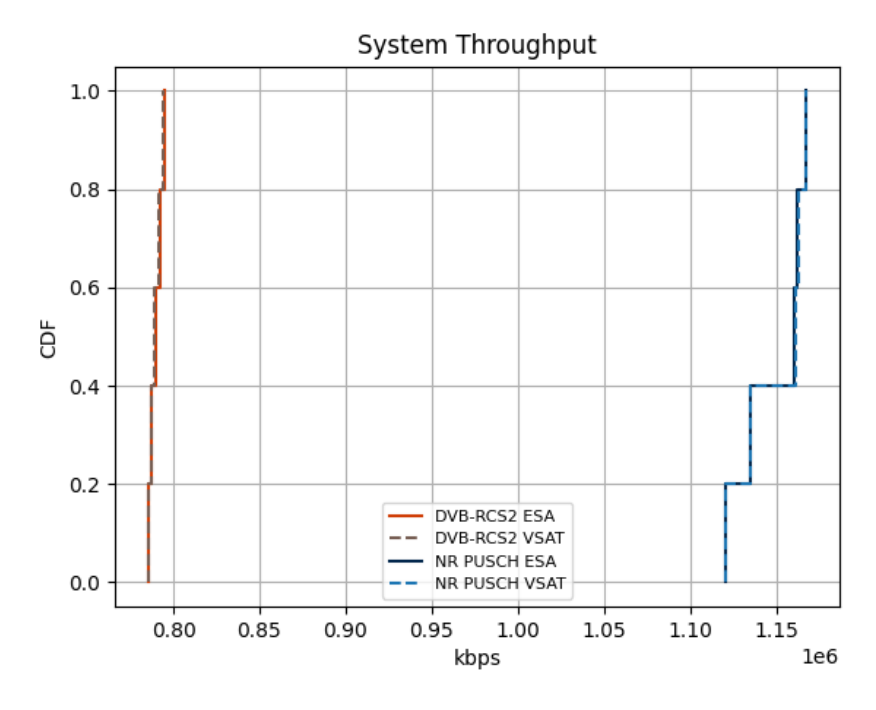


Figure 20. User throughput, DVB-RCS2 vs. NR PUSCH, ideal Doppler compensation.



Figure~21.~System~throughput,~DVB-RCS2~vs.~NR~PUSCH,~ideal~Doppler~compensation.





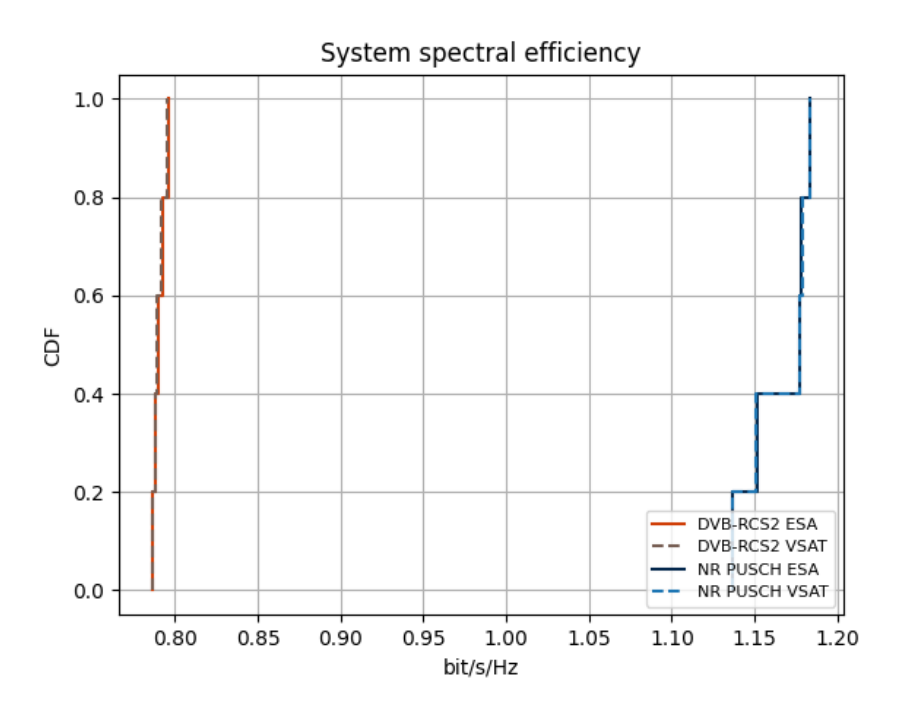


Figure 22. System spectral efficiency over 1 GHz, DVB-RCS2 vs. NR PUSCH, ideal Doppler compensation.

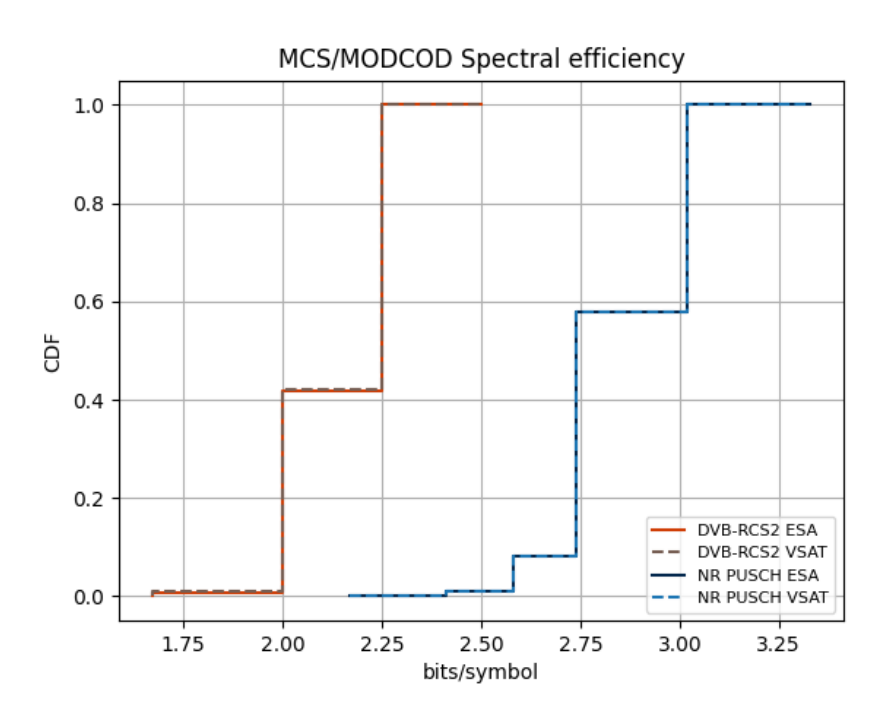


Figure 23. MCS/MODCOD spectral efficiency, DVB-RCS2 vs. NR PUSCH, ideal Doppler compensation.





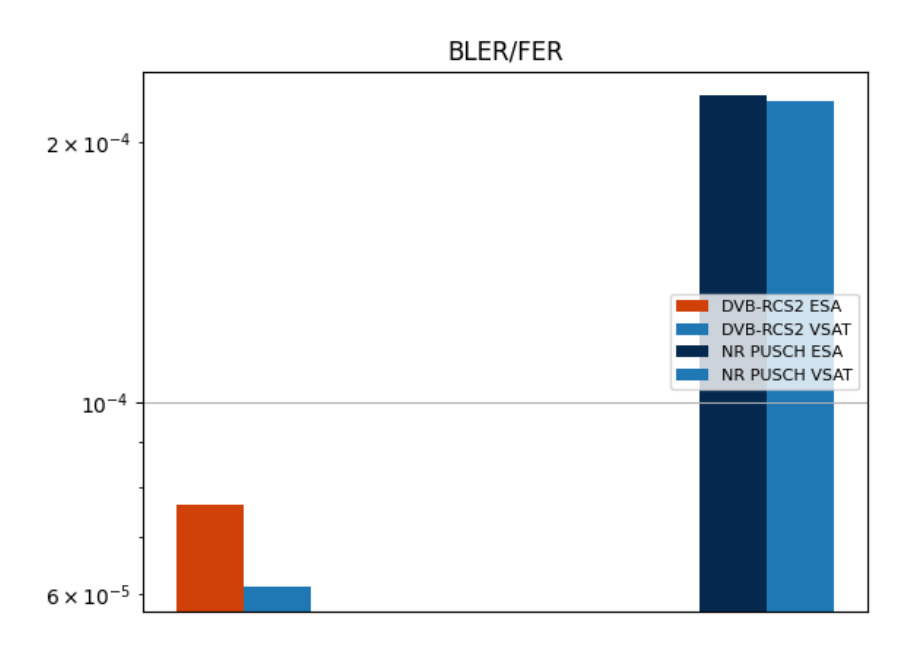


Figure 24. BLER/FER, DVB-RCS2 vs. NR PUSCH, ideal Doppler compensation.

4.2.2 Burst-mode DVB-S2X waveforms vs. NR PUSCH

The coupling loss, SNR and SINR results are presented in Figure 25, Figure 26 and Figure 27, respectively. The results are effectively almost identical with the previous section (4.2.1), refer to the analysis there.





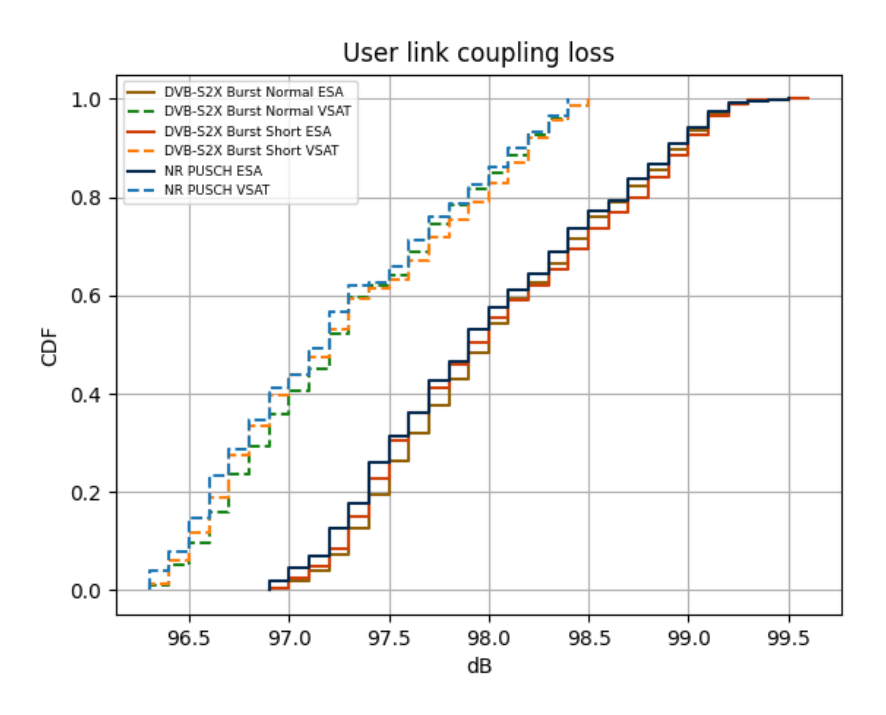


Figure 25. User link coupling loss, DVB-S2X vs. NR PUSCH, ideal Doppler compensation.

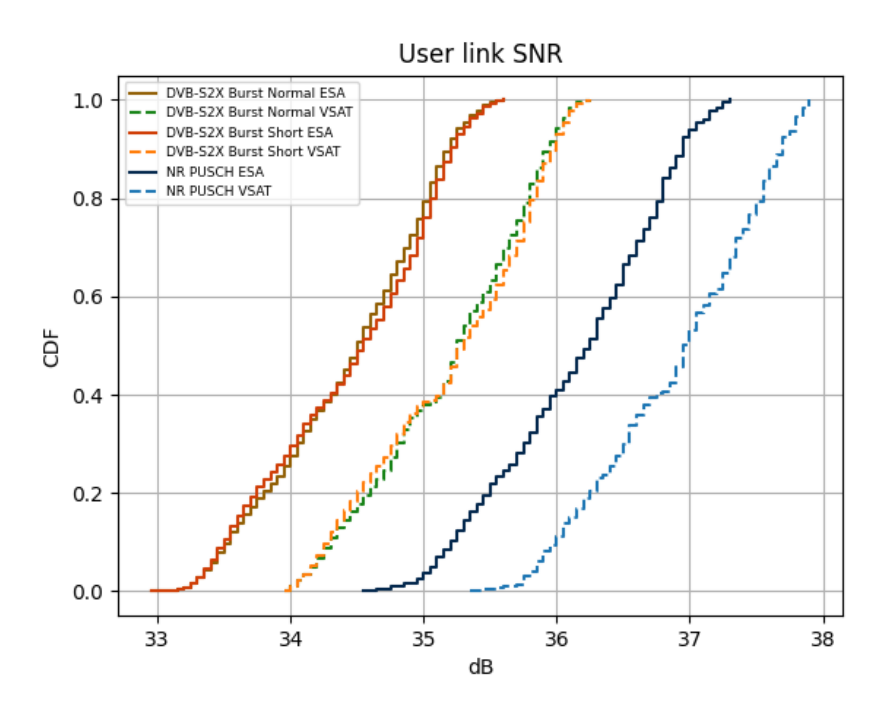


Figure 26. User link SNR, DVB-S2X vs. NR PUSCH, ideal Doppler compensation.





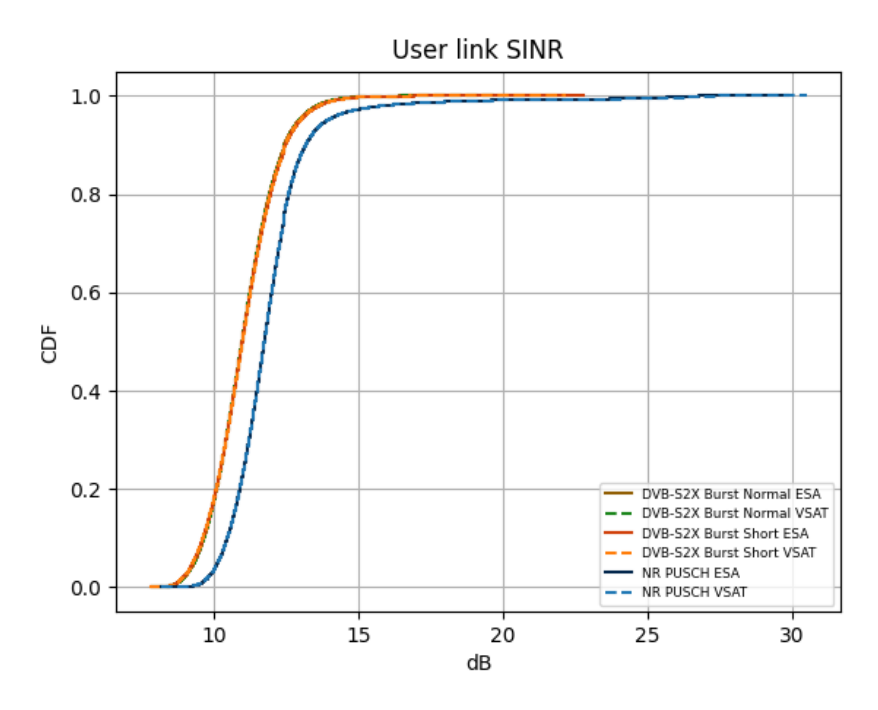


Figure 27. User link SINR, DVB-S2X vs. NR PUSCH, ideal Doppler compensation.

The performance of the technologies is presented with user- and system throughput, and system spectral efficiency (over 1 GHz) in Figure 28, Figure 29 and Figure 30, respectively. The user throughput shows a noticeable gain in favor of NR PUSCH compared to DVB-S2X waveforms, although much smaller than what was observed for DVB-RCS2. The system level metrics reflect the user level results, the performance being slightly better for NR PUSCH. The gap in throughput is mainly due to the better spectral efficiency observed for the MCS used by NR PUSCH, presented in Figure 31. Although the DVB-S2X frames have a smaller overhead than NR TBs, the spectral efficiency difference is large enough to provide NR with better overall performance. One factor affecting the observed MCS/MODCOD spectral efficiency is the robustness of the ACM, which can be indirectly analyzed through the FER/BLER, presented in Figure 32. The figure shows that the current ACM configuration is slightly less robust for NR PUSCH (larger FER), providing generally slightly higher spectral efficiency. However, the difference in the resource structures between the technologies affects the required robustness of the ACM, and for DVB-S2X frames using the Multi Frequency Time Division Multiple Access (MF-TDMA) scheme, the ACM configuration provides a big challenge, resulting in generally requiring a more robust ACM configuration to reach small FER.





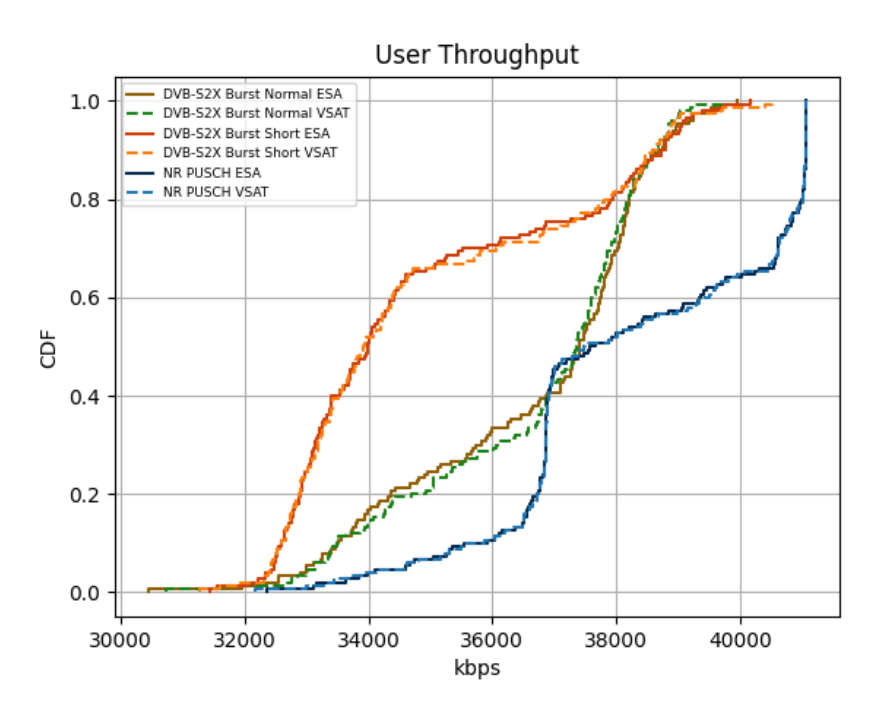
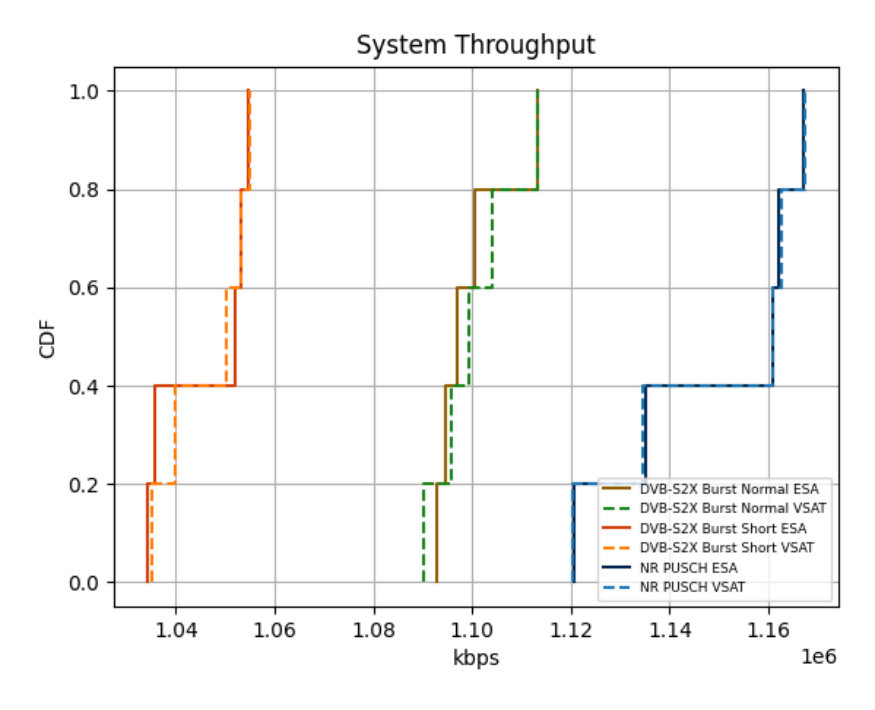


Figure 28. User throughput, DVB-S2X vs. NR PUSCH, ideal Doppler compensation.



Figure~29.~System~throughput,~DVB-S2X~vs.~NR~PUSCH,~ideal~Doppler~compensation.





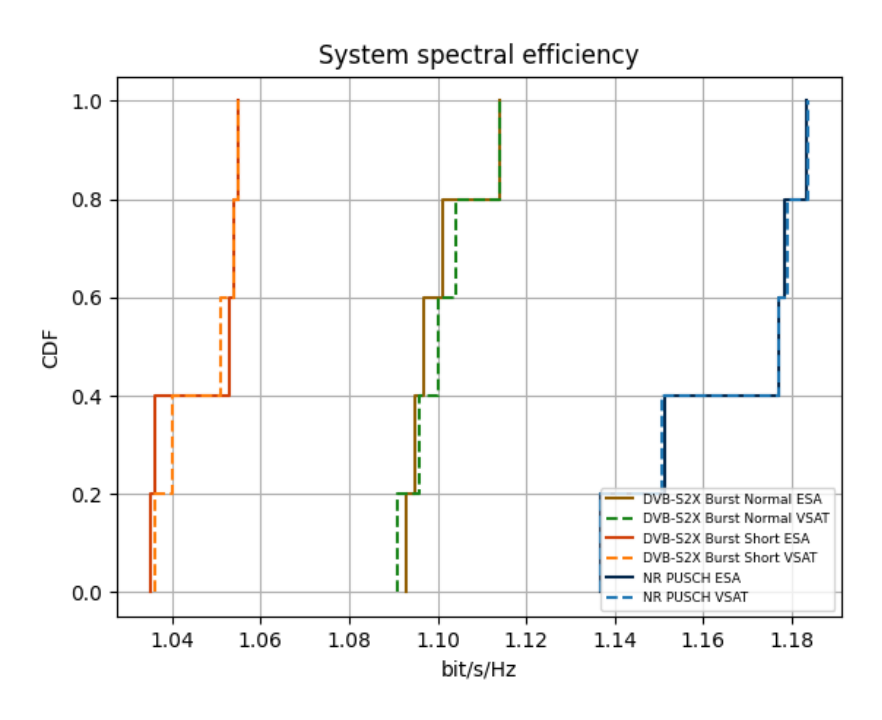


Figure 30. System spectral efficiency over 1 GHz, DVB-S2X vs. NR PUSCH, ideal Doppler compensation.

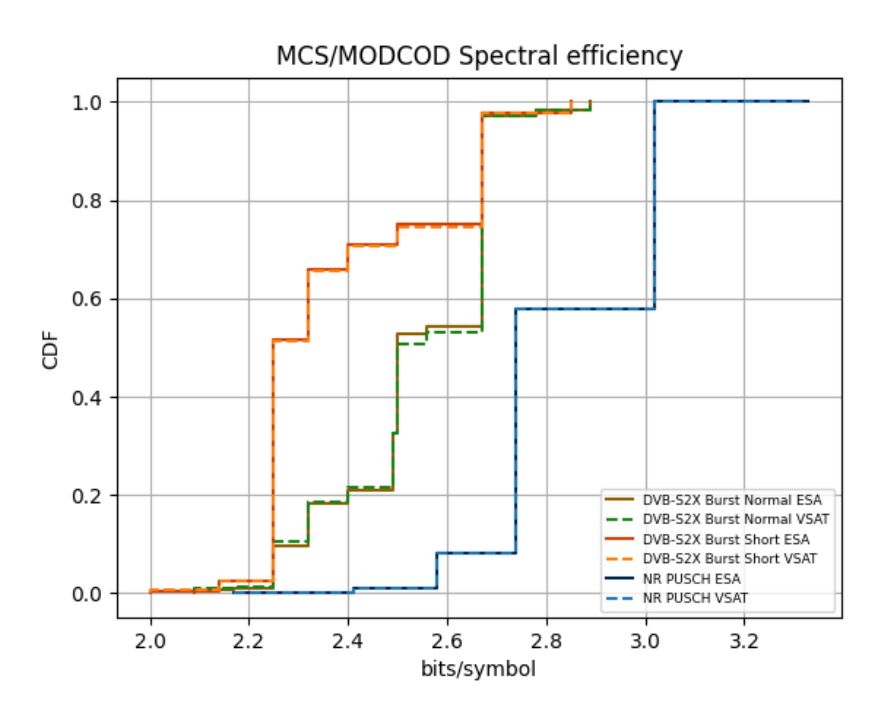


Figure 31. MCS/MODCOD spectral efficiency, DVB-S2X vs. NR PUSCH, ideal Doppler compensation.





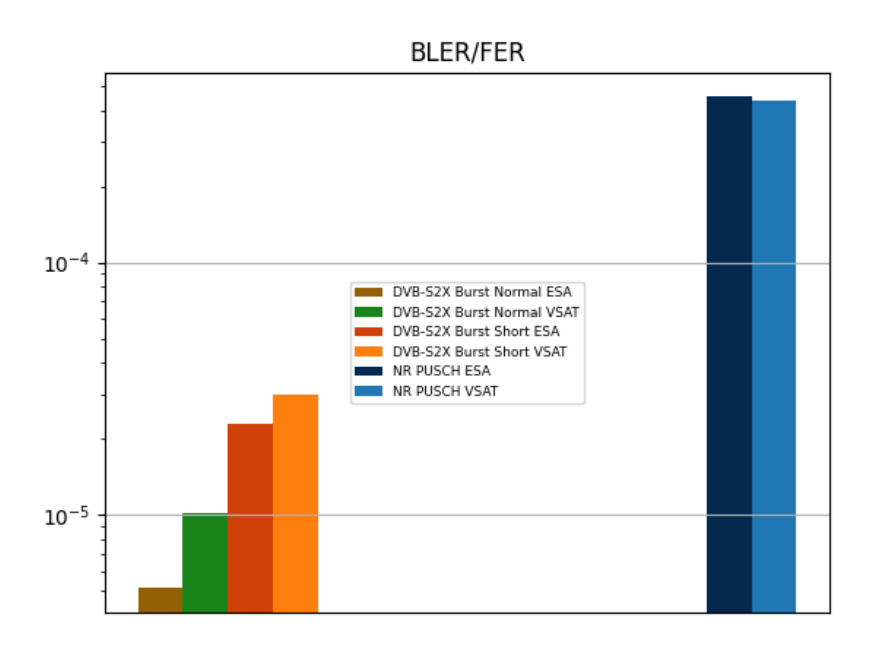


Figure 32. BLER/FER, DVB-S2X vs. NR PUSCH, ideal Doppler compensation.

4.2.3 Continuous carrier DVB-S2X waveforms vs. NR PUSCH

The coupling loss, SNR and SINR results are presented in Figure 33, Figure 34 and Figure 35, respectively. The results are effectively almost identical with the previous sections (4.2.1 and 4.2.2), refer to the analysis there.





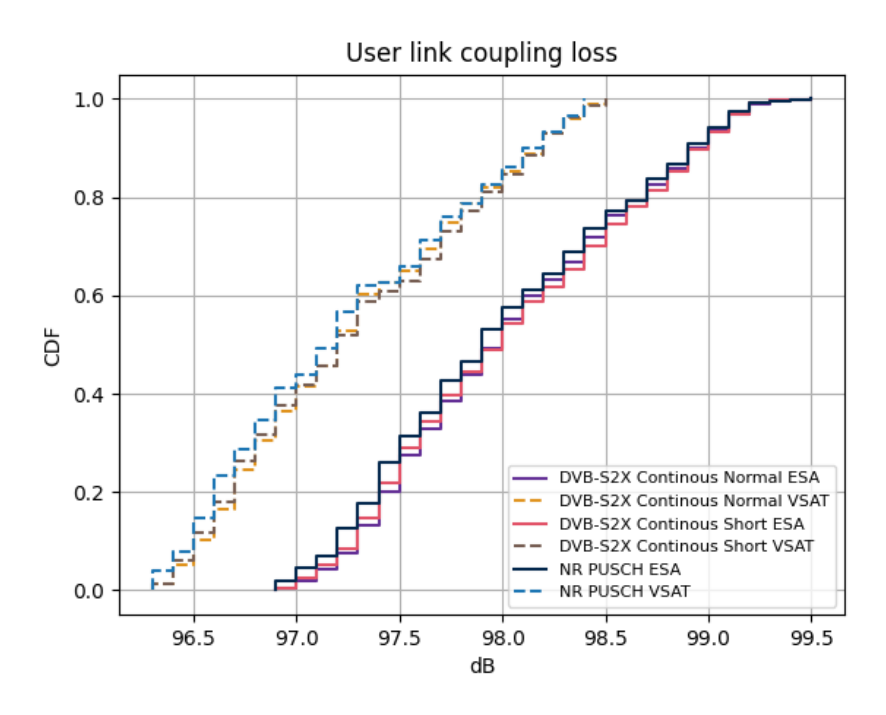


Figure 33. User link coupling loss, continuous DVB-S2X vs. NR PUSCH, ideal Doppler compensation.

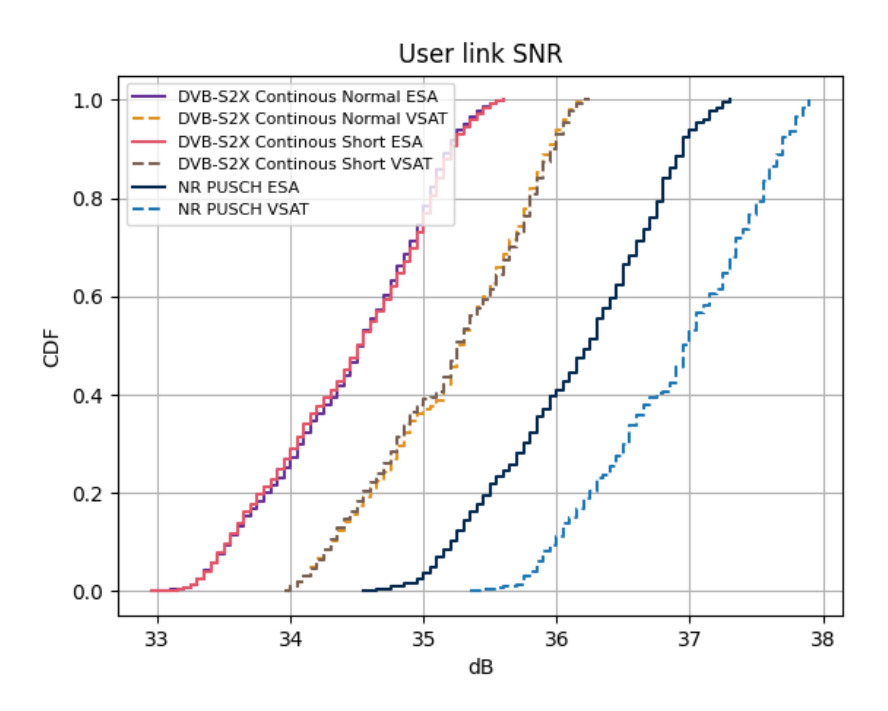


Figure 34. User link SNR, continuous DVB-S2X vs. NR PUSCH, ideal Doppler compensation.





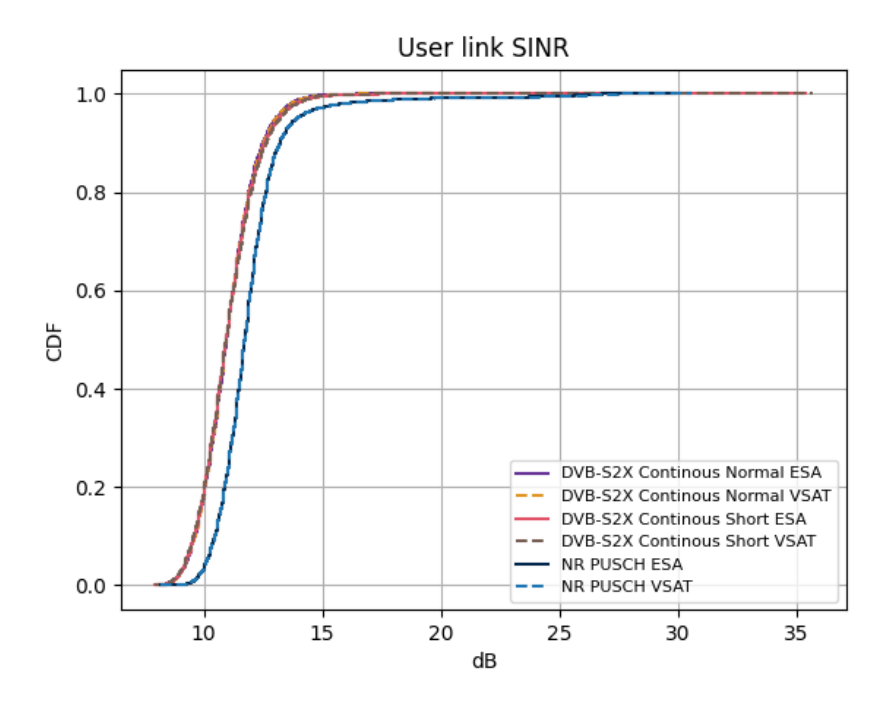


Figure 35. User link SINR, continuous DVB-S2X vs. NR PUSCH, ideal Doppler compensation.

The performance of the technologies is presented with user- and system throughput, and system spectral efficiency (over 1 GHz) in Figure 36, Figure 37 and Figure 38, respectively. Both the user- and system level results are mostly similar to what was observed for DVB-S2X bursts, although the continuous carriers can be observed to have a slightly better performance, compared to the bursts, mainly due to the better resource occupancy and more focused resource usage (only 20 UTs allocated for a longer period). The gain for NR is mainly due to the better spectral efficiency observed for the MCS used by NR PUSCH, presented in Figure 39. The realized FER/BLER is presented in Figure 40.





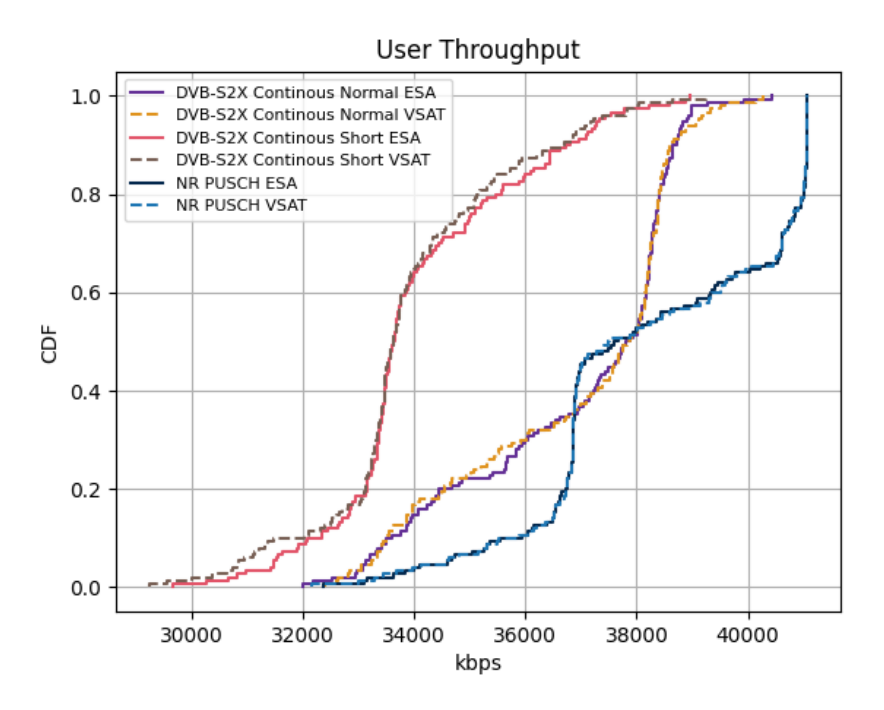
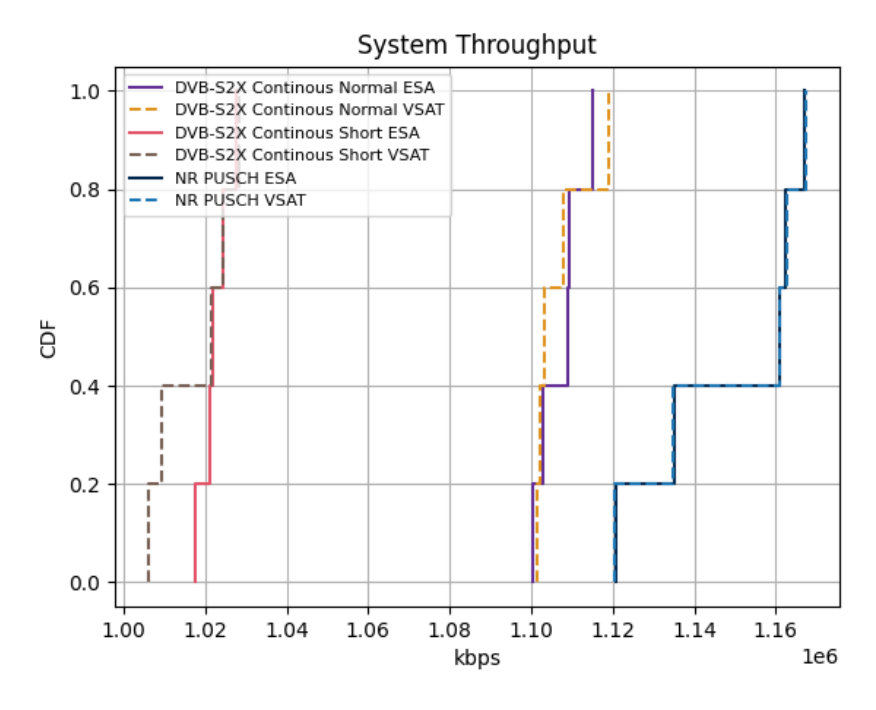


Figure 36. User throughput, continuous DVB-S2X vs. NR PUSCH, ideal Doppler compensation.



Figure~37.~System~throughput,~continuous~DVB-S2X~vs.~NR~PUSCH,~ideal~Doppler~compensation.





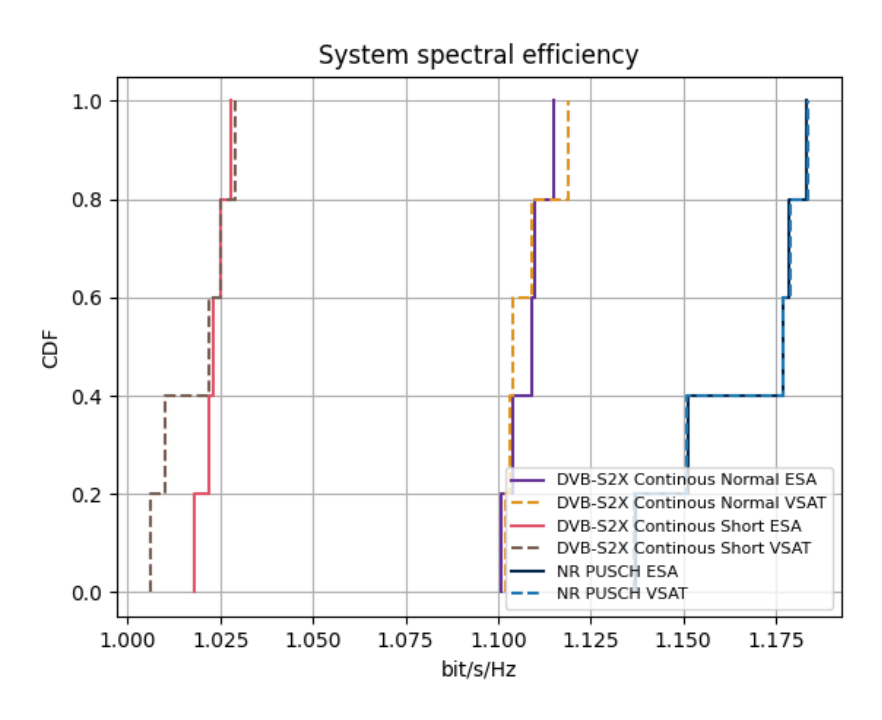


Figure 38. System spectral efficiency over 1 GHz, continuous DVB-S2X vs. NR PUSCH, ideal Doppler compensation.

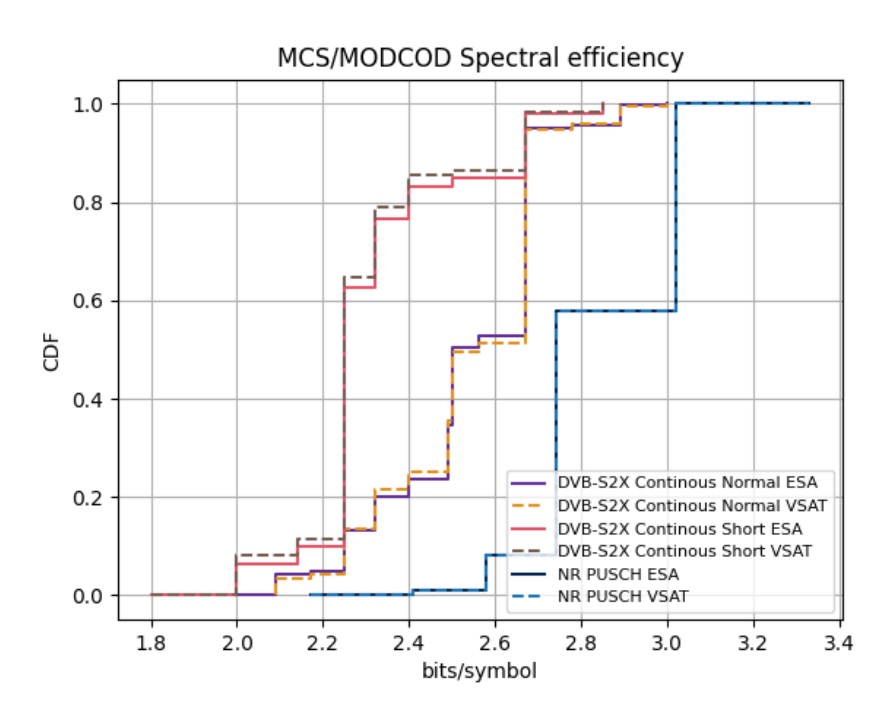


Figure 39. MCS/MODCOD spectral efficiency, continuous DVB-S2X vs. NR PUSCH, ideal Doppler compensation.





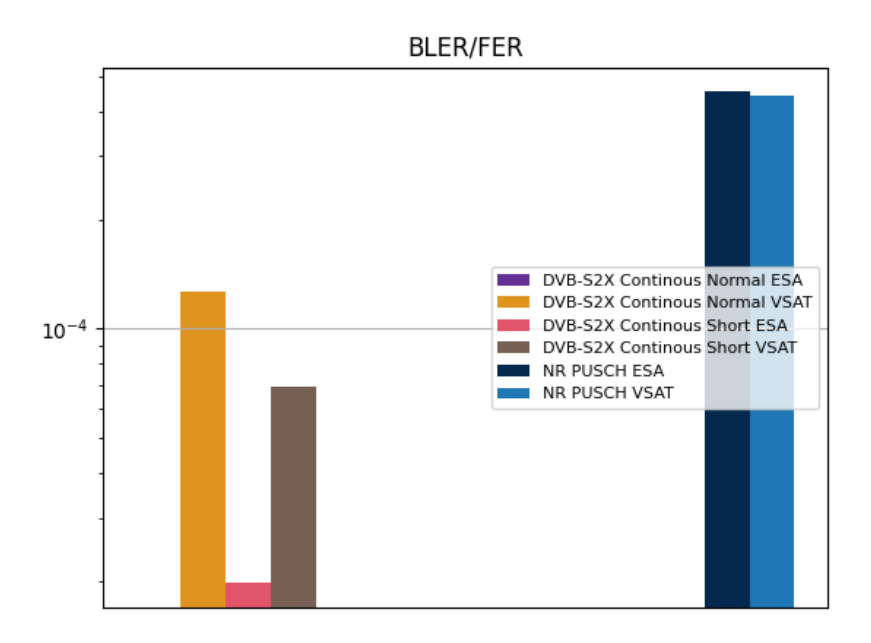


Figure 40. BLER/FER, continuous DVB-S2X vs. NR PUSCH, ideal Doppler compensation.

4.2.4 Summary

The technology comparison in ideally compensated Doppler conditions is summarised below in Table 5. The table shows an average throughput of similar magnitude for NR PUSCH and DVB-S2X Normal frames, operating with both continuous carriers and bursts within the MF-TDMA structure, however DVB-S2X Normal frames can be seen to have around 4% loss in gain. DVB-S2X Short frames and DVB-RCS2 waveforms provide comparatively much lower performance, with around 9-11% loss for DVB-S2X Short frames and around 31% loss for DVB-RCS2. The inclusion of ESA terminals causes minimal change to the results compared to conventional VSAT terminals.





Table 5. Summary table, ideal Doppler compensation.

Ideal Doppler compensation									
Antenna type	Scenario	Realized FER	5 th %-ile user tput [kbps]	50 th %- ile user tput [kbps]	95 th %- ile user tput [kbps]	User tput average [kbps]	Tput average gain over NR PUSCH		
	NR PUSCH	4.40E-04	34585.50	37478.20	41064.90	38307.99	0.00 %		
	DVB-RCS2	6.12E-05	24415.90	26955.60	27662.50	26317.25	-31.30 %		
	DVB-S2X, Normal	1.02E-05	33124.50	37358.40	38849.40	36683.00	-4.24 %		
VSAT	DVB-S2X, Short	2.99E-05	32418.30	33904.60	38897.00	34889.89	-8.92 %		
VSAI	Continuous carrier DVB-S2X, Normal	1.26E-04	33217.30	37832.60	39118.40	36892.44	-3.70 %		
	Continuous carrier DVB-S2X, Short	6.94E-05	30830.70	33611.00	37213.30	33931.69	-11.42 %		
	NR PUSCH	4.52E-04	34609.10	37582.70	41064.90	38306.23	0.00 %		
	DVB-RCS2	7.61E-05	24537.10	26955.60	27666.00	26334.35	-31.26 %		
	DVB-S2X, Normal	5.12E-06	32993.10	37409.50	38997.40	36653.66	-4.32 %		
ESA	DVB-S2X, Short	2.28E-05	32467.50	33985.80	39056.50	34865.41	-8.99 %		
	Continuous carrier DVB-S2X, Normal	0.00E+00	33115.30	37794.70	38908.80	36910.25	-3.65 %		
	Continuous carrier DVB-S2X, Short	1.98E-05	31480.80	33616.60	37322.60	34086.42	-11.02 %		

4.3 DVB-RCS2 vs. NR NTN comparison results: Doppler compensation of synchronised non-GNSS terminal

In this section, the technologies are compared, assuming a 97.5% compensated Doppler, based on findings of the frequency error of non-Global Navigation Satellite System (GNSS) terminals that have





synchronised to the network by other means [30]. The comparison is split into 3 sections: DVB-RCS2 waveforms vs. NR PUSCH, DVB-S2X waveforms vs. NR PUSCH and continuous mode DVB-S2X vs. NR PUSCH. The simulation parameters specific to this comparison are given below in Table 6.

Table 6. Simulation specific parameters, 97.5% Doppler compensation.

Parameter	Value
Doppler compensation	97.5%, according to section 2.3.1.
ACM configuration	DVB-RCS2: 300ms minimum window
	DVB-S2X Burst: 300ms minimum window &
	0.6/0.4 dB ACM offset for Normal/Short frames
	DVB-S2X Continuous: 400ms minimum window
	& 1 dB ACM offset
	NR PUSCH: 150ms average window
UT type	VSAT vs. ESA

4.3.1 DVB-RCS2 waveforms vs. NR PUSCH

The coupling loss, SNR and SINR results are presented in Figure 41, Figure 42 and Figure 43, respectively. The coupling loss varies across technologies due to the Doppler shift in receiver frequency. This difference shows that the Doppler degradation is more pronounced in technologies utilizing smaller sub-bands within the NR subcarrier architecture. Additionally, the figure shows the effect of scanning loss when using ESAs. The SNR shows lower total noise for NR compared to DVB-RCS2. This is caused by the fact that the DVB waveform after filtering contains additional noise from the roll-off frequency bands, whereas the NR waveform does not. The SINR is significantly higher for DVB-RCS2 compared to NR due to the ICI. The smaller NR subcarriers exhibit greater sensitivity to frequency shifts than the larger frequency band carriers in DVB-RCS2, leading to increased performance degradation in NR.





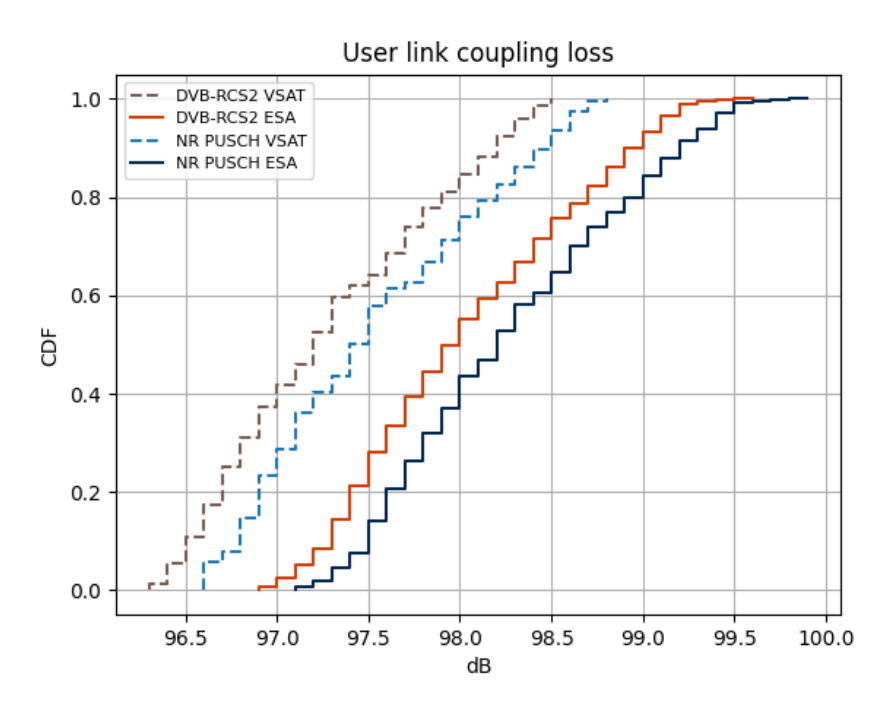
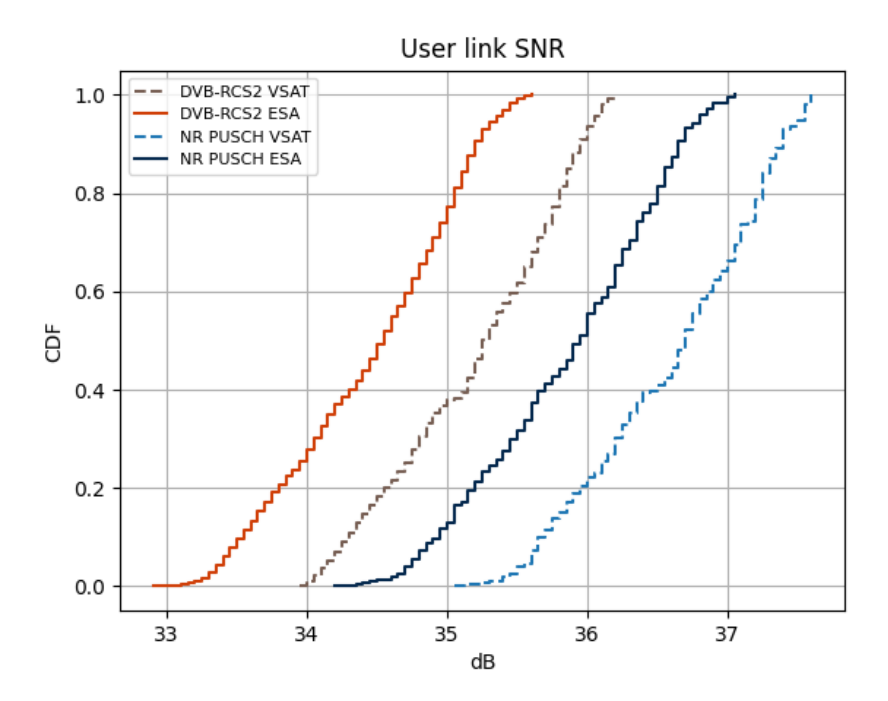


Figure 41. User link coupling loss, DVB-RCS2 vs. NR PUSCH, 97.5% Doppler compensation.



Figure~42.~User~link~SNR,~DVB-RCS2~vs.~NR~PUSCH,~97.5%~Doppler~compensation.





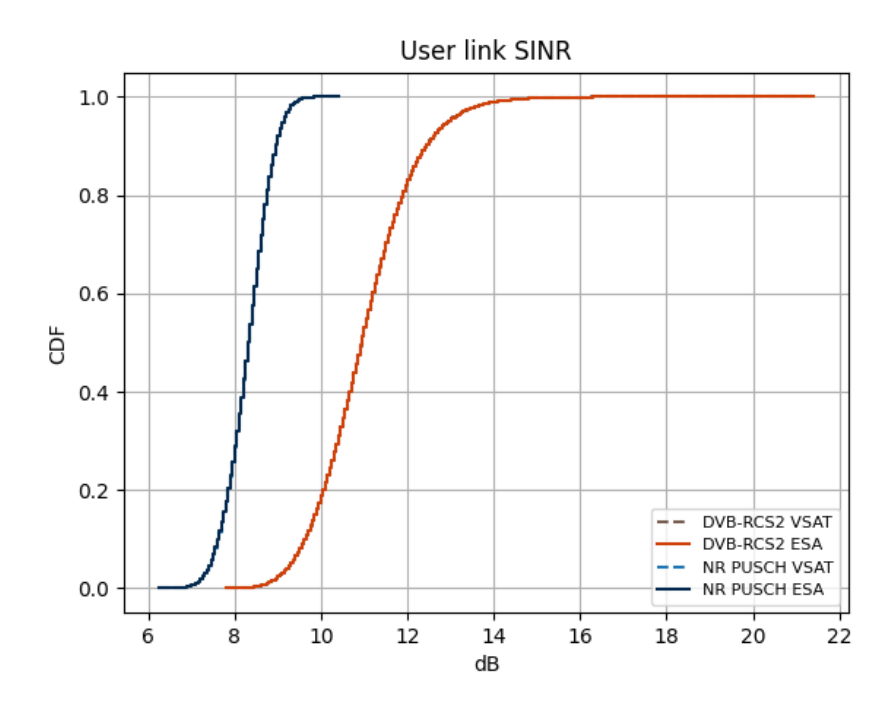


Figure 43. User link SINR, DVB-RCS2 vs. NR PUSCH, 97.5% Doppler compensation.

The performance of the technologies is presented with user- and system throughput, and system spectral efficiency in Figure 44, Figure 45 and Figure 46, respectively. User and system throughput are comparable across technologies, with NR PUSCH exhibiting a slight advantage. The MCS/MODCOD spectral efficiency is presented in Figure 47. While DVB-RCS2 achieves higher spectral efficiency per utilized MCS/MODCOD, NR PUSCH attains greater throughput due to reduced overhead and generally larger data payloads in NR TBs compared to the typical payload sizes of DVB-RCS2 waveforms. The realized FER/BLER of the comparison is presented in Figure 48.





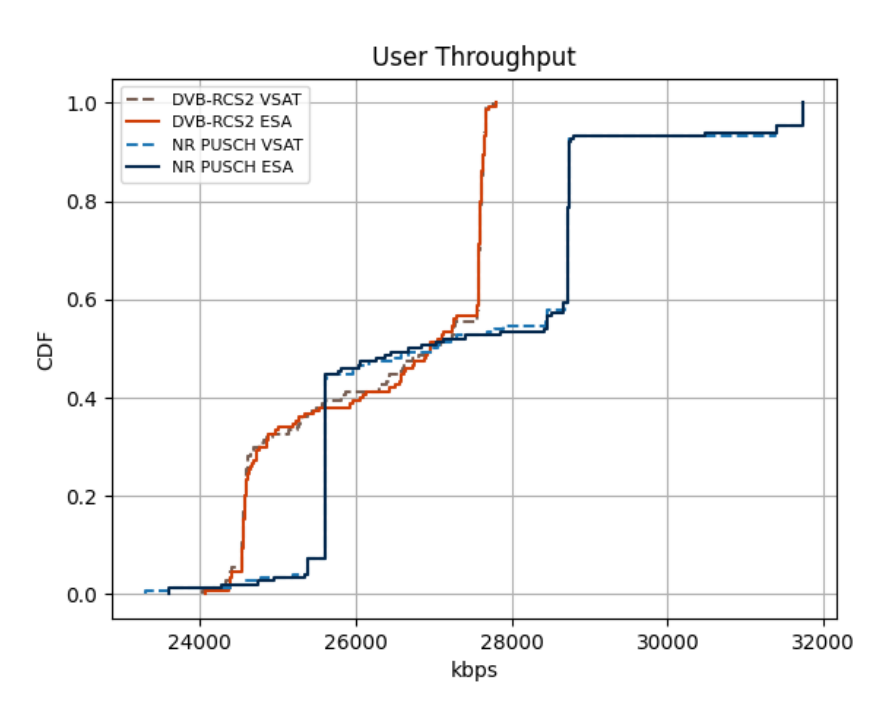
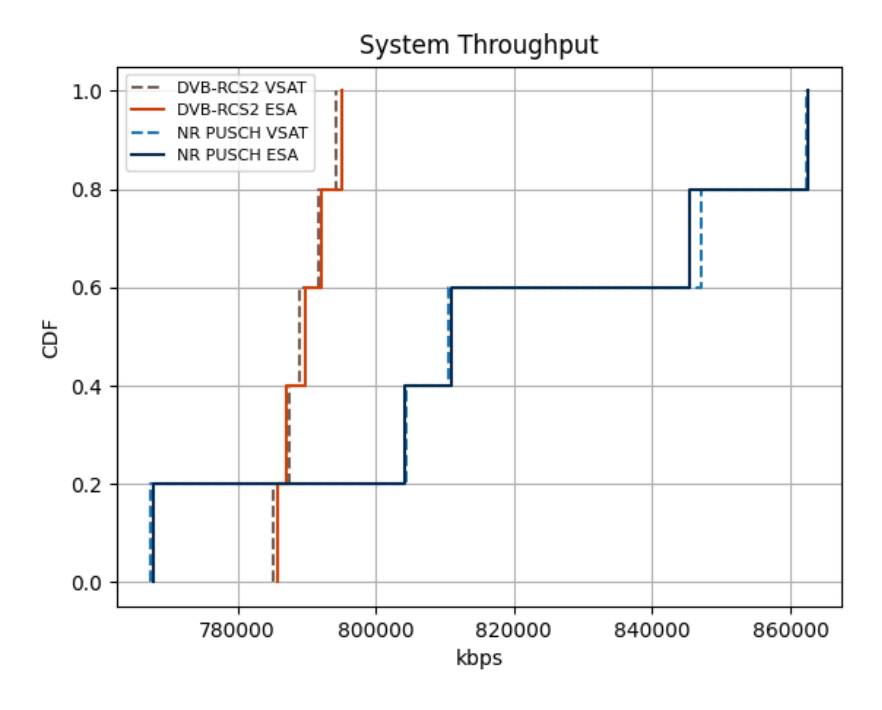


Figure 44. User throughput, DVB-RCS2 vs. NR PUSCH, 97.5% Doppler compensation.



Figure~45.~System~throughput,~DVB-RCS2~vs.~NR~PUSCH,~97.5%~Doppler~compensation.





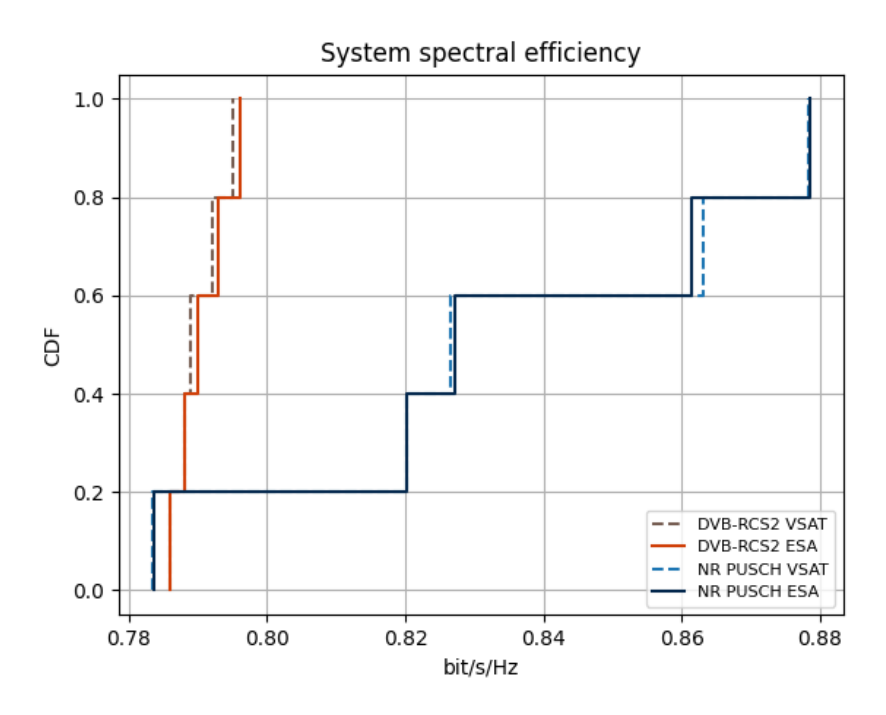


Figure 46. System spectral efficiency over 1 GHz, DVB-RCS2 vs. NR PUSCH, 97.5% Doppler compensation.

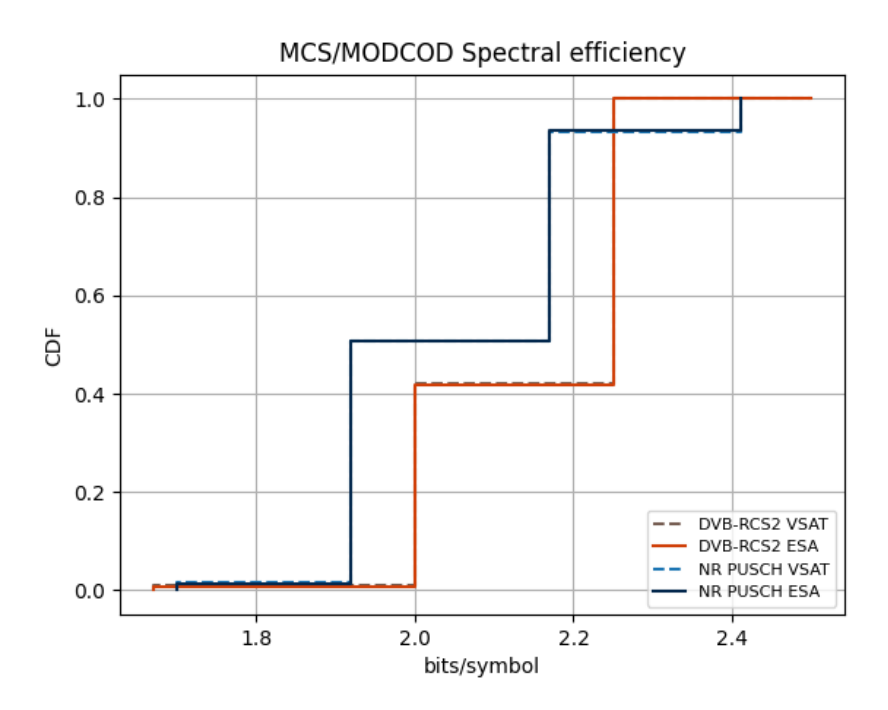


Figure 47. MCS/MODCOD spectral efficiency, DVB-RCS2 vs. NR PUSCH, 97.5% Doppler compensation.





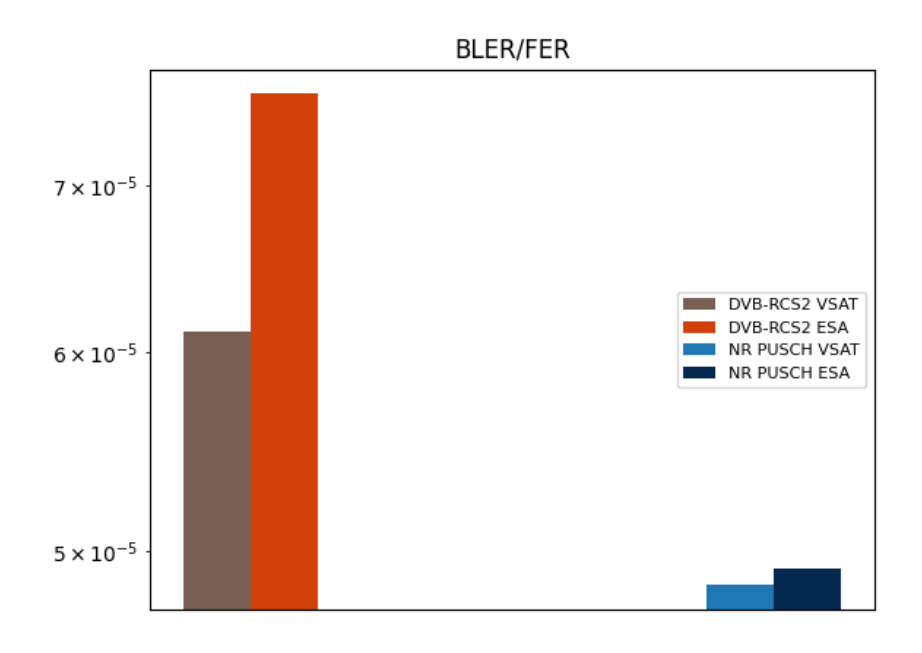


Figure 48. BLER/FER, DVB-RCS2 vs. NR PUSCH, 97.5% Doppler compensation.





4.3.2 Burst-mode DVB-S2X waveforms vs. NR PUSCH

The coupling loss, SNR and SINR results are presented in Figure 49, Figure 50 and Figure 51, respectively. The results showcase the same effects as in the previous section 4.3.1.

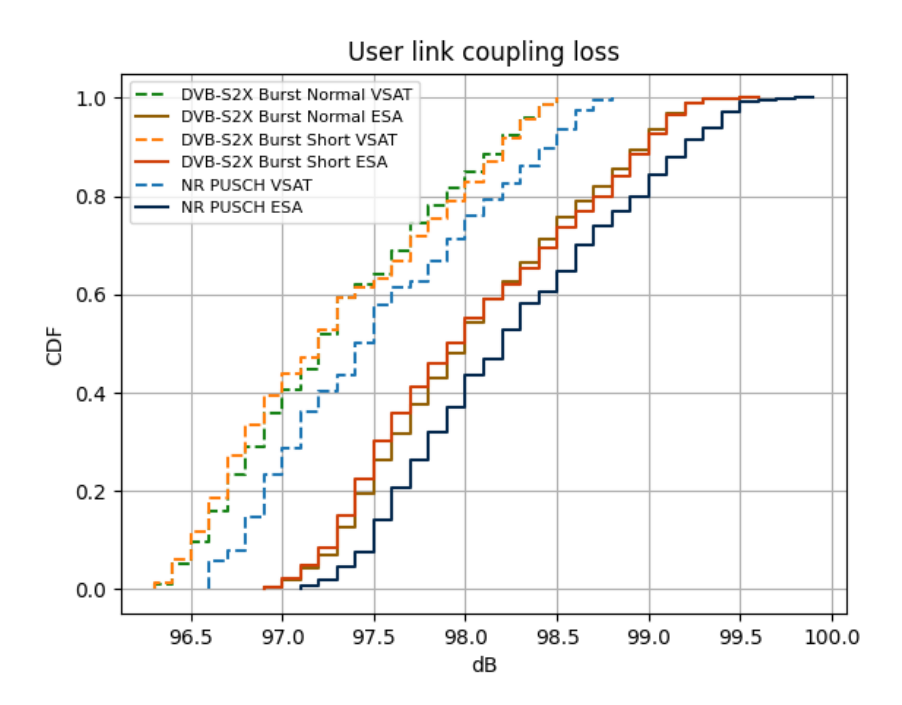


Figure 49. User link coupling loss, DVB-S2X vs. NR PUSCH, 97.5% Doppler compensation.





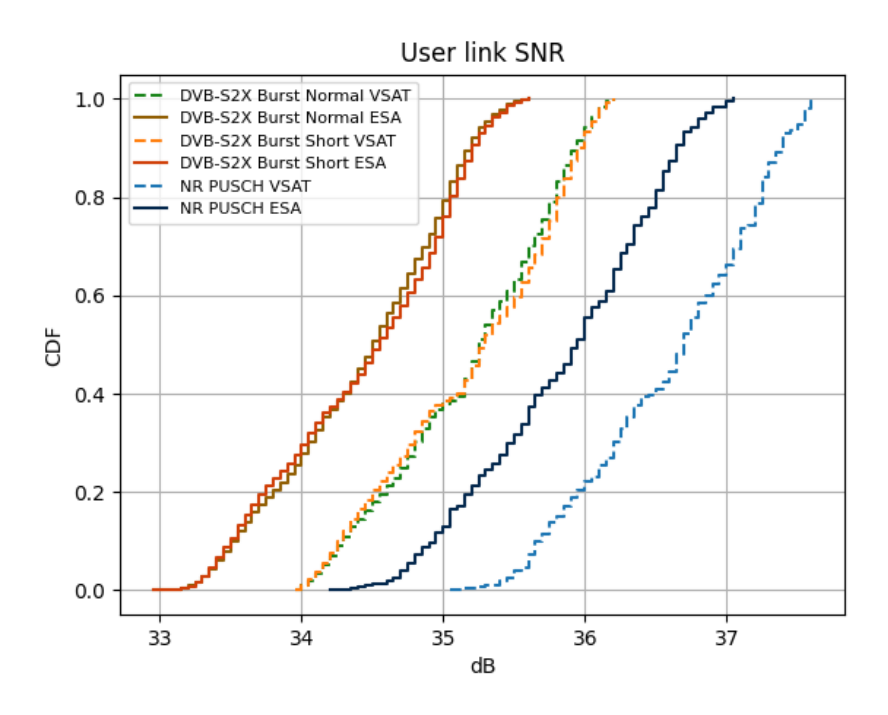


Figure 50. User link SNR, DVB-S2X vs. NR PUSCH, 97.5% Doppler compensation.

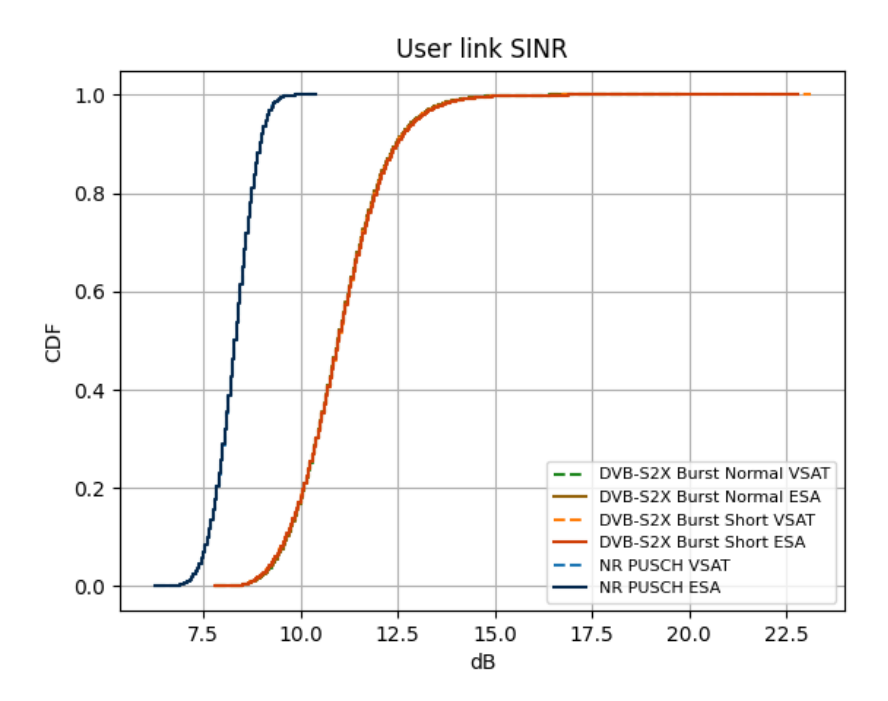


Figure 51. User link SINR, DVB-S2X vs. NR PUSCH, 97.5% Doppler compensation.

The performance of the technologies is presented with user- and system throughput, and system spectral efficiency in Figure 52, Figure 53 and Figure 54, respectively. The user throughput shows a noticeable gain in favor of DVB-S2X waveforms compared to NR PUSCH. The system level metrics align with user-level results, demonstrating higher performance for DVB-S2X waveforms in both





normal and short frame configurations. Normal frames achieve higher throughput due to reduced overhead compared to short frames. The MCS/MODCOD spectral efficiency distribution in Figure 55 shows a noticeable gain in spectral efficiency for DVB-S2X, also affecting the performance. The realized FER/BLER of the comparison is presented in Figure 56.

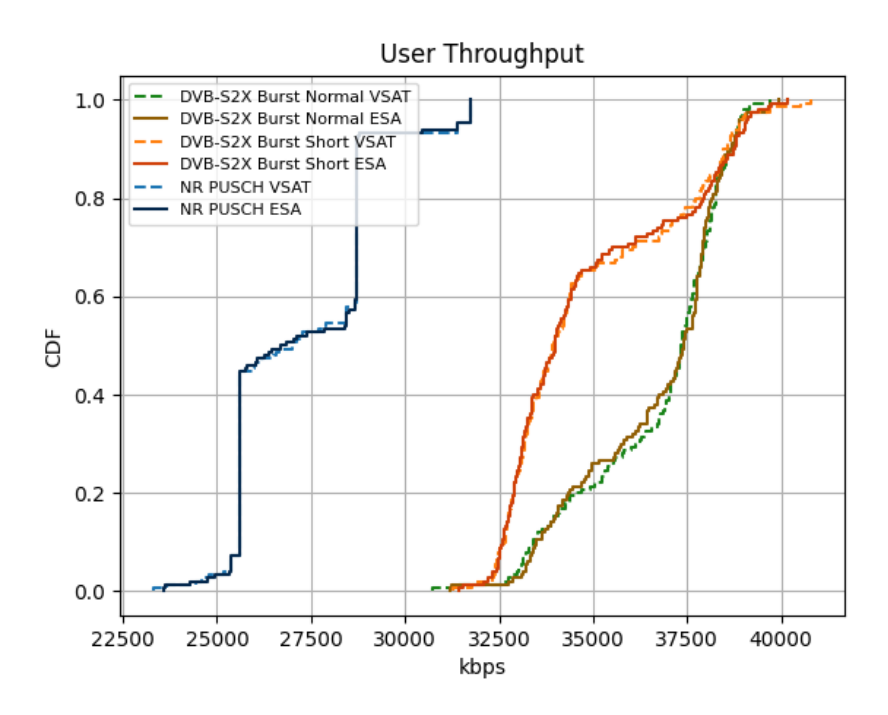


Figure 52. User throughput, DVB-S2X vs. NR PUSCH, 97.5% Doppler compensation.





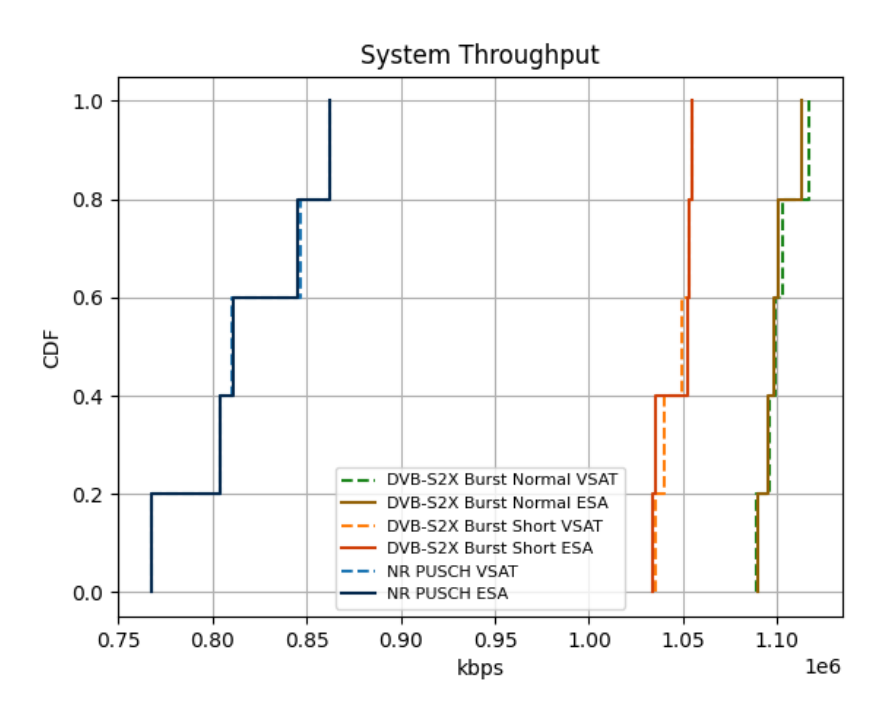
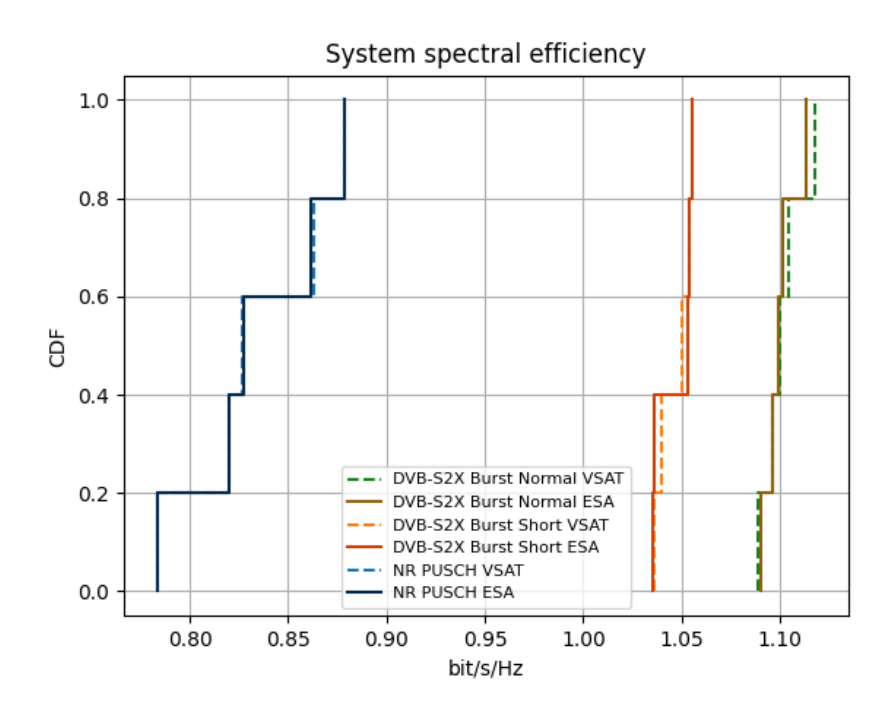


Figure 53. System throughput, DVB-S2X vs. NR PUSCH, 97.5% Doppler compensation.



Figure~54.~System~spectral~efficiency~over~1~GHz,~DVB-S2X~vs.~NR~PUSCH,~97.5%~Doppler~compensation.





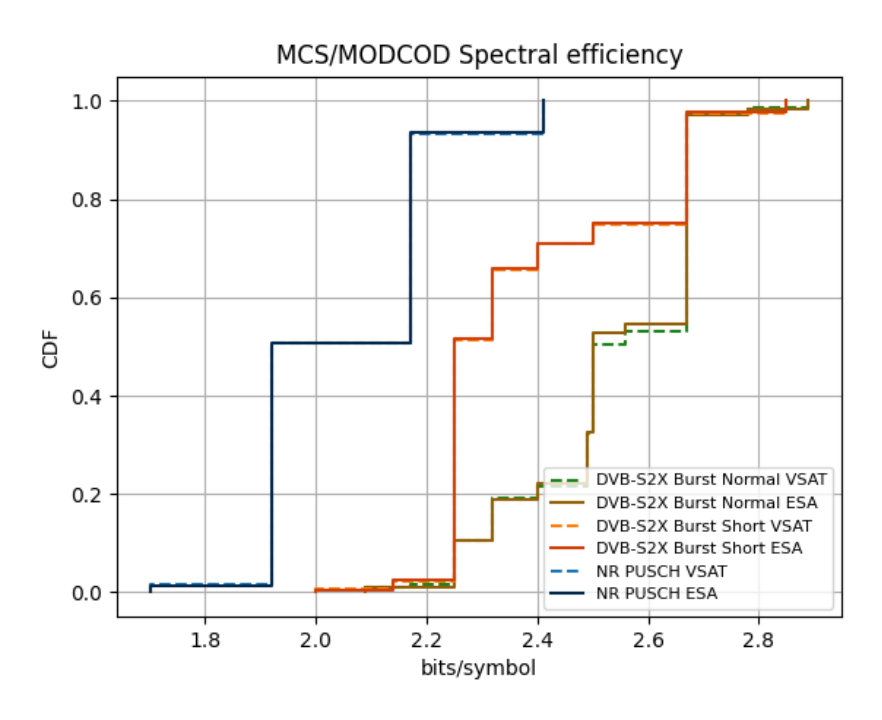


Figure 55. MCS/MODCOD spectral efficiency, DVB-S2X vs. NR PUSCH, 97.5% Doppler compensation.

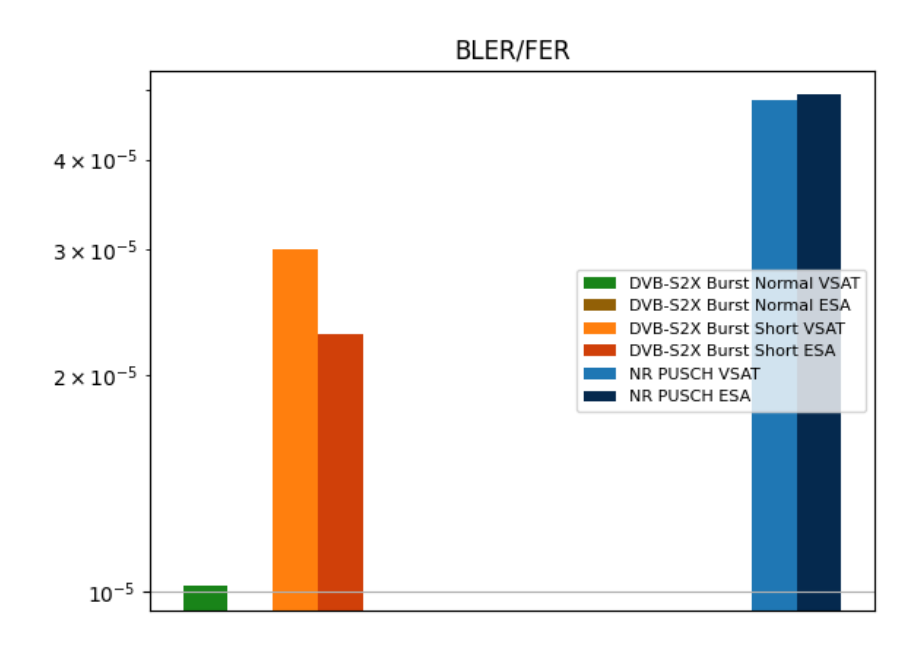


Figure 56. BLER/FER, DVB-S2X vs. NR PUSCH, 97.5% Doppler compensation.





4.3.3 Continuous carrier DVB-S2X waveforms vs. NR PUSCH

The coupling loss, SNR and SINR results are presented in Figure 57, Figure 58 and Figure 59, respectively. The results showcase the same effects as in previous two sections 4.3.1 and 4.3.2.

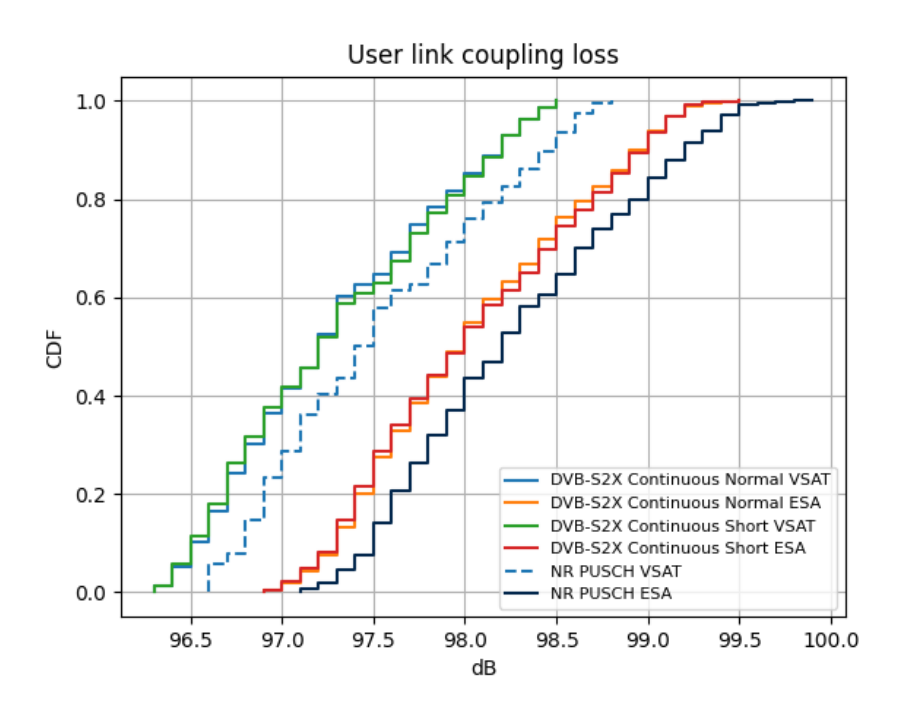


Figure 57. User link coupling loss, continuous DVB-S2X vs. NR PUSCH, 97.5% Doppler compensation.





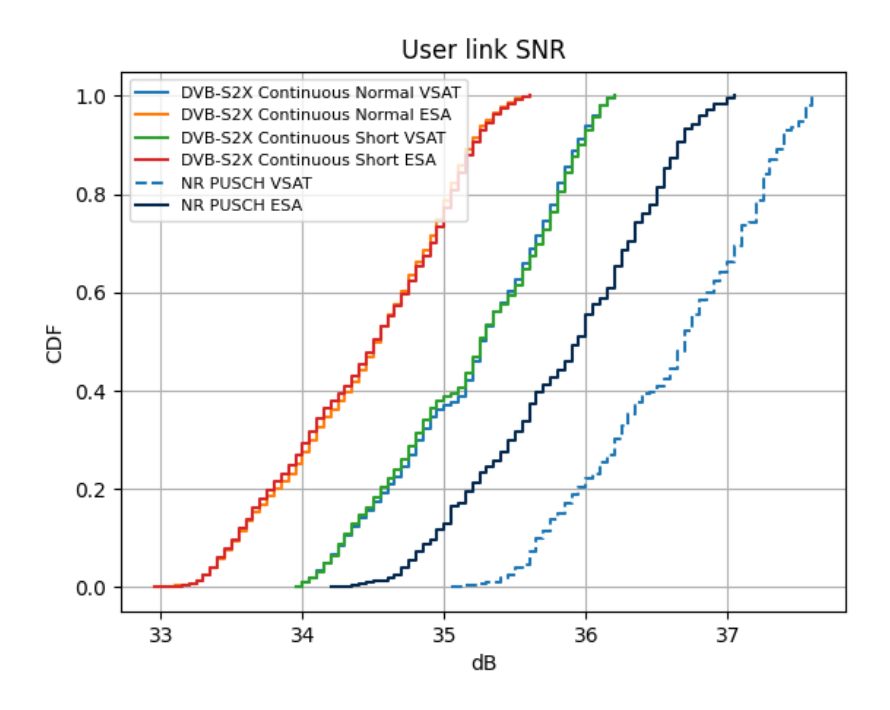


Figure 58. User link SNR, continuous DVB-S2X vs. NR PUSCH, 97.5% Doppler compensation.

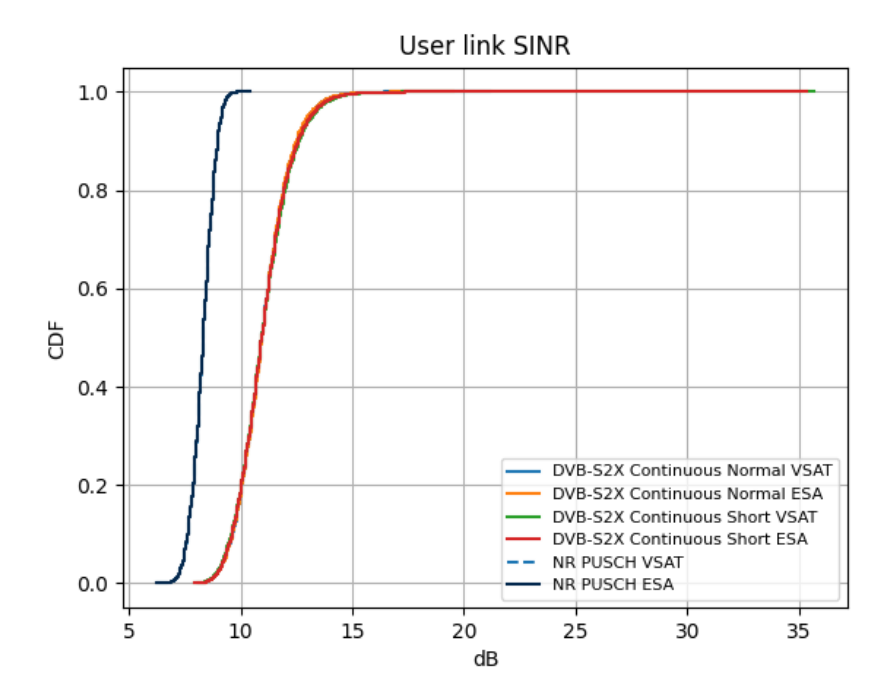


Figure 59. User link SINR, continuous DVB-S2X vs. NR PUSCH, 97.5% Doppler compensation.

The performance of the technologies is presented with user- and system throughput, and system spectral efficiency in Figure 60, Figure 61 and Figure 62, respectively. Similar to DVB-S2X burst mode





results in 4.3.2, the user throughput shows better performance for continuous mode DVB-S2X waveforms compared to NR PUSCH. The results show that DVB-S2X Normal frames achieve higher throughput due to the reduced overhead compared to Short frames. The realized FER/BLER of the comparison is presented in Figure 64. The MCS/MODCOD spectral efficiency is presented in Figure 63.

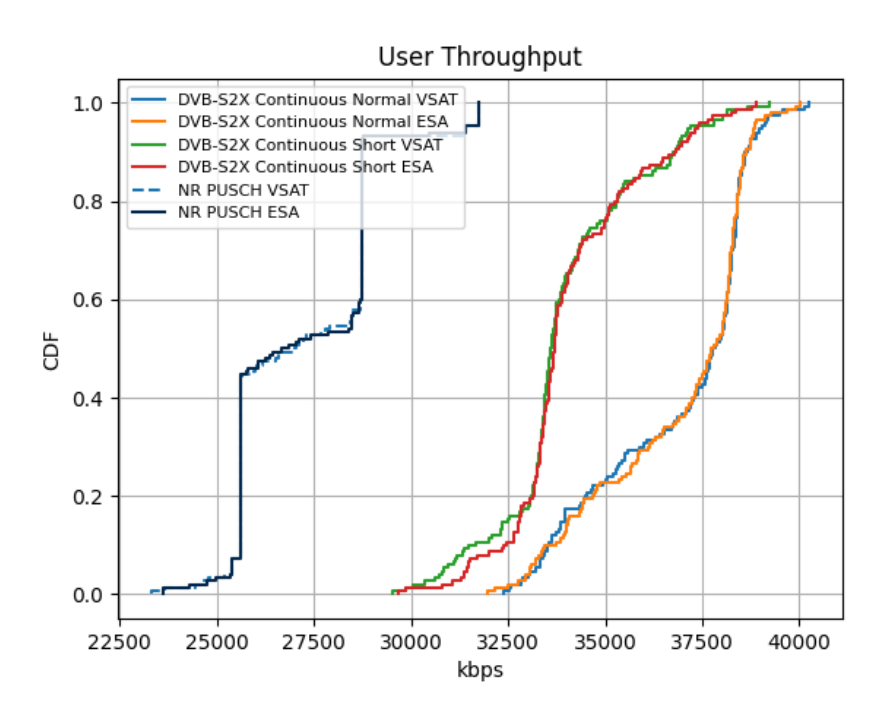


Figure 60. User throughput, continuous DVB-S2X vs. NR PUSCH, 97.5% Doppler compensation.

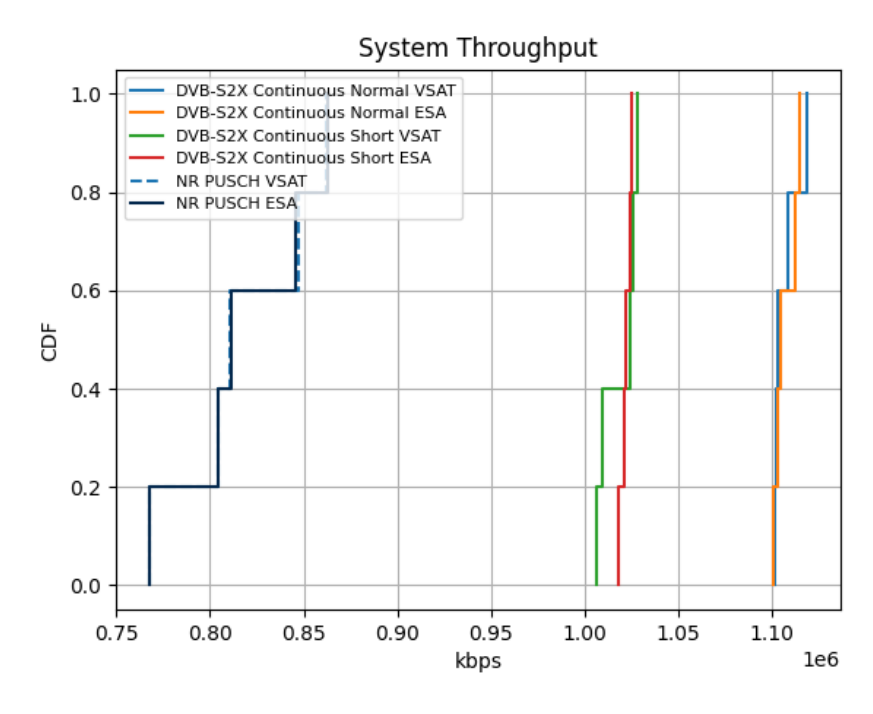


Figure 61. System throughput, continuous DVB-S2X vs. NR PUSCH, 97.5% Doppler compensation.

57





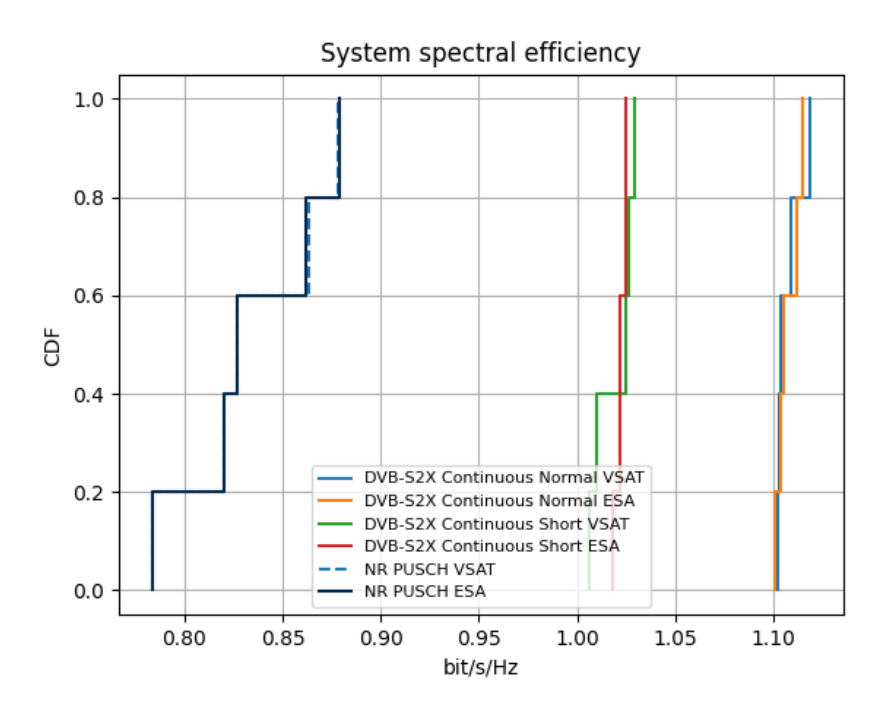


Figure 62. System spectral efficiency over 1 GHz, continuous DVB-S2X vs. NR PUSCH, 97.5% Doppler compensation.

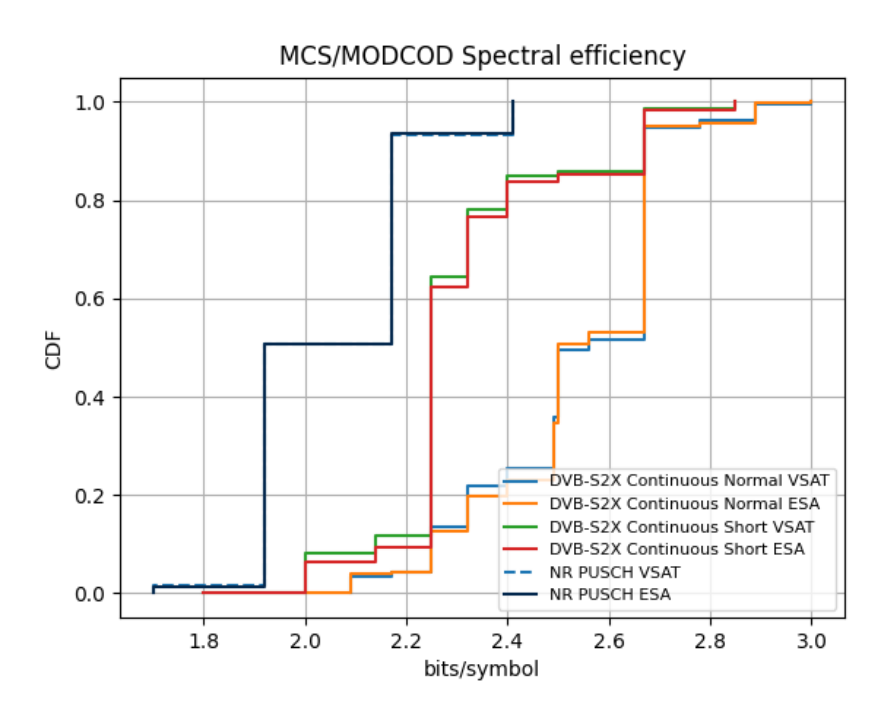


Figure 63. MCS/MODCOD spectral efficiency, continuous DVB-S2X vs. NR PUSCH, 97.5% Doppler compensation.





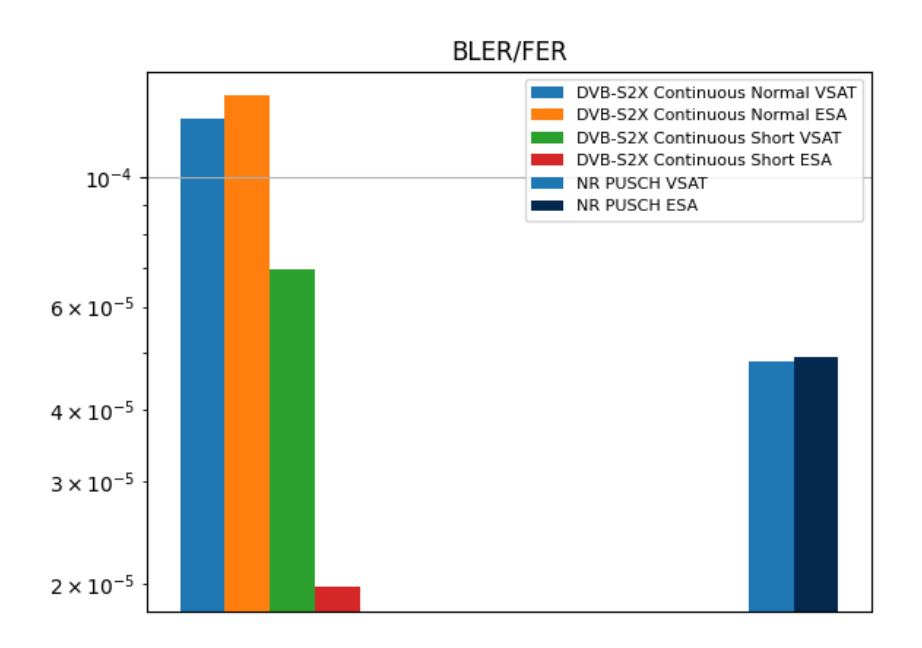


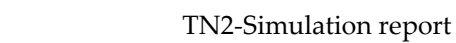
Figure 64. BLER/FER, continuous DVB-S2X vs. NR PUSCH, 97.5% Doppler compensation.

4.3.4 Summary

The technology comparison in 97.5% compensated Doppler conditions is summarised below in Table 7. The table shows an average throughput gain of around 35% for DVB-S2X Normal frames, compared to NR PUSCH, operating with both continuous carriers and bursts within the MF-TDMA structure. DVB-S2X Short frames provide comparatively slightly lower gain, around 25.5-28.5%. For DVB-RCS2 waveforms, a slight loss in gain is observed at around -3%, compared to NR PUSCH. The inclusion of ESA terminals causes minimal change to the results compared to conventional VSAT terminals.

97.5% Doppler compensation Tput 5th %-50th %-95th %-User tput average ile user ile user Antenna ile user Realized FER Scenario average gain type tput tput tput [kbps] over NR [kbps] [kbps] [kbps] **PUSCH** NR PUSCH 4.8437 E-05 25389 26991.4 31398.1 0 % 27276.615 VSAT DVB-RCS2 3.4544 E-04 24451.4 27243.9 27732.3 26429.758 -3.10 % 37282 39118.2 DVB-S2X, Normal 9.9680 E-06 32985.8 36699.503 34.55 %

Table 7. Summary table, 97.5% Doppler compensation.







	DVB-S2X, Short	2.6417 E-05	32437.1	33973.8	39261.1	35061.211	28.54 %
	Continuous carrier DVB-S2X, Normal	1.2684 E-04	33346.2	37941.4	38924.7	36948.005	35.46 %
	Continuous carrier DVB-S2X, Short	4.4556 E-05	31728.2	33644.3	37853.4	34258.309	25.60 %
ESA	NR PUSCH	4.9218 E-05	25389	26674.4	31398.1	27273.681	0 %
	DVB-RCS2	3.2409 E-04	24391.8	27253.7	27729.7	26414.054	-3.15 %
	DVB-S2X, Normal	0	32798	37392.4	39088.1	36695.197	34.54 %
	DVB-S2X, Short	4.3599 E-05	32493.7	33979.9	39458.2	35037.112	28.46 %
	Continuous carrier DVB-S2X, Normal	3.0543 E-04	33350.9	37881.8	39107.9	37053.55	35.86 %
	Continuous carrier DVB-S2X, Short	3.7216 E-05	31665.1	33686.3	37953	34256.616	25.60 %





4.4 DVB-RCS2 vs. NR NTN comparison results: Doppler compensation of GNSS terminal

In this section, the technologies are compared, assuming a 99.3% compensated Doppler, based on the minimum required compensation for this scenario to fulfil frequency error requirements for satellite terminals specified by 3GPP [31]. This limitation applies to the NR waveform of Orthogonal Frequency Division Multiplex (OFDM), which has much tighter frequency synchronization requirements than the single-carrier DVB. The comparison is split into 3 sections: DVB-RCS2 waveforms vs. NR PUSCH, DVB-S2X waveforms vs. NR PUSCH and continuous mode DVB-S2X vs. NR PUSCH. The simulation parameters specific to this comparison are given below in Table 8.

Table 8. Simulation specific parameters, 99.3% Doppler compensation.

Parameter	Value			
Doppler compensation	99.3%, according to section 2.3.1.			
ACM configuration	DVB-RCS2: 300ms minimum window			
	DVB-S2X Burst: 300ms minimum window &			
	0.6/0.4 dB ACM offset for Normal/Short frames			
	DVB-S2X Continuous: 400ms minimum window			
	& 1 dB ACM offset			
	NR PUSCH: 5ms average window			
UT type	VSAT vs. ESA			

4.4.1 DVB-RCS2 waveforms vs. NR PUSCH

The coupling loss, SNR and SINR results are presented in Figure 65, Figure 66 and Figure 67, respectively. The coupling loss has negligible differences between technologies, mainly due to the Doppler shift in received frequency. The effect of the Doppler shift is more pronounced in NR due to the physical waveform of NR being more susceptible to the error in frequency. Additionally, the coupling loss shows the effect of scanning loss when using ESAs. The SNR shows lower total noise for NR compared to DVB-RCS2. This is caused by the fact that the DVB waveform after filtering contains additional noise from the roll-off frequency bands, whereas the NR waveform does not. The SINR is noticeably higher for DVB- RCS2 compared to NR due to the ICI, caused by Doppler. However, the observed SINR for NR is now better than with worse Doppler compensation (presented in section 4.3.1), as is to be expected.





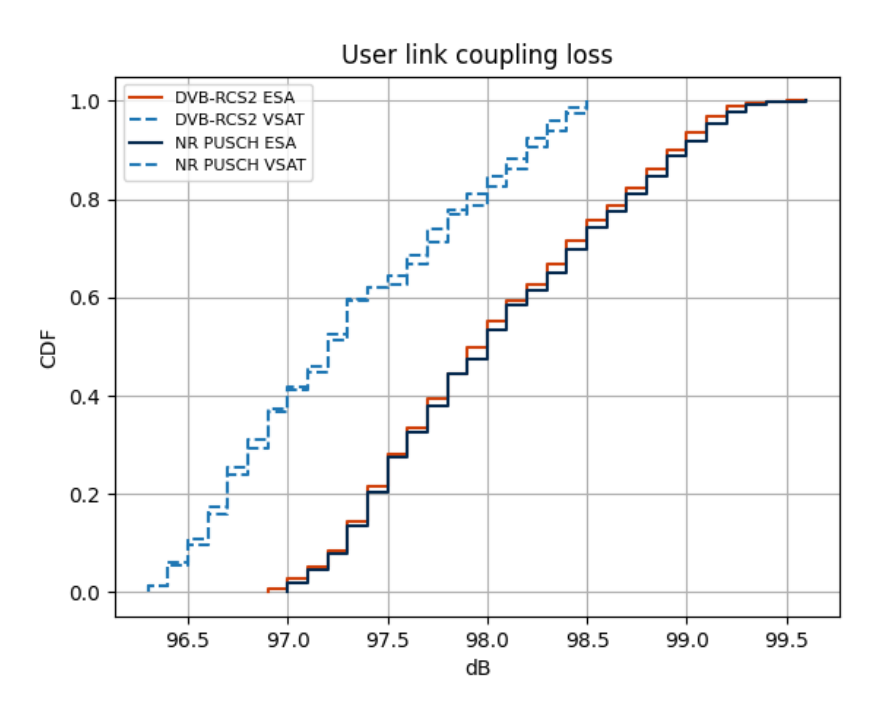


Figure 65. User link coupling loss, DVB-RCS2 vs. NR PUSCH, 99.3% Doppler compensation.

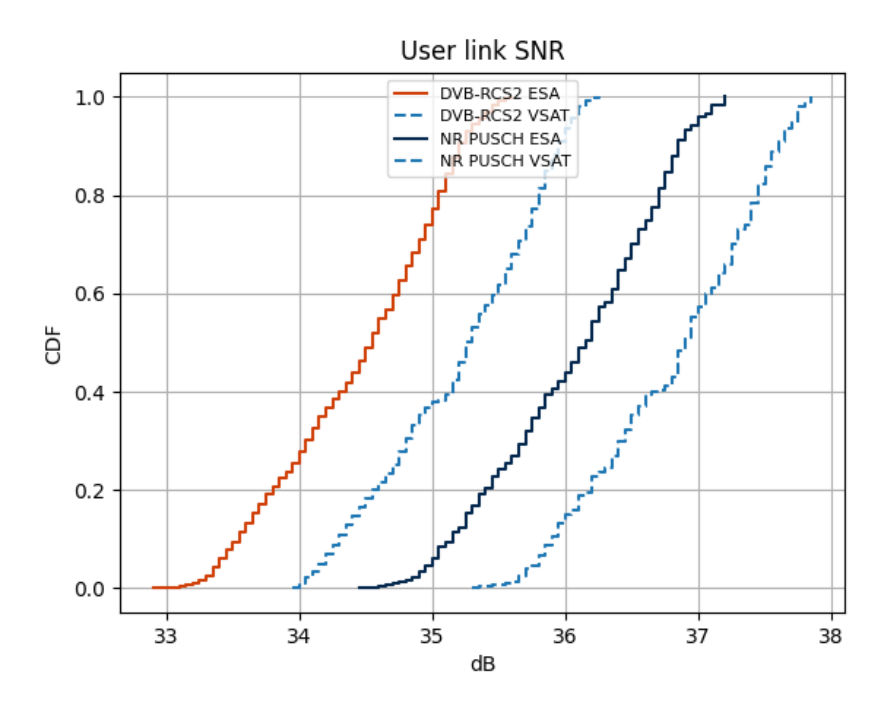


Figure 66. User link SNR, DVB-RCS2 vs. NR PUSCH, 99.3% Doppler compensation.





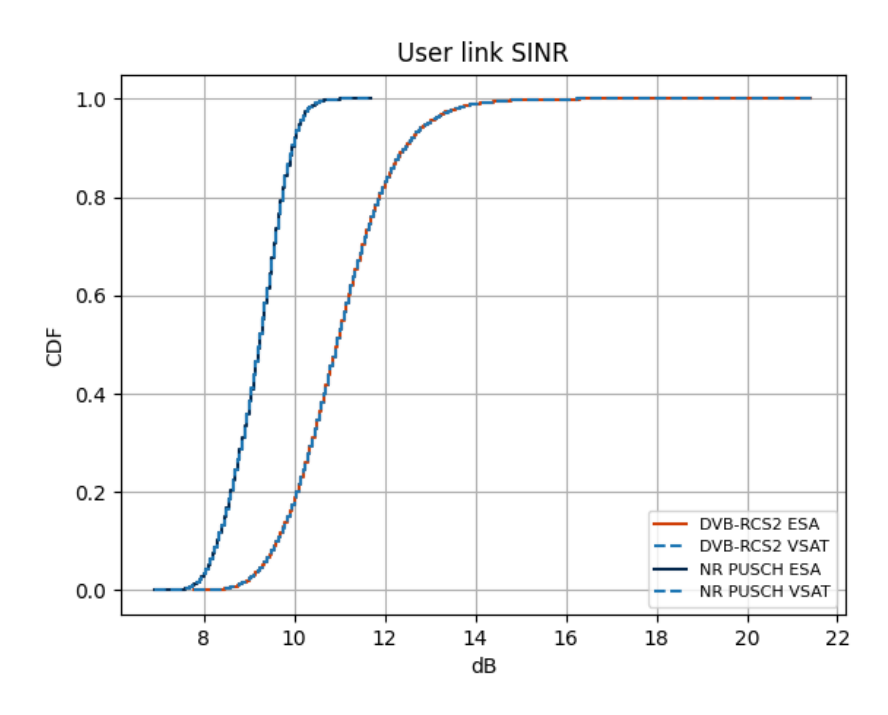


Figure 67. User link SINR, DVB-RCS2 vs. NR PUSCH, 99.3% Doppler compensation.





The performance of the technologies is presented with user- and system throughput, and system spectral efficiency (over 1 GHz) in Figure 68, Figure 69 and Figure 70, respectively. The throughput performance is noticeably better for NR. Compared to the previous section 4.3.1, it can be observed that with better alignment in frequency, NR experiences a notable performance gain, while DVB-RCS2 does not. The system level results reflect the user-level results. The MCS/MODCOD spectral efficiency distribution is presented in Figure 71, where it can be observed that the spectral efficiency per transmission is generally better for NR, resulting from the decreased error in frequency alignment and consequently better SINR. The realized FER/BLER of the comparison is presented in Figure 72.

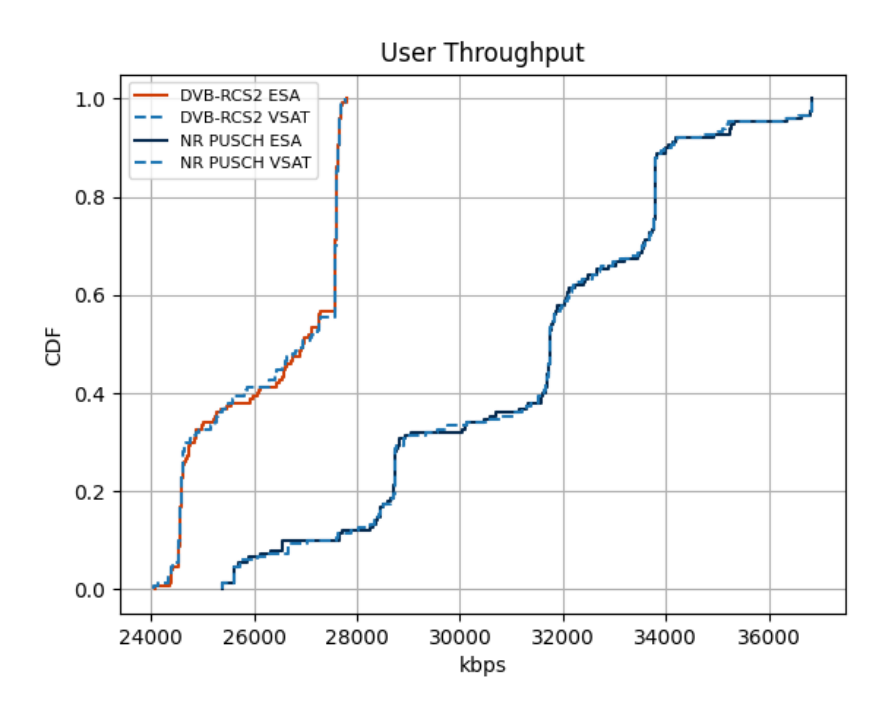


Figure 68. User throughput, DVB-RCS2 vs. NR PUSCH, 99.3% Doppler compensation.





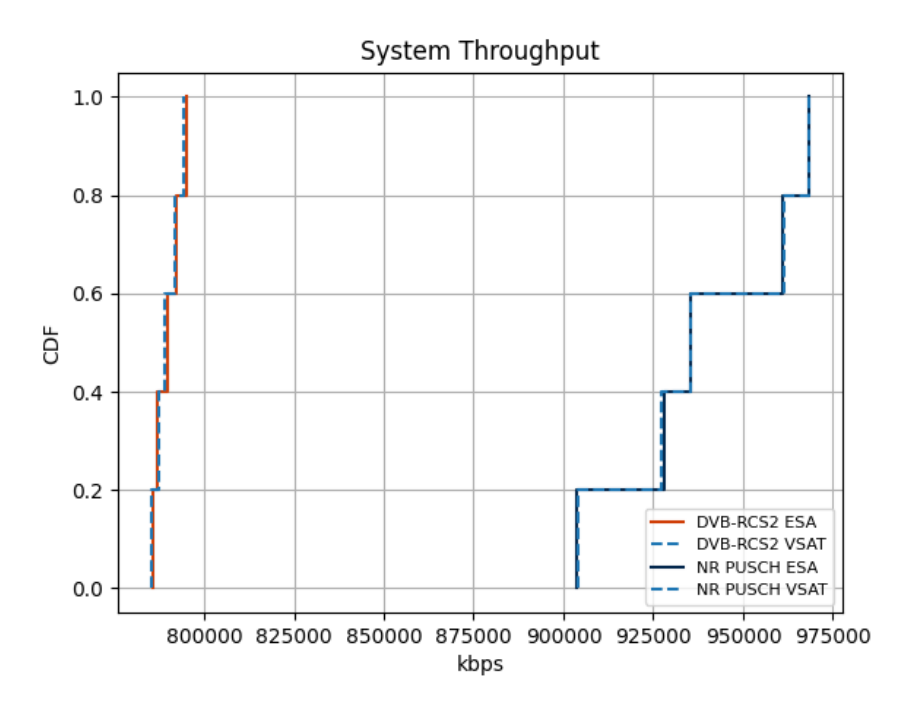
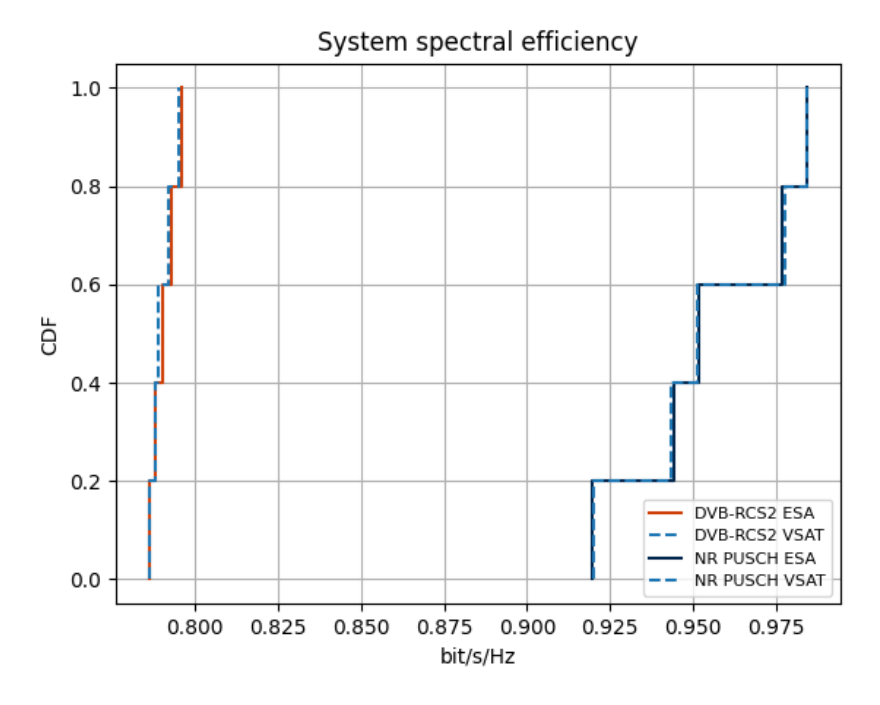


Figure 69. System throughput, DVB-RCS2 vs. NR PUSCH, 99.3% Doppler compensation.



Figure~70.~System~spectral~efficiency~over~1~GHz,~DVB-RCS2~vs.~NR~PUSCH,~99.3%~Doppler~compensation.





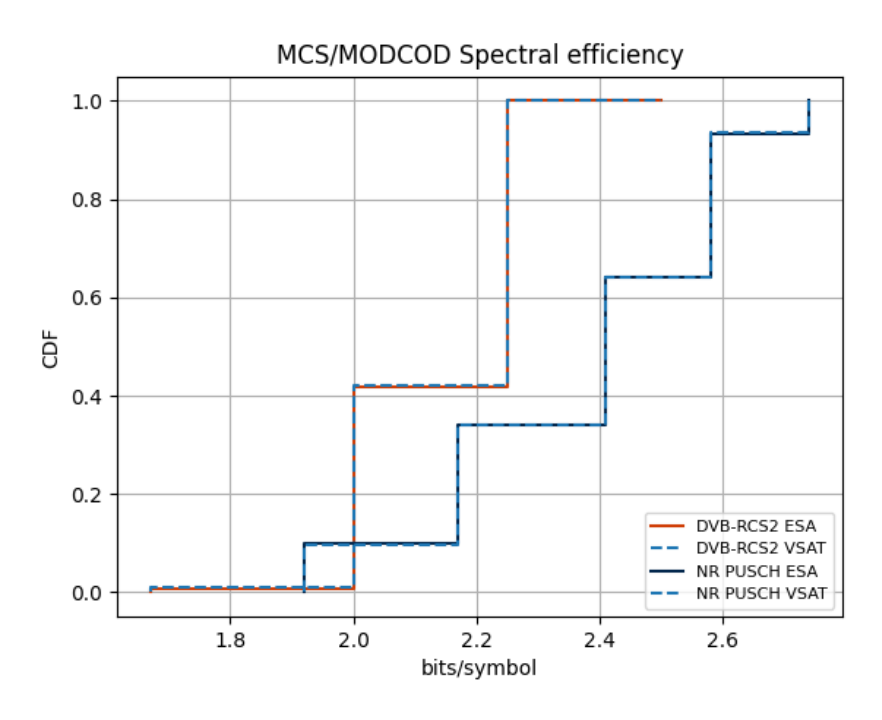


Figure 71. MCS/MODCOD spectral efficiency, DVB-RCS2 vs. NR PUSCH, 99.3% Doppler compensation.

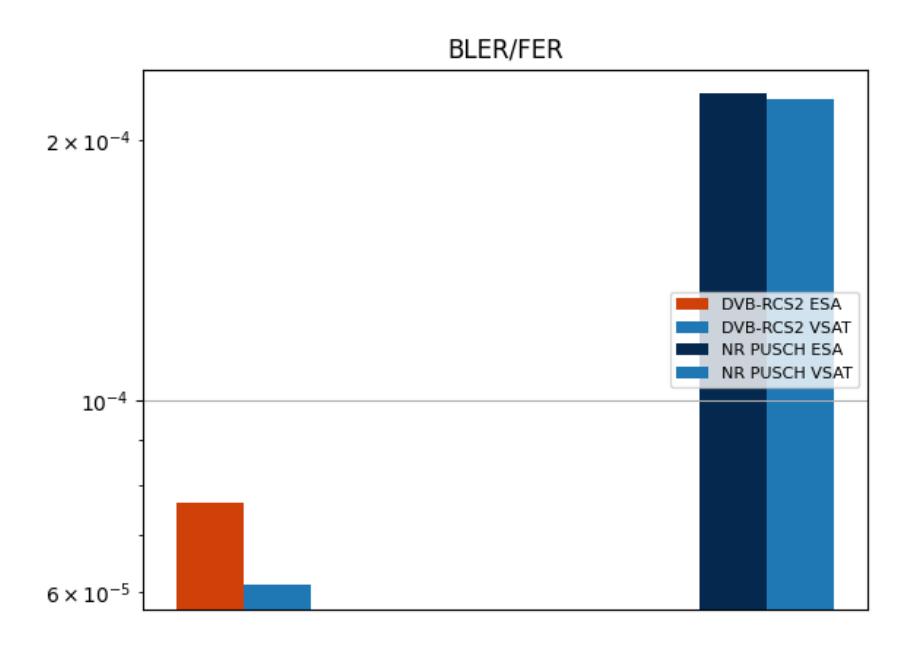


Figure 72. BLER/FER, DVB-RCS2 vs. NR PUSCH, 99.3% Doppler compensation.





4.4.2 Burst-mode DVB-S2X waveforms vs. NR PUSCH

The coupling loss, SNR and SINR results are presented in Figure 73, Figure 74 and Figure 75, respectively. The results are effectively almost identical with the previous section (4.4.1), for further analysis, refer there.

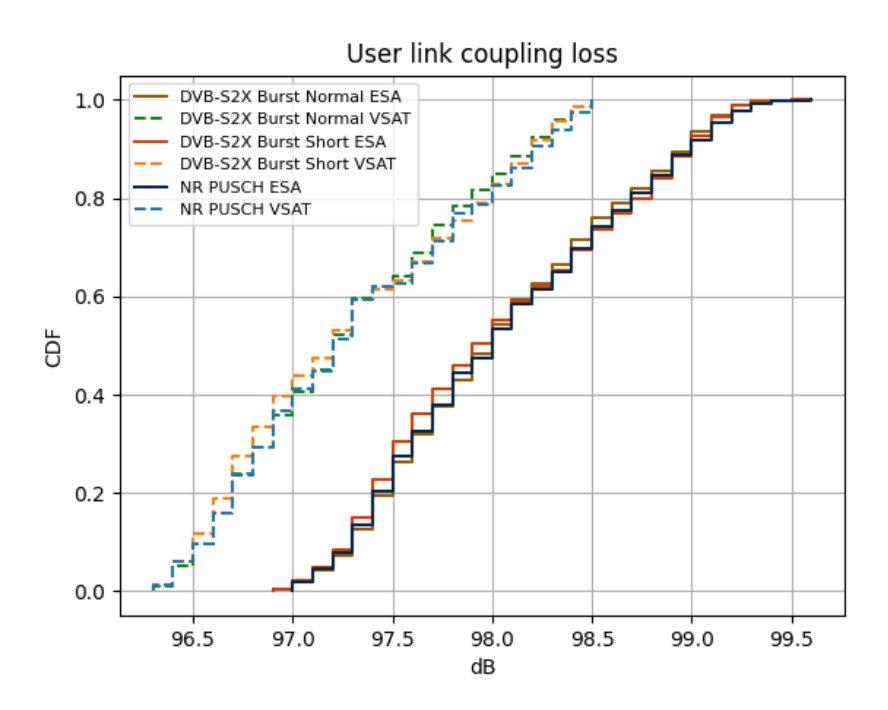


Figure 73. User link coupling loss, DVB-S2X vs. NR PUSCH, 99.3% Doppler compensation.





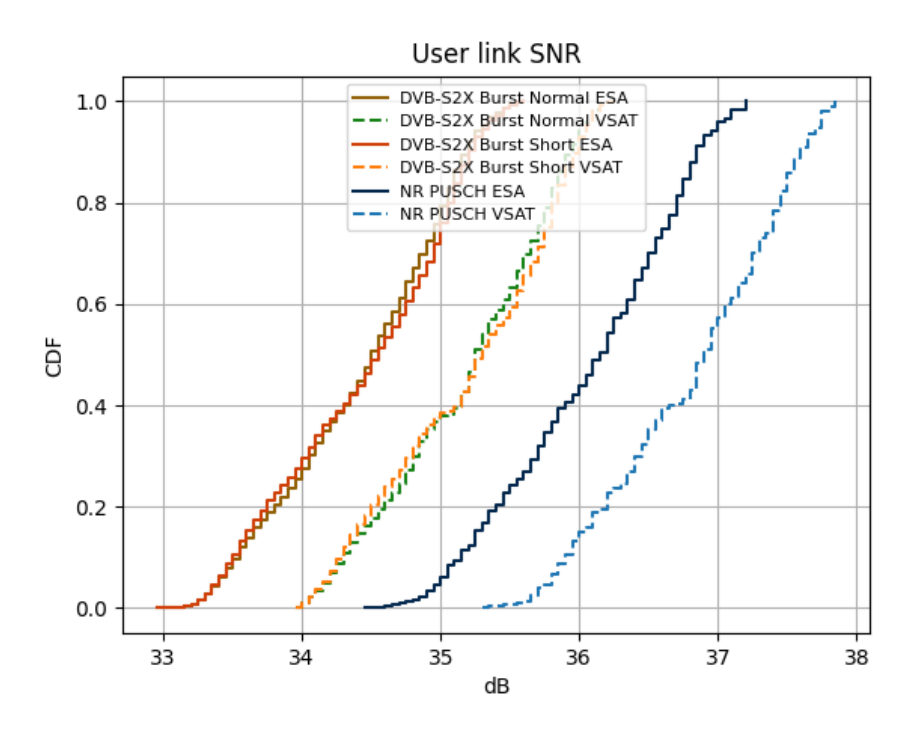


Figure 74. User link SNR, DVB-S2X vs. NR PUSCH, 99.3% Doppler compensation.

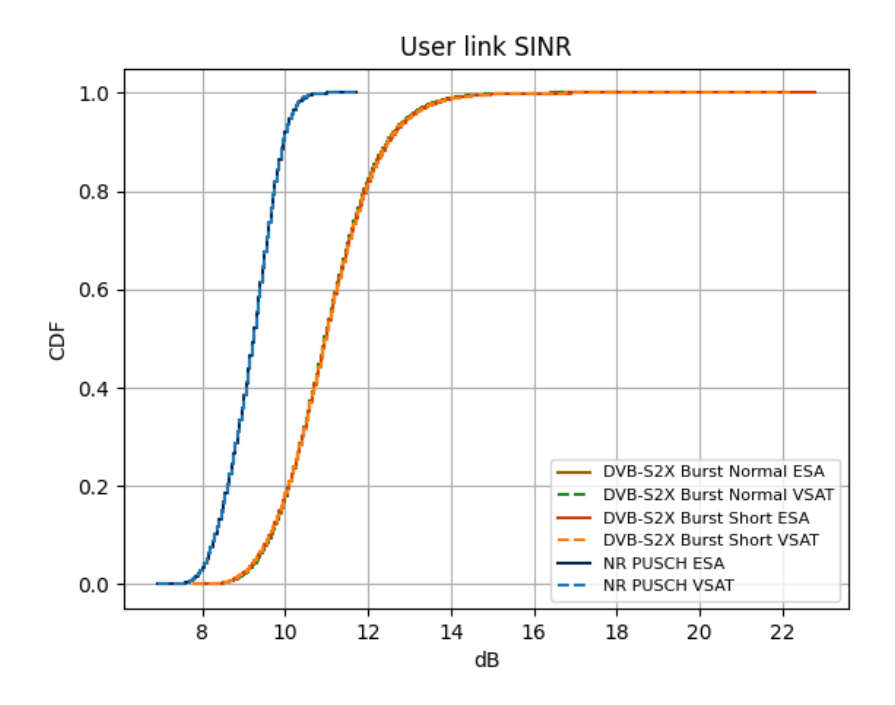
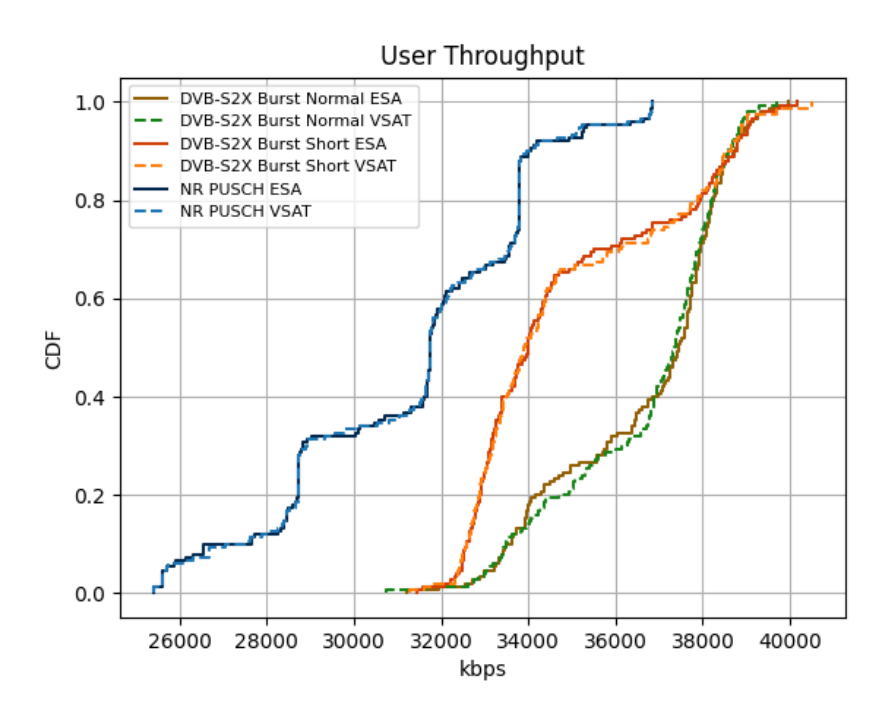


Figure 75. User link SINR, DVB-S2X vs. NR PUSCH, 99.3% Doppler compensation.





The performance of the technologies is presented with user- and system throughput, and system spectral efficiency (over 1 GHz) in Figure 76, Figure 77 and Figure 78, respectively. The throughput performance is noticeably better for DVB-S2X. Compared to the previous section 4.3.2, it can be observed that with better alignment in frequency, NR experiences a notable performance gain. However, the lower overhead of the DVB-S2X frames still provides higher overall performance. The system level results reflect the user-level results. The MCS/MODCOD spectral efficiency distribution is presented in Figure 79, where it can be observed that the spectral efficiency per transmission is generally better for NR, resulting from the decreased error in frequency alignment and consequently better SINR. DVB-S2X uses slightly less efficient MODCODs, caused by the robust ACM. The realized FER/BLER of the comparison is presented in Figure 80.



Figure~76.~User~throughput,~DVB-S2X~vs.~NR~PUSCH,~99.3%~Doppler~compensation.





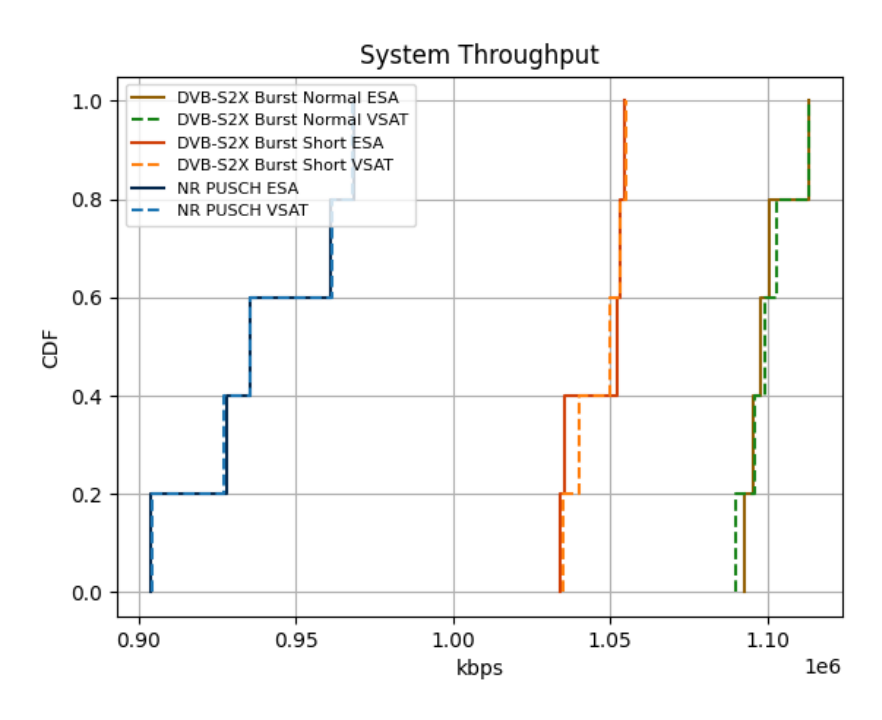
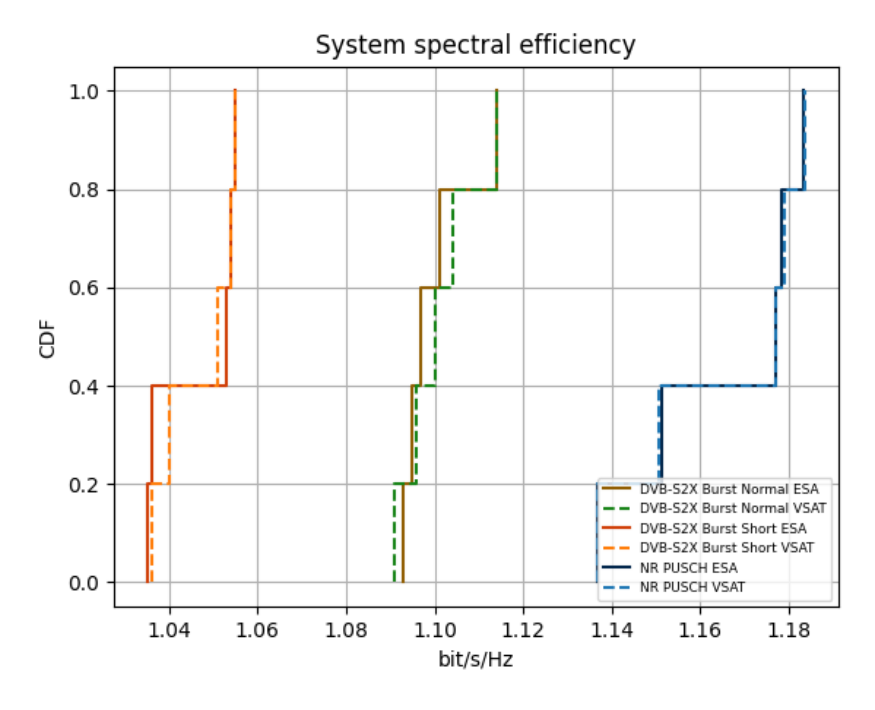


Figure 77. System throughput, DVB-S2X vs. NR PUSCH, 99.3% Doppler compensation.



Figure~78.~System~spectral~efficiency,~DVB-S2X~vs.~NR~PUSCH,~99.3%~Doppler~compensation.





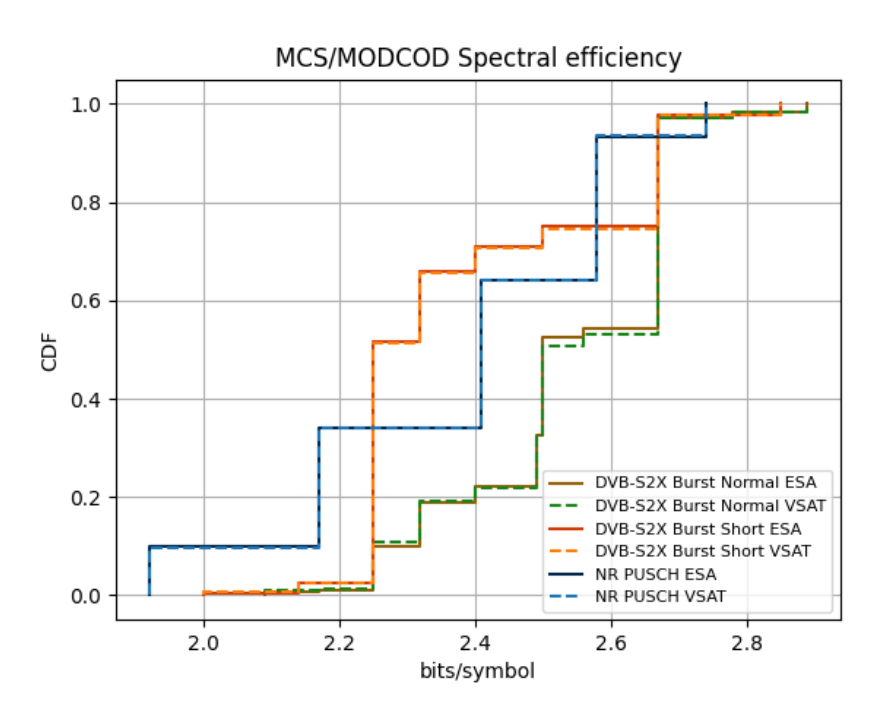


Figure 79. MCS/MODCOD spectral efficiency, DVB-S2X vs. NR PUSCH, 99.3% Doppler compensation.

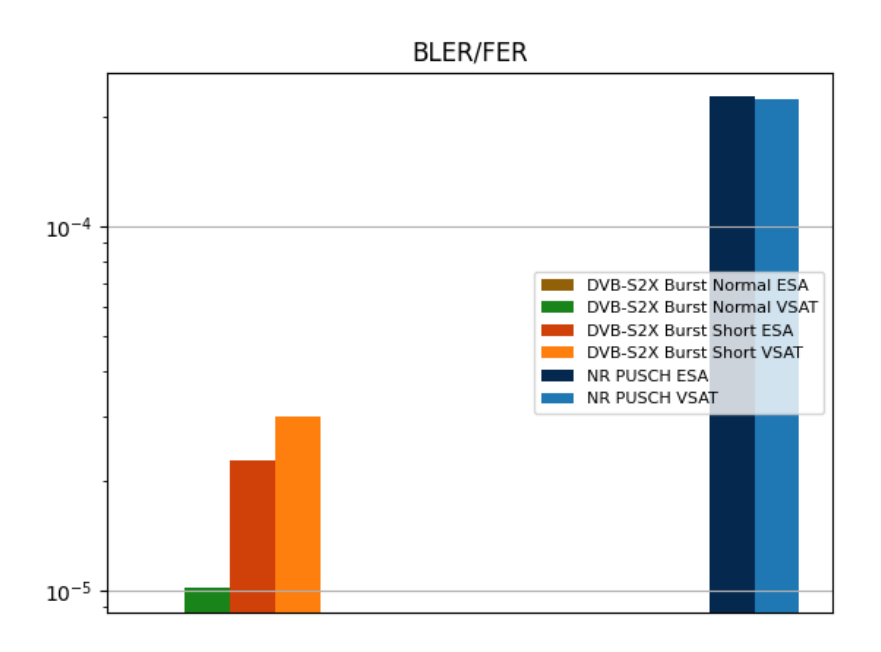


Figure 80. BLER/FER, DVB-S2X vs. NR PUSCH, 99.3% Doppler compensation.





4.4.3 Continuous carrier DVB-S2X waveforms vs. NR PUSCH

The coupling loss, SNR and SINR results are presented in Figure 81, Figure 82 and Figure 83, respectively. The results are effectively almost identical with the previous section (4.4.1), for further analysis, refer there.

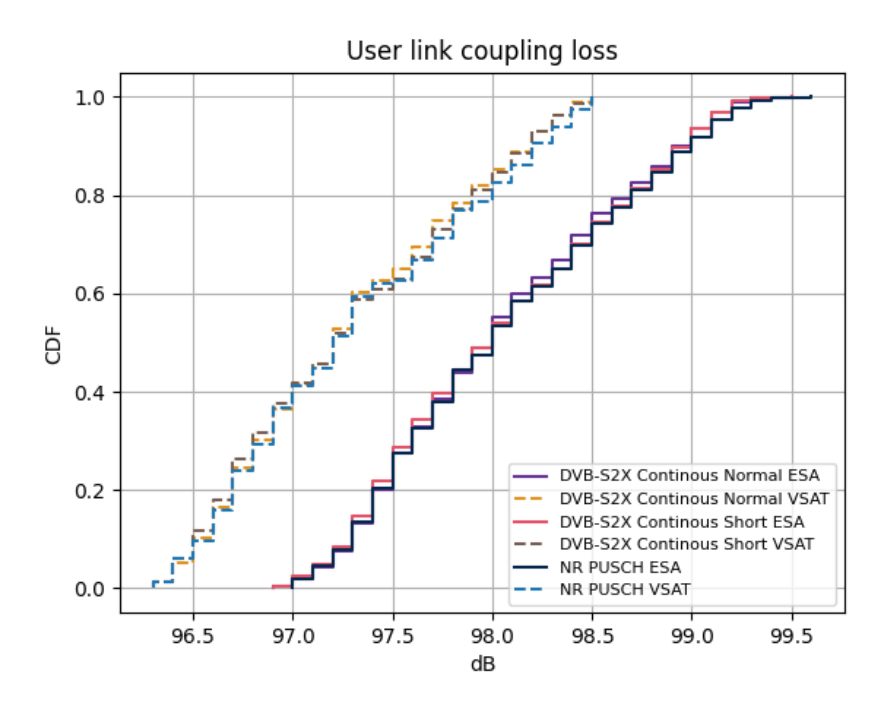


Figure 81. User link coupling loss, continuous DVB-S2X vs. NR PUSCH, 99.3% Doppler compensation.





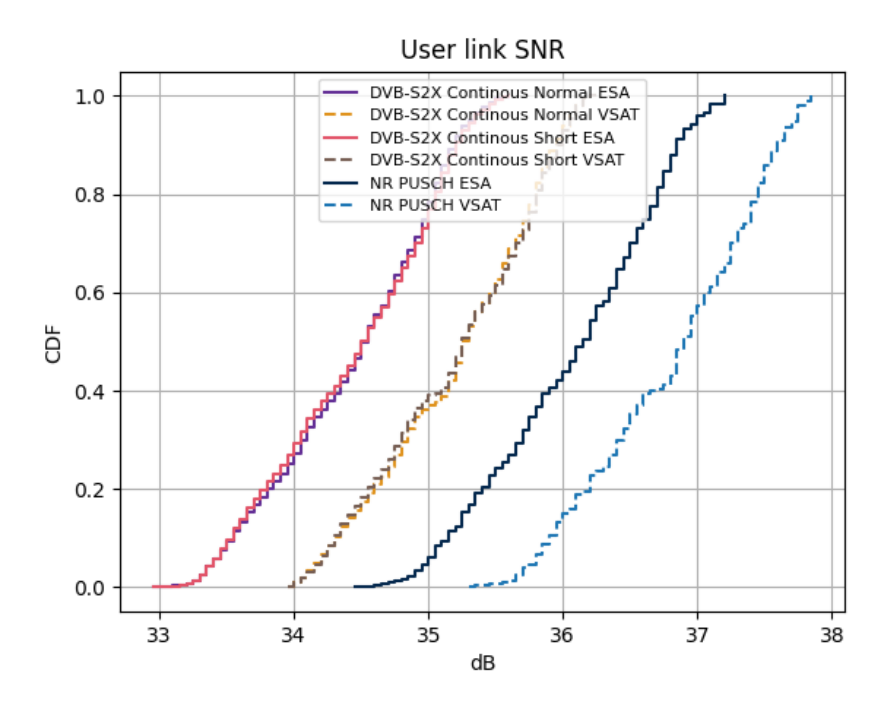


Figure 82. User link SNR, continuous DVB-S2X vs. NR PUSCH, 99.3% Doppler compensation.

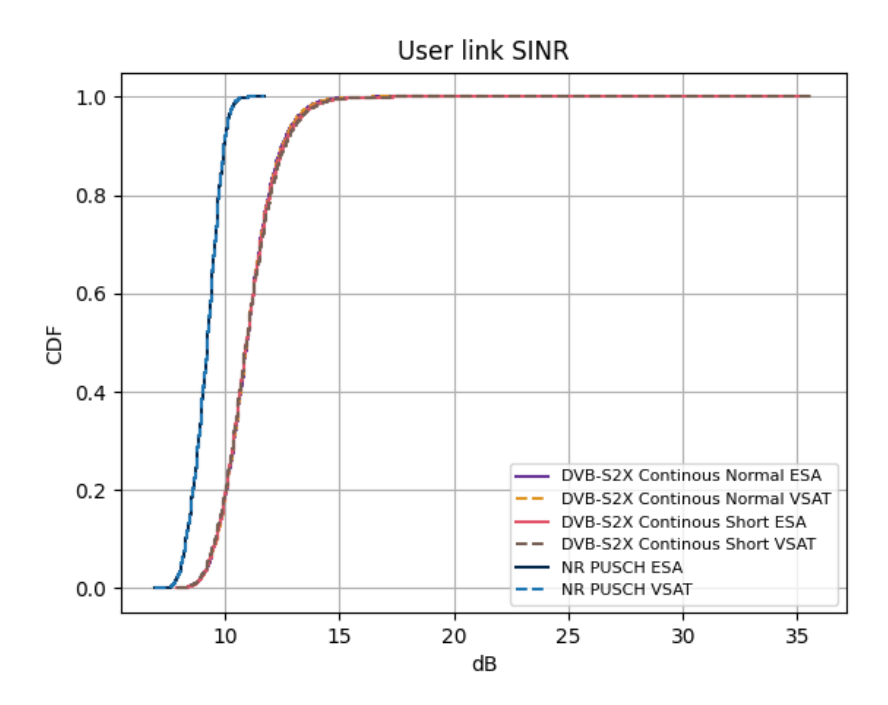


Figure 83. User link SINR, continuous DVB-S2X vs. NR PUSCH, 99.3% Doppler compensation.

The performance of the technologies is presented with user- and system throughput, and system spectral efficiency (over 1 GHz) in Figure 84, Figure 85 and Figure 86, respectively. The throughput performance is still noticeably better for DVB-S2X, reflecting the results for DVB-S2X bursts in section 4.4.2. The system level results reflect the user-level results. The MCS/MODCOD spectral efficiency





distribution is presented in Figure 87, where it can be observed that the spectral efficiency per transmission is generally better for NR, resulting from the decreased error in frequency alignment and consequently better SINR. DVB-S2X uses slightly less efficient MODCODs, caused by the robust ACM. The realized FER/BLER of the comparison is presented in Figure 88.

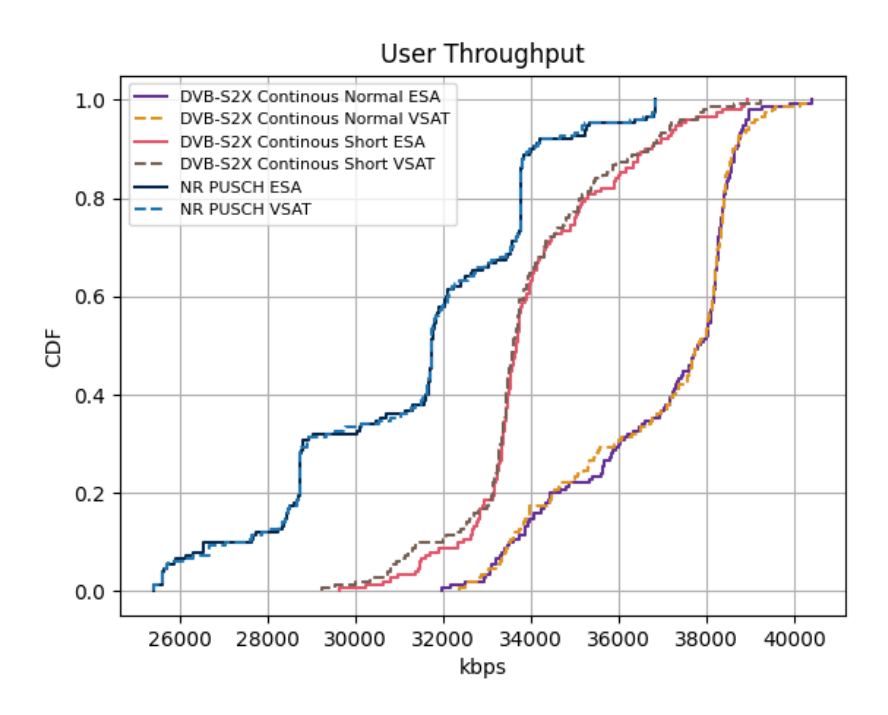


Figure 84. User throughput, continuous DVB-S2X vs. NR PUSCH, 99.3% Doppler compensation.





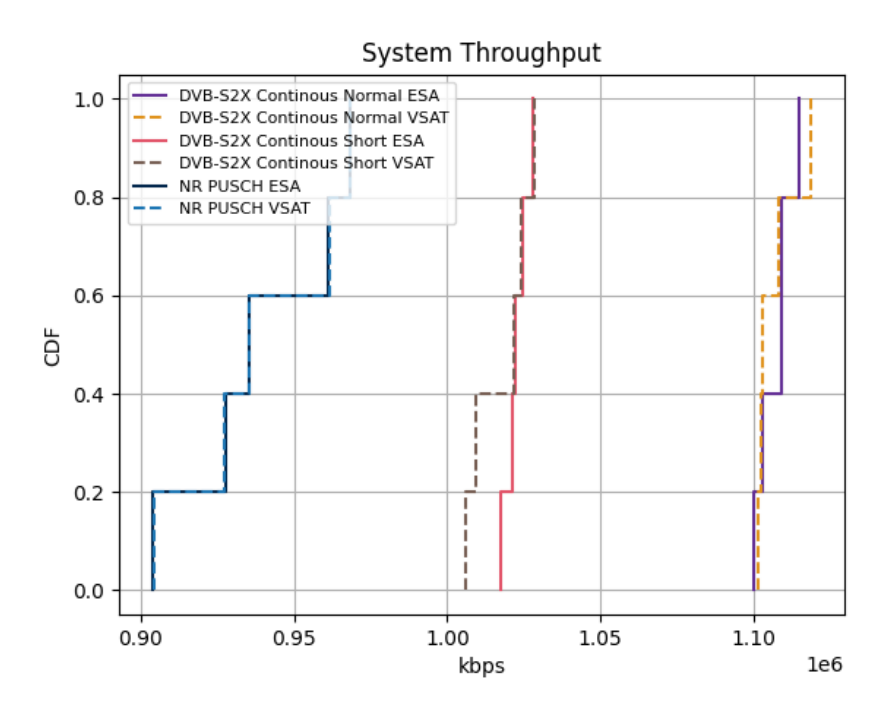


Figure 85. System throughput, continuous DVB-S2X vs. NR PUSCH, 99.3% Doppler compensation.

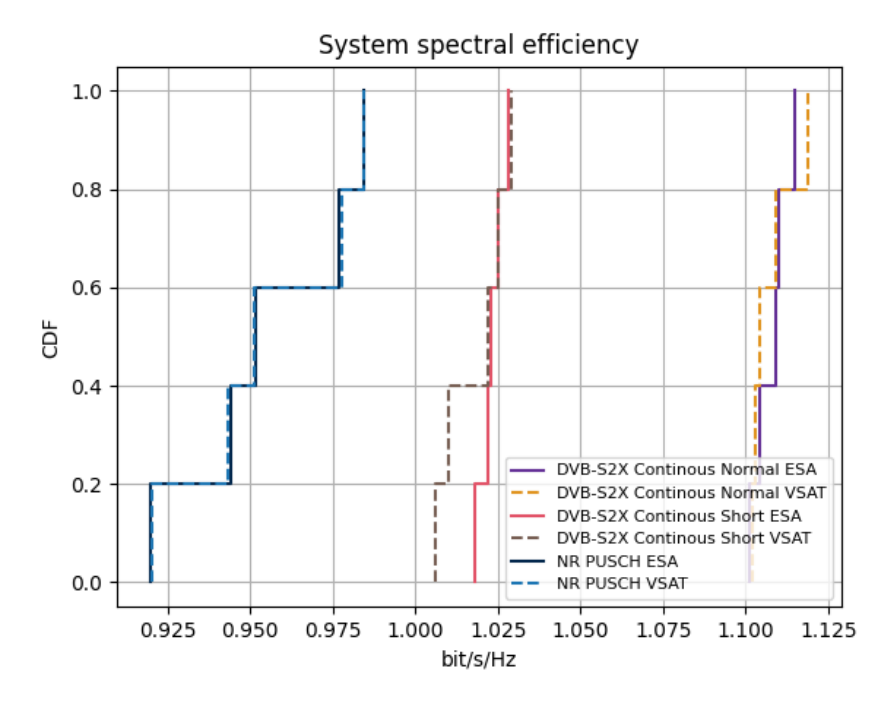


Figure 86. System spectral efficiency, continuous DVB-S2X vs. NR PUSCH, 99.3% Doppler compensation.





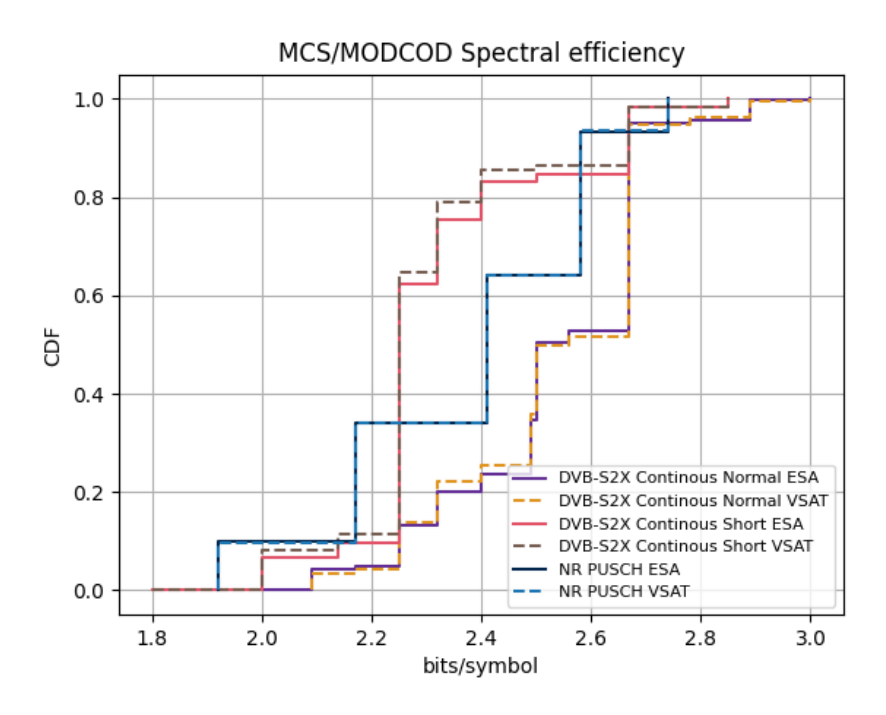


Figure 87. MCS/MODCOD spectral efficiency, continuous DVB-S2X vs. NR PUSCH, 99.3% Doppler compensation.

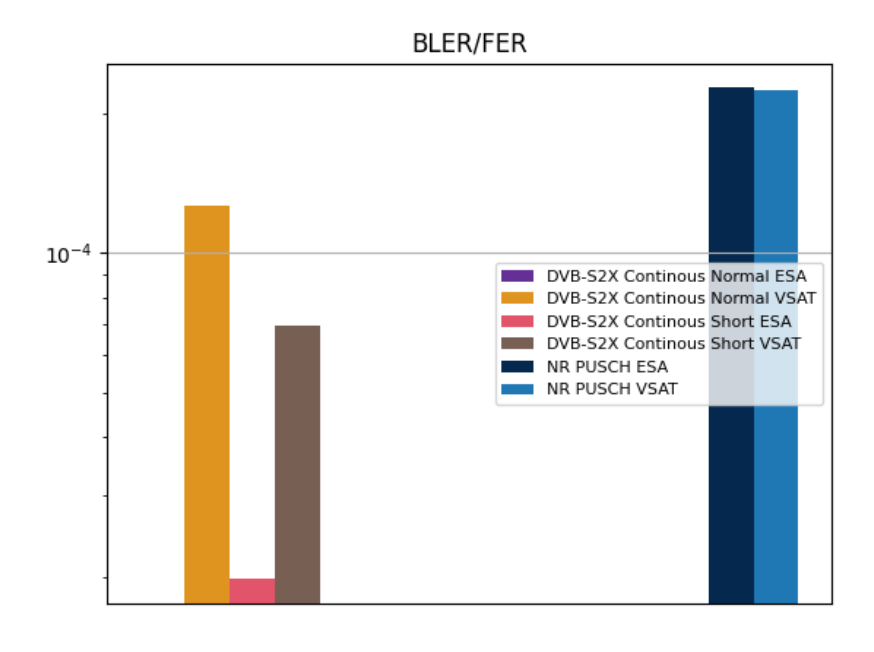


Figure 88. BLER/FER, continuous DVB-S2X vs. NR PUSCH, 99.3% Doppler compensation.





4.4.4 Summary

The technology comparison in 99.3% compensated Doppler conditions is summarised below in Table 9. The table shows an average throughput gain of around 17-18% for DVB-S2X Normal frames, compared to NR PUSCH, operating with both continuous carriers and bursts within the MF-TDMA structure. DVB-S2X Short frames provide comparatively slightly lower gain, around 8-11%. For DVB-RCS2 waveforms, a noticeable loss in gain is observed at around -16%, compared to NR PUSCH. The inclusion of ESA terminals causes minimal change to the results compared to conventional VSAT terminals.

Table 9. Summary table, 99.3% Doppler compensation.

99.3% Doppler compensation								
Antenna type	Scenario	Realized FER	5 th %-ile user tput [kbps]	50 th %- ile user tput [kbps]	95 th %- ile user tput [kbps]	User tput average [kbps]	Tput average gain over NR PUSCH	
	NR PUSCH	2.24E-04	25715.60	31741.70	35229.60	31310.93	0.00 %	
	DVB-RCS2	6.12E-05	24415.90	26955.60	27662.50	26317.25	-15.95 %	
	DVB-S2X, Normal	1.02E-05	33124.50	37342.10	38849.40	36676.97	17.14 %	
VSAT	DVB-S2X, Short	2.99E-05	32418.30	33904.60	38897.00	34889.89	11.43 %	
VSAT	Continuous carrier DVB-S2X, Normal	1.26E-04	33217.30	37759.70	39037.50	36892.06	17.82 %	
	Continuous carrier DVB-S2X, Short	6.94E-05	30830.70	33611.00	37213.30	33931.69	8.37 %	
ESA	NR PUSCH	2.27E-04	25705.30	31741.70	35327.30	31310.37	0.00 %	
	DVB-RCS2	7.61E-05	24537.10	26955.60	27666.00	26334.35	-15.89 %	
	DVB-S2X, Normal	0.00E+00	33231.50	37441.10	39034.60	36660.16	17.08 %	
	DVB-S2X, Short	2.28E-05	32467.50	33985.80	39056.50	34865.41	11.35 %	





Continuous carrier DVB-S2X, Normal	0.00E+00	33115.30	37794.70	38908.80	36910.21	17.88 %
Continuous carrier DVB-S2X, Short	1.98E-05	31464.40	33679.30	37427.30	34088.58	8.87 %

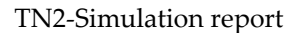
5 Conclusions

The performance of the NR NTN and DVB return link was evaluated at system level in a LEO regenerative satellite payload scenario, utilizing 3GPP LEO-600 satellite calibration scenarios and 3GPP VSAT characteristics. The Doppler effect, observed as a shift in frequency, is a critical phenomenon in LEO systems due to the high relative speed of the satellites compared to the ground users. This comparison modelled the Doppler shift as a degradation of the received power and additional ICI resulting from the frequency shift. Additionally, losses from electronically steering the beam pattern of a user terminal were modelled.

System level evaluations compared DVB-RCS2 to 3GPP NTN NR under three different Doppler compensation values: full (ideal) compensation, 99.3% compensation for the Doppler shift, and 97.5% compensation for the Doppler shift. DVB return link included the standardized linear modulation RCS2 waveforms as well as the newly introduced DVB-S2X waveforms. DVB-S2X waveforms were evaluated with two different carrier configurations, Continuous and Burst mode, and both Normal and Short frames were assessed separately.

NR PUSCH was observed to be more susceptible to Doppler degradation compared to DVB. This effect can be attributed to the physical layer architecture of NR, utilizing OFDM, where the frequency shift relative to the receiver's bandwidth is greater than in DVB carriers. Two different Doppler compensation values with residual frequency error were evaluated, and it was observed that all DVB return link variations demonstrate an increase in performance gain over NR PUSCH as the residual Doppler shift i.e., error in frequency synchronization, increased. However, with ideal compensation, NR PUSCH was seen to perform better overall than the DVB waveforms. The scanning losses associated with the use of ESAs did not appear to affect the performance, as the scenarios were dominated by interference and the loss in gain affected only slightly the SNR. In this context, the small reduction in the received power of the desired signal is counterbalanced by the reduction in the received power of the interference signals.

It is important to note that the presented results are highly sensitive to changes in the simulated configuration e.g., ACM and channel estimation parameters. The results showed that while DVB-S2X has generally better spectral efficiency for modulation and coding at the same SINR levels, the MF-TDMA resource structure is not optimal for DVB-S2X waveforms and required a robust ACM configuration to reach the intended error rates. Nevertheless, the presented results provide a clear picture of the general trend and magnitude of the performance of each technology, when Doppler







effects are applied. This comparison could be improved in the future by e.g., letting the users make ACM decisions, enabled by the fact that the DVB-S2X waveforms contain a MODCOD identifier within the physical layer header, as is already supported in the specification. Another factor that could benefit the DVB system, could be to evaluate less robust ACM configurations, combined with retransmissions, which should generally raise the spectral efficiency of DVB and increase the relative performance. Although the system still needs to be carefully configured, so that the increased delay from retransmissions does not affect any one user disproportionately.





6 References

- [1] Magister Solutions, "TN1: Simulation report of DVB-S2X/RCS2 in LEO systems", DVB project, January 2025
- [2] Lauri Sormunen, Tuomas Huikko, Verneri Rönty, Erno Seppänen, Sami Rantanen, Frans Laakso, Vesa Hytönen, Mikko Majamaa and Jani Puttonen, "Simulative Comparison of DVB-S2X/RCS2 and 3GPP 5G NR NTN Technologies in a Geostationary Satellite Scenario", arXiv, 2025, arXiv:2502.13704
- [3] Jani Puttonen, Lauri Sormunen, Henrik Martikainen, Sami Rantanen and Janne Kurjenniemi, "A System Simulator for 5G Non-Terrestrial Network Evaluations", IEEE International Symposium on a World of Wireless, Mobile and Multimedia Networks (WoWMoM), Non-Terrestrial Networks in 6G Wireless workshop, June 7-11, 2021.
- [4] ESA AO 8985 "Support to Standardisation of Satellite 5G Component", https://artes.esa.int/projects/alix.
- [5] Network Simulator 3 (ns-3), https://www.nsnam.org/
- [6] NS-3 module to simulate 3GPP 5G networks, Centre Tecnologic Telecomunicacions Catalunya, https://5g-lena.cttc.es/
- [7] 3GPP Technical Report TR 38.901 "Study on channel model for frequencies from 0.5 to 100 GHz".
- [8] 3GPP Technical Report TR 38.811 "Study on New Radio (NR) to support non-terrestrial networks".
- [9] 3GPP Technical Report TR 38.821, "Solutions for NR to support non-terrestrial networks (NTN)"
- [10]3GPP Tdoc R1-2101289, "Discussion on HARQ for NTN", Thales, 3GPP TSG RAN WG1 #104-e, January 25th February 5th, 2021.
- [11] 3GPP Tdoc R1-2104402, "Discussion on HARQ for NTN", Magister Solutions, Thales, 3GPP TSG RAN WG1 #105-e, May 10th 27th, 2021.
- [12] H2020-SPACE-2018-2020, "Dynamic spectrum sharing and bandwidth-efficient techniques for high- throughput MIMO Satellite systems", https://www.dynasat.eu/.
- [13] Mikko Majamaa, Henrik Martikainen, Lauri Sormunen, Jani Puttonen, "Adaptive Multi-Connectivity Activation for Throughput Enhancement in 5G and Beyond Non-Terrestrial Networks", International Conference on Software, Telecommunications and Computer Networks 2022 (SoftCOM), 22 24 September 2022.
- [14] Mikko Majamaa, Henrik Martikainen, Lauri Sormunen, Jani Puttonen, "Multi-Connectivity for User Throughput Enhancement in 5G Non-Terrestrial Networks", The 18th International Conference on Wireless and Mobile Computing, Networking and Communications (WiMob), 10-12 October 2022.
- [15] Mikko Majamaa, Henrik Martikainen, Lauri Sormunen, Jani Puttonen, "Multi-Connectivity in 5G and Beyond Non-Terrestrial Networks", Journal of Communications Software and Systems, Vol. 18, No. 4, Dec 2022.
- [16] Mikko Majamaa, Henrik Martikainen, Jani Puttonen, Timo Hämäläinen, "Satellite-Assisted Multi-Connectivity in Beyond 5G", IEEE International Symposium on a World of Wireless, Mobile and Multimedia Networks (WoWMoM), Workshop on 6G Non-Terrestrial Networks (NTNs), June 2023, Boston, USA.
- [17] Henrik Martikainen, Mikko Majamaa, Jani Puttonen, "Coordinated Dynamic Spectrum Sharing Between Terrestrial and Non-Terrestrial Networks in 5G and Beyond", IEEE International

TN2-Simulation report





- Symposium on a World of Wireless, Mobile and Multimedia Networks (WoWMoM), Workshop on 6G Non-Terrestrial Networks (NTNs), June 2023, Boston, USA.
- [18] Mikko Majamaa, Henrik Martikainen, Jani Puttonen, Timo Hämäläinen, "On Enhancing Reliability in B5G NTNs with Packet Duplication via Multi-Connectivity", IEEE International Conference on Wireless for Space and Extreme Environments (WiSEE 2023), Sept 2023, Aveiro, Portugal.
- [19] ESA AO 9725, "Satellite Air interface for Railway Control Communications".
- [20] Lauri Sormunen, Henrik Martikainen, Jani Puttonen, Dorin Panaitopol, "Co-Existence of Terrestrial and Non-Terrestrial Networks on Adjacent Frequency Bands", 11th Advanced Satellite Multimedia Conference (ASMS), September 2022.
- [21] Lauri Sormunen, Henrik Martikainen, Jani Puttonen, Dorin Panaitopol, "Coexistence of Terrestrial and Non-Terrestrial Networks on Adjacent Frequency Bands", International Journal of Satellite Communications and Networking, Sep. 2023.
- [22] 3GPP Tdoc R4-2114486, "NTN co-existence calibration with THALES updated values", THALES, 3GPP TSG-RAN WG4 Meeting RAN4#100- e, August, 2021.
- [23] 3GPP Tdoc R4-2120628, "TN-NTN Coexistence Results for Phase 1", THALES, Magister Solutions Ltd, 3GPP TSG-RAN WG4 Meeting #101-e, November, 2021.
- [24] 3GPP Tdoc R4-2201839, "TN-NTN Coexistence Results Updates", THALES, Magister Solutions Ltd, 3GPP TSG-RAN WG4 Meeting #101-bis-e, January, 2022.
- [25] Baptiste Chamaillard, Albekaye Traoré, Nathan Borios, Stefano Cioni, "Physical Layer simulative comparison of DVB-S2X/RCS2 and 3GPP 5G NR-NTN technologies over Geostationary Satellite Scenario", 12th Advanced Satellite Multimedia Systems Conference, Sitges, Spain, February 26-28, 2025.
- [26] ETSI EN 301 545-2, "Digital Video Broadcasting (DVB); Second Generation DVB Interactive Satellite System (DVB-RCS2); Part 2: Lower Layers for Satellite standard".
- [27] Toni Levanen, Jukka Talvitie, Risto Wichman, Ville Syrjälä, Markku Renfors, Mikko Valkama, "Location-Aware 5G Communications and Doppler Compensation for High-Speed Train Networks", 2017 European Conference on Networks and Communications (EuCNC), Oulu, Finland, 2017, pp. 1-6, doi: 10.1109/EuCNC.2017.7980755.
- [28] ESA, "Multi Access RelatIve performaNce compArison for GSO broadband satellite networks (MARINA)", https://connectivity.esa.int/projects/marina
- [29] R. J. Mailloux, "Phased Array Antenna Handbook, Second Edition", Artech, 2005.
- [30] Avraham Freedman, Lars Erup, Fernando Díaz Canales, David Peilow, Peter Nayler, Vittoria Mignone, Kimmo Kaario, Tuomas Huikko, and Verneri Rönty, "DVB standard support of NGSO systems", preprint, Authorea, February 28, 2025.
- [31]3GPP TS 38.101-5, "NR; User Equipment (UE) radio transmission and reception; Part 5: Satellite access Radio Frequency (RF) and performance requirements"